THE MORPHOLOGY OF THE AXOLOTL

(AMBYSTOMA MEXICANUM)

OPTIC TECTUM

by

Carolyn Ann Ingham

(Department of Behavioural Biology,

Research School of Biological Sciences,

Australian National University)

A thesis submitted for the degree of

Master of Science

at the

Australian National Univeristy

May 1980

To Richard

STATEMENT

This thesis describes original research carried out in the Department of Behavioural Biology at the Australian National University, from June 1978 to May 1980.

C. A. Ingham.

(C. A. Ingham)

Some of this work has been presented (1), some published (2), and some has been submitted for publication (3).

(1) INGHAM, C. A. (1979) The optic synapses in the axolotl tectum - An ultrastructural study. *Proceedings of APPS*, 10, 47P.

(2) INGHAM, C. A. and GÜLDNER, F-H. (1980) Constant occurrence of an ipsilateral retinotectal projection in the axolotl *(Ambystoma mexicanum)* revealed by horseradish peroxidase tracing. *Neurosci. Lett.* 17, 17-22.

(3) INGHAM, C. A. and GÜLDNER, F-H. (1980) Identification and morphometric evaluation of optic nerve afferents in the axolotl *(Ambystoma mexicanum)* optic tectum. *Cell and Tiss. Res.*

ACKNOWLEDGEMENTS

Special thanks are due to Dr. Fritz Güldner who suggested I should do an MSc. and then supervised my work with enthusiasm throughout the two years.

I am indebted to Professor Richard Mark for allowing me to undertake a Master of Science degree on a part-time basis whilst being employed as a laboratory technician. I also thank him for invaluable discussions and help when required.

Thanks are also extended to Dr. Ian Morgan for devoting so much time and effort to critically reading the manuscript.

I would like to thank the staff of the E.M. unit, illustrations, computer services, and photography for expert and friendly assistance.

I am grateful to my sister Sally for typing this thesis expertly.

Finally, I thank Richard for enticing me to Australia and Canberra, as well as giving his unerring support.

SUMMARY

1. The retino-tectal projection in the axolotl was studied using the diffusion of horseradish peroxidase along the cut optic nerve, by both light and electron microscopy. Filled nerve fibres and terminals were found throughout the superficial part of the contralateral optic tectum. No lamination of fibres or terminals was apparent. A small ipsilateral retino-tectal projection was also found. It was concentrated in the rostral tectum particularly the dorsomedial and ventrolateral areas. Ultrastructurally, the filled optic synapses looked similar in both the contralateral and the ipsilateral tecta.

2. The neurons in the tectum were studied using Golgi techniques. The cell type stained most frequently was oriented radially and branched throughout the plexiform layers. A second radially-oriented cell type was observed, which only branched in the outer plexiform layer of the tectum (that part receiving optic input). Horizontal and multipolar cells were also seen. The above cell types were situated in the cellular layers of the axolotl tectum. A small number of cells varying in shape were found in the superficial tectal layers.

3. The optic nerve terminals of the retinal afferents to the tectum were identified ultrastructurally using the techniques of filling with horseradish peroxidase, and degeneration. The mitochondria in filled structures had a characteristic electron-lucent matrix. After both eyes had been removed, terminals with these pale mitochondria almost completely

disappeared from the area known to receive optic input. In this area the presence of pale mitochondria was therefore nearly always diagnostic of the retinal origin of a bouton. The synapses were similar to those assumed to be of retinal origin in other vertebrates.

4. Identified optic synapses were morphometrically analysed. The results were compared with published data on optic synapses in the rat suprachiasmatic nucleus. Apart from the slightly smaller size of axolotl optic nerve terminals and their mitochondria, the parameters considered were very similar in the optic boutons of the two areas in the two species.

TABLE OF CONTENTS

1. INTRODUCTION

1. INTRODUCTION

1.1 THE VERTEBRATE OPTIC TECTUM

The optic tectum forms the roof of the mid-brain or mesencephalon. The homologous structure is usually termed the superior colliculus in mammals (Sprague, 1975; Ingle, 1973a). As the name implies the optic tectum is a component in the visual system, receiving a major retinal input in all vertebrates. The retino-tectal projection is retinotopically organised. The temporal retina (nasal field) projects rostrally, the nasal retina (temporal field) projects caudally, the ventral retina (superior field) medially, and the dorsal retina (inferior field) laterally (Scalia, 1976). In lower vertebrates the optic tectum forms a relatively large proportion of the brain.

In general, the morphology of the tecta of vertebrates has been studied in some detail both by light and electron microscopy. Degeneration and, more recently, autoradiographic, horseradish peroxidase and cobalt techniques have been employed to demonstrate the retinal projection to the tectum (for example, see Jackway and Riss, 1972; Guillery and Updyke, 1976; - urodeles; Scalia, 1976; Lázár, 1978 - anurans; Repérant *et al*, 1976 - fish; Repérant *et al*, 1978 - reptiles; Repérant, 1973 - birds; Mai, 1976 - mammals). Golgi techniques have been widely used to show the structure of neurons and terminal axonal arbors within the tectum (Gruberg, 1969 - urodeles; Scalia, 1976; Székely and Lázár, 1976 - anurans; Vanegas *et al*, 1974; Meek and Schellart, 1978 - fish; Butler and Ebbesson, 1975 - reptiles; La Vail and Cowan, 1971 - birds; Sterling, 1971; Mathers, 1977 - mammals). The ultra-

structure of the optic tectum has also been investigated by electron microscopy, especially that part receiving optic input (Székely and Lázár, 1976 - anurans; Laufer and Vanegas, 1974 - fish; Hayes and Webster, 1975; Angaut and Repérant, 1976 - birds; Sterling, 1971; Lund, 1972; Mathers, 1977 - mammals).

The main function of the optic tectum is, at least in lower vertebrates, orientation and capture of prey (Ingle, 1976). In a free-moving animal, activation of a focal region of the tectum by electrical stimulation, causes turning of the head, eyes, or body toward that spatial region retinotopically mapped upon the activated tectal area. This is known as the visual grasp reflex (Ingle, 1973a). When a visual, prey-like stimulus is moved into the animal's visual field the orientation toward that stimulus can be followed by a snapping action i.e. capture of prey. However, this action depends upon other factors such as the size of the stimulus or the motivation of the animal (Riss and Ingle, 1973; Ingle, 1973a).

1.2 THE AMPHIBIAN TECTUM

The optic tecta of anuran amphibians such as frogs and toads have been studied in some detail, physiologically and behaviourally (for reviews see Grüsser and Grüsser-Cornehls, 1976; Grüsser-Cornehls and Himstedt, 1976; Ingle, 1973a, 1976), as well as morphologically. These species have been used for studying the mature visual system as well as for studies of development, regeneration and plasticity (for review see Keating and Kennard, 1976). Their use in this regard is due to the ability of their retinal ganglion cells to regenerate nerves and reform precise connections (Keating and Kennard, 1976).

In this study the axolotl has been chosen as the subject of a morphological study of the optic tectum. The axolotl is a urodele amphibian. Urodeles have not been studied in as much detail as the anurans, however they may prove to be useful subjects for the type of studies described

above. Urodeles appear to have a relatively simple optic tectum without the multiple lamination found in anuran amphibians (Potter, 1969, 1972; Székely and Lázár, 1976). Golgi studies on *Ambystoma tigrinum* (Herrick, 1942; Gruberg, 1969) suggest that there are few cell types. If the morphological simplicity is paralleled by functional simplicity, this animal could provide some basic information on tectal circuitry which should aid in the understanding of the more complicated tectal structure of other vertebrates.

1.3 AIMS

The precise aims were firstly, to see which part of the tectum the retina projected to in the axolotl tectum using a tracing technique. The method used involved filling the optic nerve with horseradish peroxidase and thereby labelling the nerve fibres and their terminations. It was also applied for ultrastructural examination of the retino-tectal terminals (Mason and Robson, 1979; Robson and Mason, 1979). Secondly the types of cells in the axolotl tectum were studied using Golgi staining with a view to establishing which cell types received optic input directly and which cell types were likely to send efferent axons to other parts of the brain. Finally, the ultrastructure of the optic nerve terminals and their post-synaptic elements was examined after establishing that optic terminals could be recognised due to the presence of characteristic mitochondria. At the ultrastructural level a population of synapses can be identified by a tracing technique (such as horseradish peroxidase) or by destroying the neurons which give rise to the synapses and observing which ones disappear. The optic boutons were morphometrically analysed.

The literature cited on the subject of the optic tectum in this introduction is a fraction of that available. It serves only to give a broad outline of the sort of work carried out in this field. The studies relevant to this thesis will be discussed in detail after presenting my own

results and observations.

2. METHODS

FIG. 1 The three varieties of axolotl used in this study. a, pigmented body and eyes. b, pigmented eyes. c, no pigment at all. Calibration bar = 2cm.


a


b


c

ADDENDUM

TABLE: Number of axolotls with various pigment characteristics used in each experiment.

Experiment	Pigmentation			Total Number by experiment
	Pigmented eyes and skin	Pigmented eyes pink bodies	Albino, i.e. pink eyes and bodies	
1. HRP - light microscopy				
(a) Experimental	2	5	-	7
(b) Control	1	1	-	2
2. HRP - electron microscopy				
(a) Experimental	1	1	-	2
(b) Control	-	1	-	1
3. Golgi study	19	19	14	52
4. Ultrastructural study of degeneration of retinal afferent terminals	4	3	-	7
5. Ultrastructural study of general features of the optic neuropile	2	2	-	4
6. Morphometric study of optic synapses	3	2	-	5
TOTAL NUMBERS BY PIGMENTATION	32	34	14	TOTAL - ALL ANIMALS 80

2. METHODS

Three varieties of axolotl were used in this study. They either had pigmented eyes and skin, pigmented eyes and pink bodies or were totally albino with pink eyes and bodies (Fig. 1). Their length varied between 9 and 18cms. Albino mammals have abnormal retinofugal pathways (see Guillery and Updyke, 1976). In this study, no further reference will be made to the colour of the animals, as these factors did not appear to affect the results. It should be noted, however, that animals used for morphometric studies all had pigmented retinae. The size of the animals did not appear to affect the results.

2.1 LIGHT AND ELECTRON MICROSCOPICAL INVESTIGATION OF THE RETINO-TECTAL PROJECTION USING HORSERADISH PEROXIDASE (HRP) TRACING TECHNIQUES

Nine axolotls were used. The techniques employed involved the movement of HRP (Boehringer Mannheim,GmbH) from a cut end of the optic nerve to the terminals. The cytoplasm of the nerve and its terminals is filled with HRP so that after producing a visable reaction product it resembles a Golgi impregnated neuron (Mason and Robson, 1979; Robson and Mason, 1979).

Each axolotl was anaesthetised in 0.5% MS222 (tricaine methane-sulphate; Sandoz) in tap water, one optic nerve was cut just behind the eye and bathed in distilled water for 1 min. After removing surplus water, a small piece of gel-foam (Upjohn) saturated with a concentrated solution of HRP (in 1µl of distilled water) was inserted between the cut ends of the nerve. The skin was then glued back into place above the eye with isobutyl-

2-Cyanoacrylate (Ethicon, GmbH). After 66-72h the animals were anaesthetised, perfused with 0.1M sodium cacodylate buffer, 0.005% calcium chloride (pH7.2) and then with 3% glutaraldehyde, 3% paraformaldehyde (or alternatively 1.5% glutaraldehyde), 0.005% calcium chloride in 0.1M sodium cacodylate buffer (pH 7.2). The optic tecta were removed and immersed in the same fixative for 4h at 4°C. After rinsing overnight in 5% sucrose in buffer at 4°C, the tecta were processed for light and electron microscopy, using various methods.

The first method was that described by Riley and Marchand (1978), itself a modification of that suggested by Mesulam (1976), procedure 8. 60µm frozen sections were washed in distilled water and then incubated in: 50mg benzidine dihydrochloride, 100mg sodium nitroprusside, 10ml 0.2M sodium acetate buffer, pH 5.0), 90ml distilled water and 10 drops 0.1M cobalt chloride, for 20 mins. After addition of 4ml 0.3% hydrogen peroxide incubation was continued for another 25 mins. The sections were then transferred to a stabilising solution (9% sodium nitroprusside in, 0.2M sodium acetate buffer (pH 5.0): ethanol: distilled water, 5:50:45), at 0-4°C for 20 mins. The sections were washed in several changes of distilled water after which they were mounted on gelatinised slides and counterstained with 1% neutral red.

The second method was that of Malmgren and Olsson (1977). 60µm frozen sections were collected, and after rinsing in 0.1M sodium cacodylate buffer (pH 7.2), were incubated in the dark at room temperature in 10ml 0.1M sodium cacodylate - HCL buffer (pH 5.1), 20mg diaminobenzidine and 0.1ml 1% hydrogen peroxide for 30 mins. After rinsing in buffer the sections were mounted and counterstained lightly with 5% cresyl violet.

The third method was that of Malmgren and Olsson (1977) for electron microscopy. 200-300µm slices of optic tectum were incubated in 10ml 0.1M sodium cacodylate - HCL buffer (pH 5.1), and 20mg diaminobenzidine for 30 mins., after which 0.1ml 1% hydrogen peroxide was added and the

incubation continued for another 60 mins. Both stages were carried out in the dark at room temperature.

Sections from three animals were processed according to the first method (alternate sections only in two animals), sections from four animals were processed according to the second method (alternate sections only in two animals), and sections from four animals were processed according to the third method.

Two of the latter were dehydrated and embedded in araldite. Thick sections (approximately 100µm) were cut by hand from the araldite block and examined under the light microscope together with the other five preparations. The extent of the ipsilateral and contralateral retino-tectal projection was determined and drawings were made with the aid of a camera lucida attachment. For electron microscopy, the tecta from the remaining two animals were post-fixed for 1.5h in 1% osmium tetroxide, dehydrated and embedded in araldite. Thick and thin sections were taken from the medio-dorsal area of both ipsilateral and contralateral tecta (more rostral part). The thin sections were examined unstained and stained (with lead citrate (Reynolds,1963) and 10% uranyl acetate in 50% alcohol (Lewis and Knight, 1977)) using an Hitachi 500 electron microscope. To obtain a very approximate estimate of the relative proportions of ipsi- and contra-lateral optic nerve terminals in the tectum, 35 random survey pictures (initial magnification x 7,000, final magnification x 17,500) were taken through the ipsi- and contra-lateral optic neuropile, and the number of filled presynaptic elements with synaptic vesicles were counted.

Three animals, where the optic nerve and terminals were not filled with HRP (one for electron microscopy, two for light microscopy) served as controls. Dense reaction product in blood vessels showed the reaction was carried out successfully. No intrinsic peroxidase activity could be detected by light or electron microscopy, in neuronal elements of either tectum.

2.2 GOLGI STUDY

Fifty two axolotl tecta were examined in this study. Three Golgi methods were applied: the rapid Golgi method (modified from Palay and Chan-Palay, 1974), the Golgi-Kopsch method (modified from Meek and Schellart, 1978) and the Golgi-Cox method (Ramón-Moliner, 1970). Staining times were varied in an attempt to obtain the best results (Table 1). The tecta from all animals were coated with fresh egg yolk according to Schroeder (1973), prior to placing in 25ml of the staining fluid. Cotton wool lay on the base of each bottle to ensure sufficient access of the stain to all parts of the brain. All the bottles were stored in the dark at room temperature, during the staining process.

In the rapid Golgi method (GR) the animal was anaesthetised in 0.5% MS222 and then perfused through the heart with 0.1M sodium cacodylate buffer (pH 7.2), for 30 secs., followed by 1% glutaraldehyde, 1% paraformaldehyde, in 0.1M sodium cacodylate buffer (pH 7.2), for about 5 mins. The tecta were then removed from the brain and immersed in the above fixative at 0-4^{o}C for varying periods of time (see Table 1). After coating in egg yolk, the tissue was placed in 2.4% potassium dichromate, 0.2% osmium tetroxide, in distilled water. After varying periods of time (see Table 1) the tissue was removed, patted on gauze and rinsed in a small volume of 0.75% aqueous silver nitrate for differing time periods (see Table 1). The tissue was then dehydrated in a routine fashion, the first solution being 0.5% silver nitrate in 50% ethanol followed by a graded series of alcohols and epoxypropane. Finally, the tissue was embedded in a soft mixture of araldite (20ml resin, 10ml hardener, 12 drops accelerator, 33 drops dibutyl phthallate).

In the Golgi-Kopsch (GK) method the tissue was fixed as above. After coating in egg yolk, it was placed in 1.5% potassium dichromate, 5% glutaraldehyde, in distilled water for various times. It was then

GR			GK			GC		
NO. OF ANIMALS	FIXATION TIME H	STAIN TIME H $K_2Cr_2O_7/AgNO_3$	NO OF ANIMALS	FIXATION TIME H	STAIN TIME H $K_2Cr_2O_7/AgNO_3$	NO. OF ANIMALS	STAIN USED	STAIN TIME DAYS
2	4	15/3	6	2-4	48/24*	1	GC	3.5
2	12	6/1.5	1	2-4	48/24(x2)	1	GC	7
19	4-8	10/2*	4	12	48/24	2	GC	21
2	12	6/3	2	4	24/24	1	½GC	3.5
						5	½GC	7*
						2	½GC	14
						1	¼GC	3.5
						1	¼GC	7
25			13			14		

TABLE 1 Table showing the fixation and staining times as well as the number of animals used for each method.

* Methods considered most successful, although all methods were used for analysis.

placed in 0.75% aqueous silver nitrate and processed as described above. In the Golgi-Cox (GC) method, the animal was anaesthetised in 0.5% MS222, after which the brain was removed as quickly as possible and the tecta coated with egg yolk. They were then placed in a mixture of solutions A and B (Ramón-Moliner, 1970). A contained 1g potassium dichromate, 1g mercuric chloride, dissolved in 85ml distilled water and boiled for 15 mins. Solution B contained 0.8g potassium chromate and 0.5% potassium tungstate dissolved in 20ml distilled water. Various combinations of A and B and boiled distilled water were used (Meek and Schellart, 1978). They were: GC, which was A:B in the ratio 1:1; ½GC, which was A:B:H_2O in the ratio 1:1:2; and ¼GC which was A:B:H_2O in the ratio 1:1:6. The rapid procedure of Ramón-Moliner (1970), steps 1-3 only, was then followed. This consisted of rinsing the tissue in water and placing it in an impregnation fluid made up of 0.5g lithium hydroxide, 15g potassium nitrate and 100ml distilled water. The tecta were then dehydrated through a graded series of alcohols and embedded as described previously.

The araldite blocks were placed in a 60^{o}C oven for 24h to allow partial hardening. They were then either sectioned immediately or placed in a freezer until they could be sectioned. Approximately 100µm transverse sections were cut by hand under a dissecting microscope. They were floated on drops of water on a gelatinised slide and dried in a 60^{o}C oven for a further 48h. After placing in xylene for 2 mins, the slides were cover-slipped with D.P.X. mounting medium (Difco). The sections were examined under the light microscope and 48 cells were drawn at 100x magnification under oil, using a camera lucida attachment.

Gruberg (1969) divided the outer plexiform layer of the tiger salamander *(Ambystoma tigrinum)* into three, based on physiological characteristics. These consisted of an optic layer, a contralateral somesthetic layer and a bilateral somesthetic layer. They have been called PL1, PL2 and PL3 respectively in this study. These divisions were followed, and the

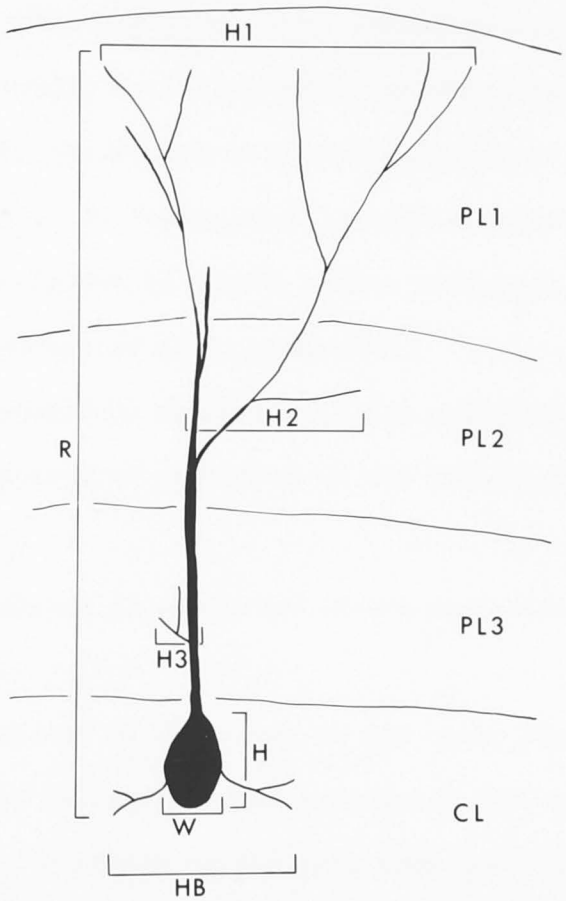

FIG. 2 Diagram showing measurements made in the Golgi study. CL, cellular layer; PL1, 2, 3, plexiform layers; R, radial extension of neuron; HB, horizontal extension of basal dendrites; H1, 2, 3, horizontal extension of dendrites in PL1, 2, 3 respectively.

inner cellular layer was also arbitrarily divided into three (Herrick, 1942), called CL1, CL2 and CL3 in this study (Fig. 4). The various parameters of the cells measured are listed below. (Also see Fig. 2).

1. Cell body, height and width.
2. Radial extension of the dendritic field of the cell in the dorso-ventral direction. This was often under-estimated due to incomplete staining or the inability to follow dendrites which became obscured by the staining of other structures in peripheral regions (see discussion of technical details). In these cases the radial extensions were not included in the calculation of a mean radial extension.
3. Maximum horizontal spread of basal dendrites.
4. Maximum horizontal spread of dendrites in the cellular layer.
5. Maximum horizontal spread of dendrites in the bilateral somesthetic layer (PL3).
6. Maximum horizontal spread of dendrites in the contralateral somesthetic layer (PL2).
7. Maximum horizontal spread of dendrites in the optic layer (PL1).

Means and standard deviations were calculated for the above parameters for each cell group. The position of the cell body and the presence of an axon were also noted. On the basis of the characteristics of their dendritic trees, cells were classified into various basic types, following a simplified version of the approach used by Meek and Schellart (1978) for studying the goldfish optic tectum. The classification of cells by the pattern of their dendritic tree was first suggested by Ramón-Moliner (1962).

2.3 ULTRASTRUCTURAL STUDY OF THE DEGENERATION OF RETINAL AFFERENT TERMINALS i.e. OPTIC SYNAPSES

Seven axolotls were anaesthetised in 0.5% MS222 and both eyes were removed from each animal.

After survival periods of 3, 4, 6, 10, 12, 14 or 56 days after the operation, the animals were anaesthetised and perfused through the heart

for 30 secs with 0.1M sodium cacodylate buffer (pH7.2), 0.005% calcium chloride, and then with 3% glutaraldehyde, 3% paraformaldehyde, 0.005% calcium chloride in 0.1M sodium cacodylate buffer (pH7.2). The brains were left in fixative at 4°C for 4h, washed in 0.1M sodium cacodylate buffer (pH7.2) for 20 mins with two changes, and then fixed with 1% osmium tetroxide in the same buffer, dehydrated in ethanol and embedded in araldite. Thin transverse sections were taken from the middle of the optic tectum, stained with 10% uranyl acetate in 50% alcohol (Lewis and Knight, 1977) and 2.7% lead citrate (Reynolds, 1963) and examined with an Hitachi 500 electron microscope. To obtain some indication of the time course of optic bouton degeneration, the numbers of dense bodies in glial cells, degenerating synapses and normal looking optic synapses were counted. Ten random survey pictures were taken (final magnification 30,000x). Presynaptic elements, optic boutons with characteristic mitochondria, dense bodies in glial cells, and degenerating synapses were counted.

Thirty five random survey pictures (final magnification 17,500x) were taken of the optic neuropile from a normal animal (see Methods 2.4), an HRP-treated animal (see Methods 2.1) and the axolotl, whose eyes had been removed 56 days prior to perfusion. Presynaptic elements containing dark and light mitochondria were counted in all preparations, taking note of the number of elements in each category containing HRP reaction product. Histograms were drawn to compare the percentage of presynaptic elements with dark and light mitochondria in each animal.

2.4 MORPHOMETRIC STUDY OF NORMAL OPTIC SYNAPSES

Nine axolotls were used in this study. Five were anaesthetised in 0.5% MS222, perfused for 30 secs with 0.1M sodium cacodylate (pH7.2), 0.005% calcium chloride, and then with 3% glutaraldehyde, 3% paraformaldehyde, 0.005% calcium chloride, in 0.1M sodium cacodylate (pH7.2). Four animals were decapitated. On ice, their skulls were opened and the brains immersed

in the above fixative within 2 mins. All nine brains were left in fixative at 4°C for 4h, washed in 0.1M sodium cacodylate buffer (pH 7.2) for 20 mins with two changes, followed by fixation with 1% osmium tetroxide in the same buffer, dehydrated in ethanol and embedded in araldite. Thin, transverse sections were taken from the middle of the optic tectum, stained with 10% uranyl acetate in 50% alcohol (Lewis and Knight, 1977) and 2.7% lead citrate (Reynolds, 1963) and examined with an Hitachi 500 electron microscope.

In five animals approximately 30 optic synapses from each animal, with mitochondria and a transversely cut synaptic apposition, were photographed to a final magnification of 60,000x. Various parameters were measured, following the check list suggested by Palay and Chan-Palay (1975), together with those added by Güldner (1978b). Perimeters and areas were calculated using an image analyser. Glial covering and length of the contact between boutonal and postsynaptic elements were measured using an opisometer. The diameters of the optic boutons were calculated by converting the area into a circle $\left(d = 2\left(\frac{area}{\pi}\right)^{\frac{1}{2}}\right)$. Diameters of mitochondria and dendrites were taken as the smallest diameter. With clear and dense-core vesicles, the average of largest and smallest diameter was taken. The thickest portion of the postsynaptic density was measured. The frequency distributions of the various parameters were drawn with the aid of a PDP-11 computer and graph plotter. This also gave means and standard deviations. These values are not usually given as most of the curves were skewed and therefore the data could not be considered as being normally distributed. Instead, ranges and peaks are generally quoted. In four normal axolotls, approximately 50 random survey pictures (final magnification 30,000x) were taken through the tectum for studying the general features of the optic neuropile. No attempt was made to estimate the numbers of optic synapses, or to compare different areas of the tectum.

3. RESULTS

FIG. 3 Drawings of the axolotl brain. a, dorsal view. b, longitudinal section.

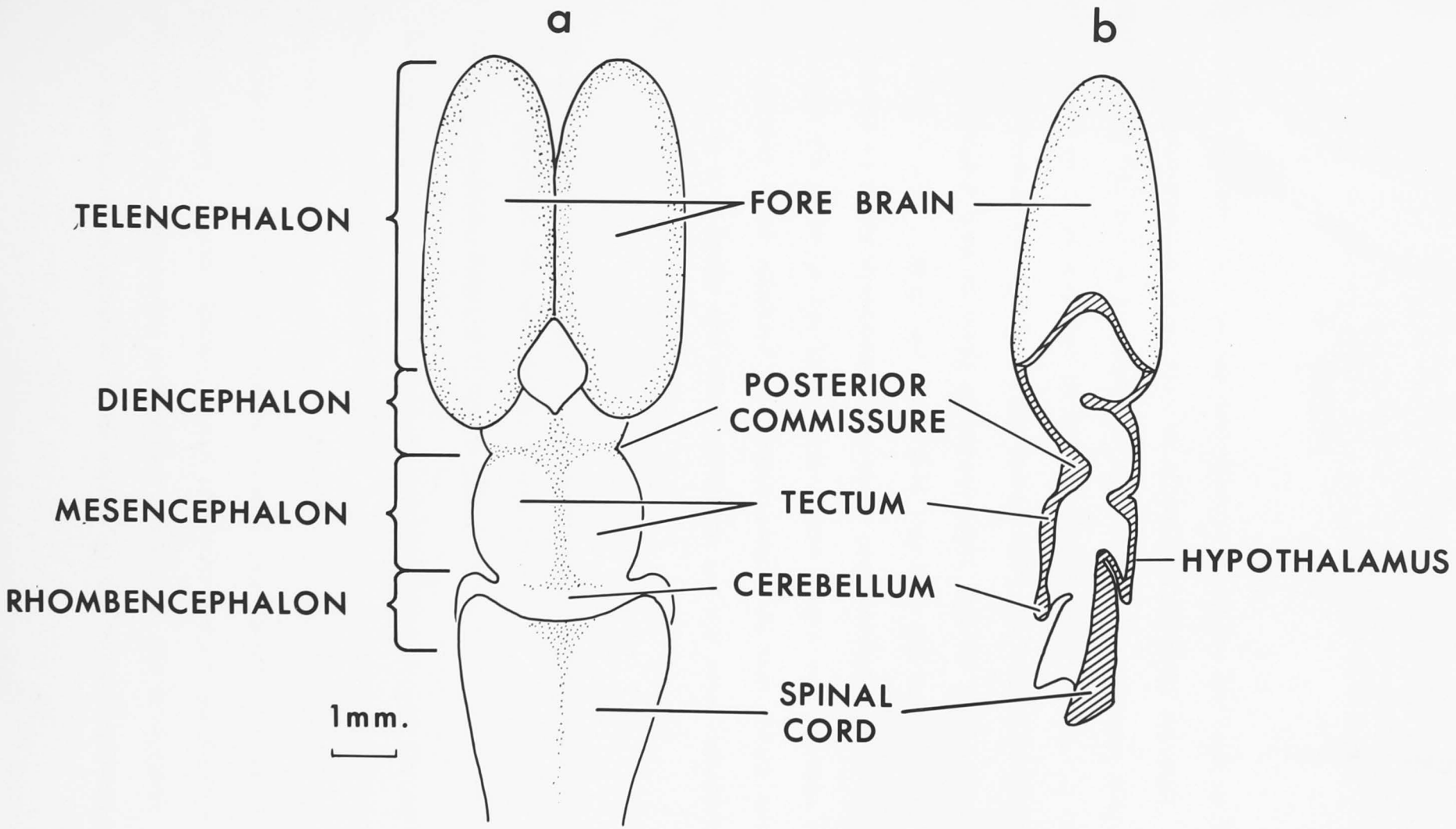
a
b
TELENCEPHALON
DIENCEPHALON
MESENCEPHALON
RHOMBENCEPHALON
FORE BRAIN
POSTERIOR COMMISSURE
TECTUM
CEREBELLUM
HYPOTHALAMUS
SPINAL CORD
1mm.

3. RESULTS

The optic tectum is a paired structure which forms the roof of the mid-brain or mesencephalon (Fig. 3). In transverse section, the most anterior part of the tectum is caudal to the posterior commissure (Fig. 4a,d). The most caudal point is anterior to the cerebellum (Fig. 4c, f). A transverse section through the middle of the tectum (Fig. 4b, e) showed that it is basically divided into an outer plexiform layer (PL1-3) and an inner cellular layer (CL1-3). Very few cells were found in the outer layer, which consisted of a few myelinated but mainly unmyelinated axons, and dendrites from the cells in the inner layer. The nuclei of the cells in the inner cellular layer appeared fairly homogeneous in size, shape and distribution. In this study the outer plexiform and the inner cellular layer were each divided into three (Fig. 4e).

3.1 LIGHT AND ELECTRON MICROSCOPIC INVESTIGATION OF THE RETINO-TECTAL PROJECTION USING THE HRP TRACING TECHNIQUE

3.1.a Light Microscopic Results (Figs. 5-13)

The contralateral retino-tectal projection extended from the most rostral point to within 200µm of the caudal extreme of the tectum (Fig. 5). Terminals (spot like reaction product) (Fig. 7) and fibres (threads of reaction product) (Fig. 7) were found throughout the superficial half of the plexiform layer (approx. 150µm). Optic fibres tended to concentrate in the upper part of the tectum but no distinct lamination was detectable (Fig. 6). The projection appeared to be denser in the rostral portion of

FIG. 4 1µm araldite transverse sections through the axolotl tectum, stained with toluidine blue.
a, anterior tectum. b, mid tectum; rectangle indicates area used for electron microscopy; c, caudal tectum. Calibration bar for a, b, c = 150µm.
d, anterior tectum; tc, tectal commissure; pc, posterior commissure; T, tectum. e, mid tectum, area used for electron microscopy as shown in rectangle of b, showing divisions of outer plexiform layers (PL1, PL2, PL3) and inner cellular layers (CL1, CL2, CL3) used in this study.
f, caudal tectum, PL plexiform layer; CL, cellular layer. Calibration bar for d, e, f = 100µm. The degree of staining in a - f is variable.

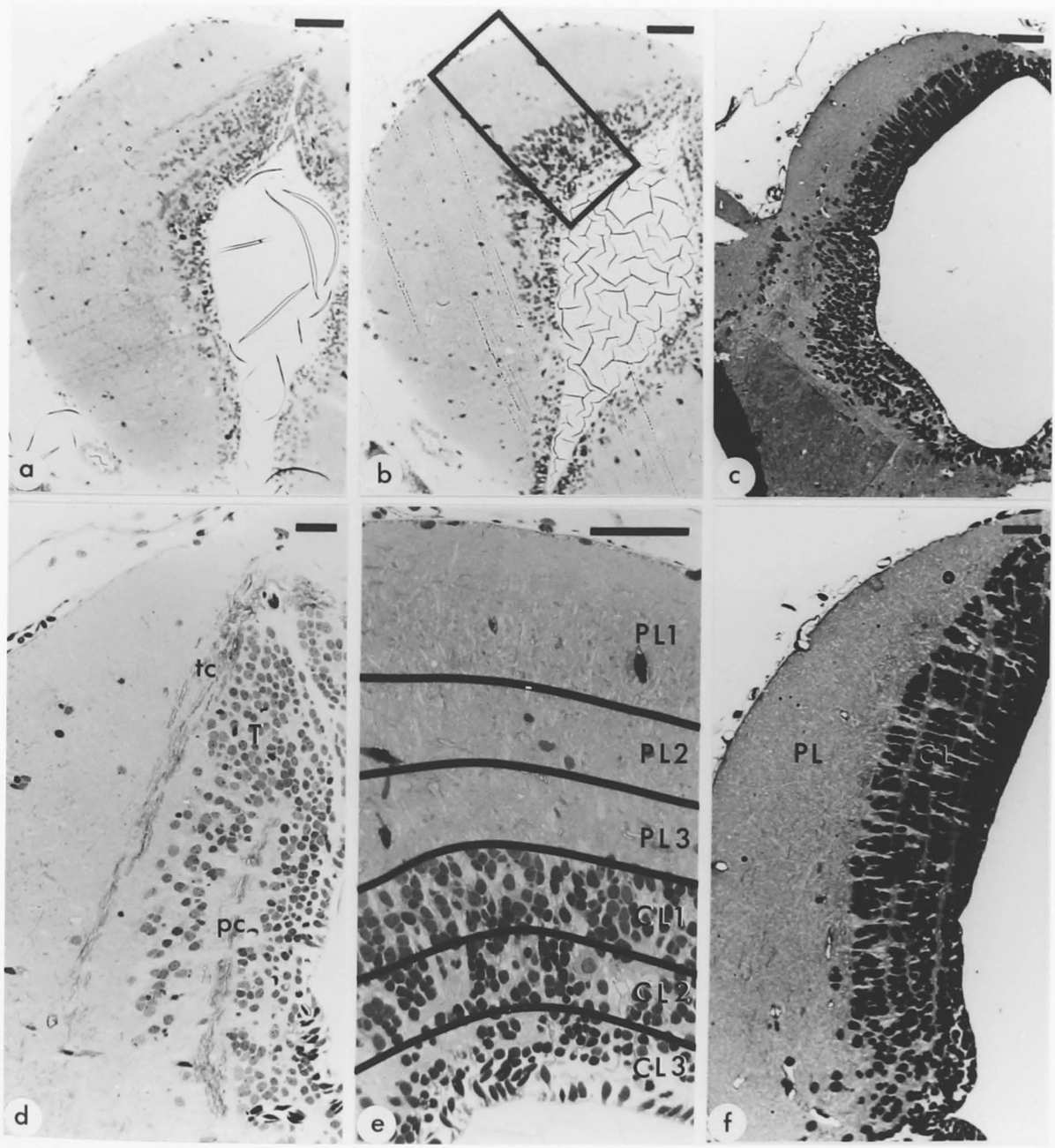
a
b
c
tc
T
pc
d
PL1
PL2
PL3
CL1
CL2
CL3
e
PL
CL
f

FIG. 5

Camera lucida drawings of typical distribution of ipsi and contralateral optic termination in the axolotl tectum. Proceeding from the top of the page rostro-caudally in 120μm steps.

C, Contralateral; I, Ipsilateral; CL, Cellular layer; PL, Plexiform layer.

Symbols on the top drawing apply throughout figure. Lines and dots represent fibres and terminals respectively.

Calibration bar = 200μm.

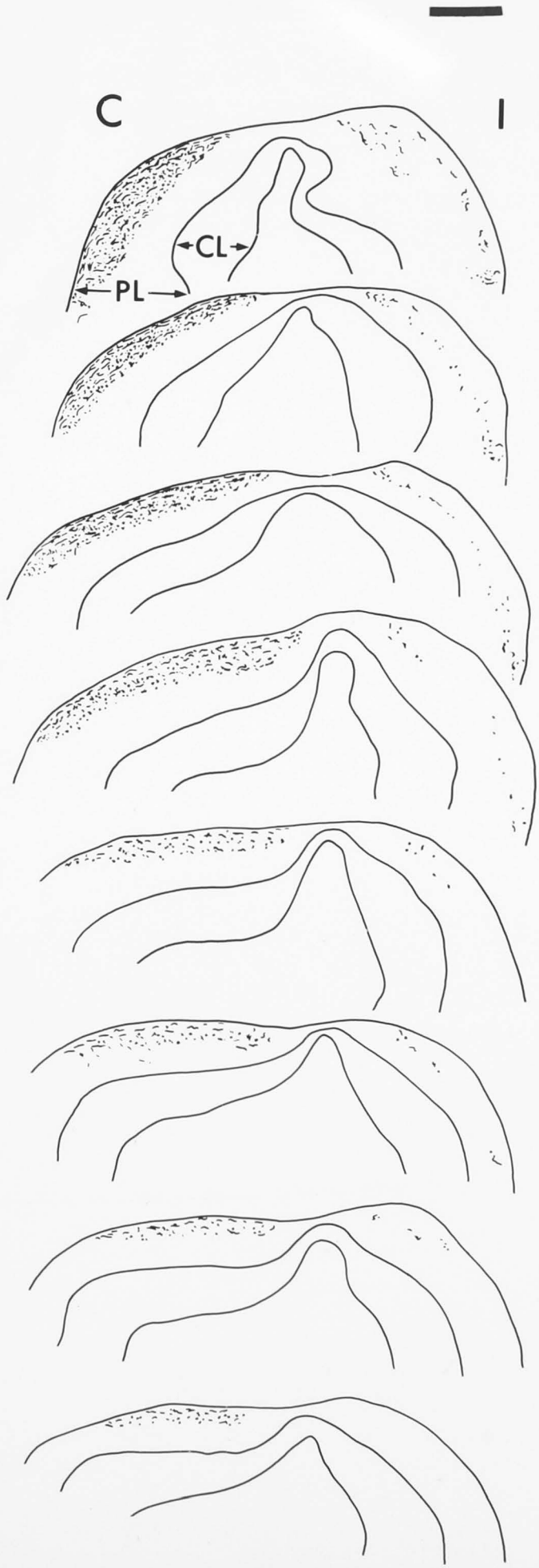
C
I
CL
PL

FIGS. 6-9 Micrographs of the contralateral retino-tectal projection shown by filling the optic nerve with HRP and reacting it with benzidine dihydrochloride.
P, pial surface.

FIG. 6 Reaction product is seen throughout the superficial half of the outer plexiform layer (PL); CL, cellular layer; V, ventricle. The ipsilateral projection cannot be seen at this magnification. Calibration bar = 150μm.

FIG. 7 Ventrolateral tectum. Threads (arrows) and specks (asterix) of reaction product can be seen, filling fibres and terminals respectively. CL, cellular layer. Calibration bar = 50μm.

FIG. 8 Darkfield micrograph of dorsomedial tectum. A bright band of reaction product can be seen in the superficial part of the contralateral tectum (arrows). Ipsilateral projection cannot be seen clearly at this magnification. Calibration bar = 100μm.

FIG. 9 Darkfield micrograph of dorsomedial, contralateral projection. Bright band of threads and dots (arrows) can be seen in superficial part of tectum. Calibration bar = 50μm.

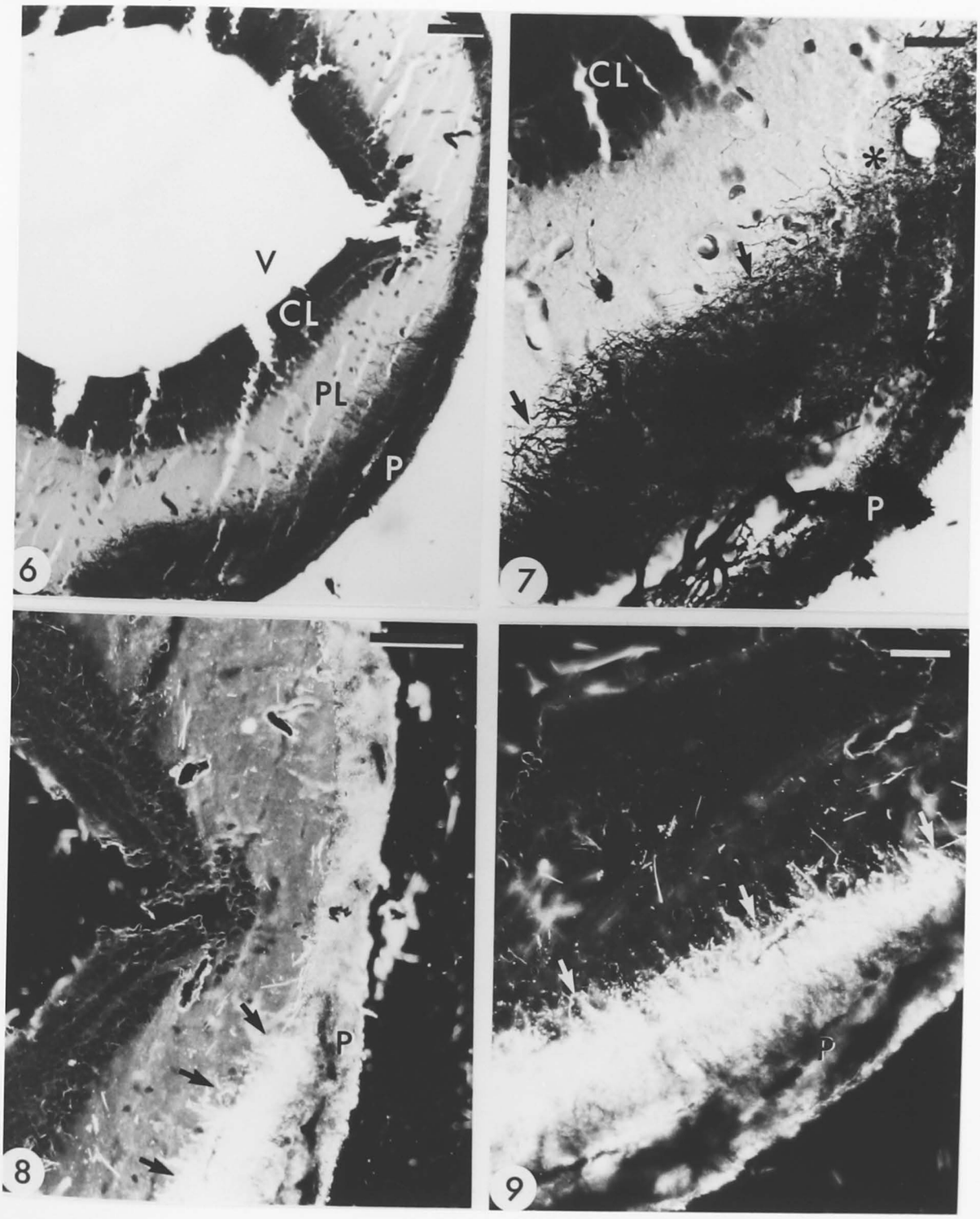
V
CL
PL
P
6
CL
*
P
7
P
8
P
9

FIGS. 10-13 Micrographs of the ipsilateral retino-tectal projection shown by filling the optic nerve with HRP and reacting it with benzidine dihydrochloride. Needle-like crystals of reaction product contaminate some of the sections (C).

FIG. 10 Ventrolateral area of the tectum. Fibres (arrows) are filled with reaction product.
Calibration bar = 50µm.

FIG. 11 Darkfield micrograph of ventrolateral area of the tectum. Fibres (arrows) and terminals (asterisk) can be seen.
Calibration bar = 50µm.

FIG. 12 Dorsomedial area of tectum. Ipsilateral retino-tectal fibres (arrows) can be seen. Calibration bar = 50µm.

FIG. 13 Dorsomedial area of tectum. Ipsilateral retino-tectal fibres (arrows) can be seen. Calibration bar = 50µm.

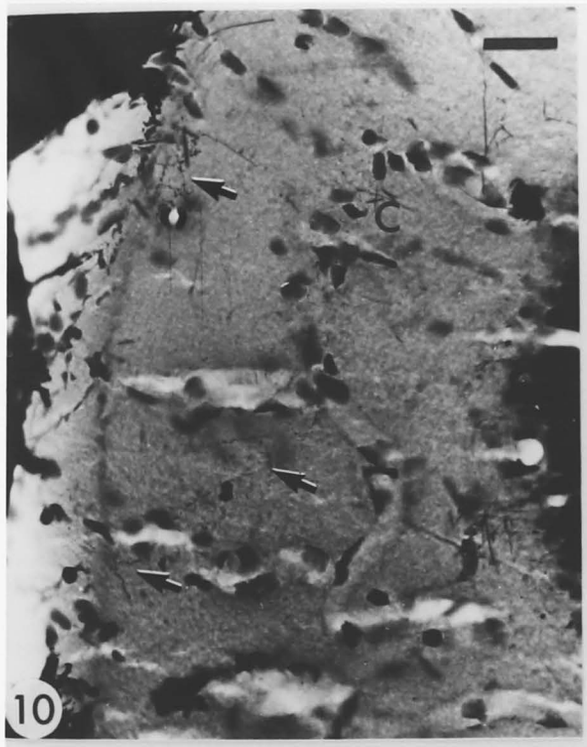

10

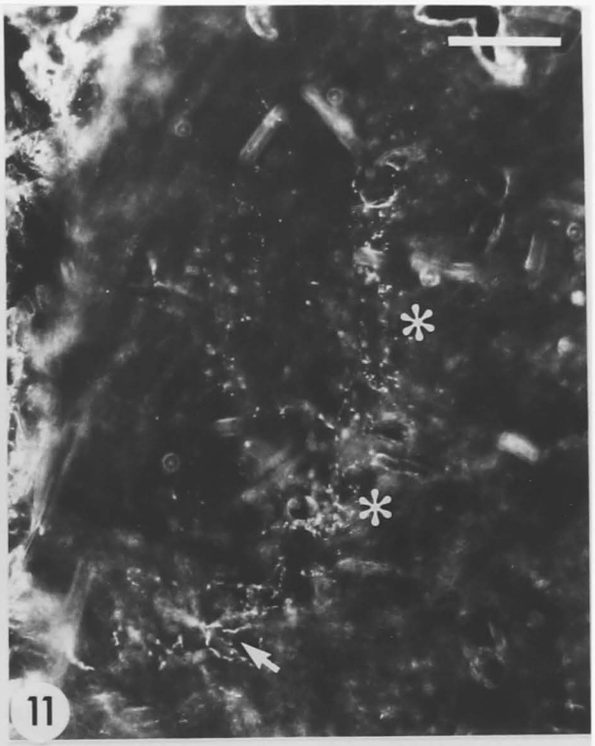

11

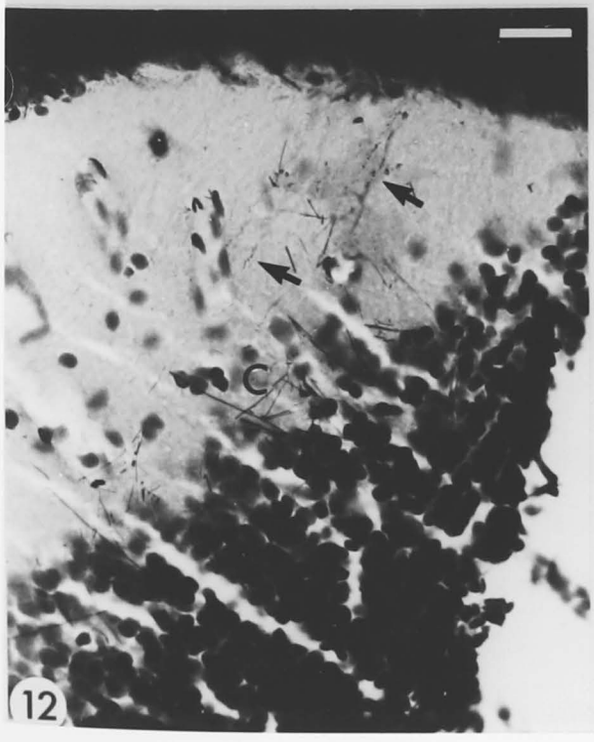

12

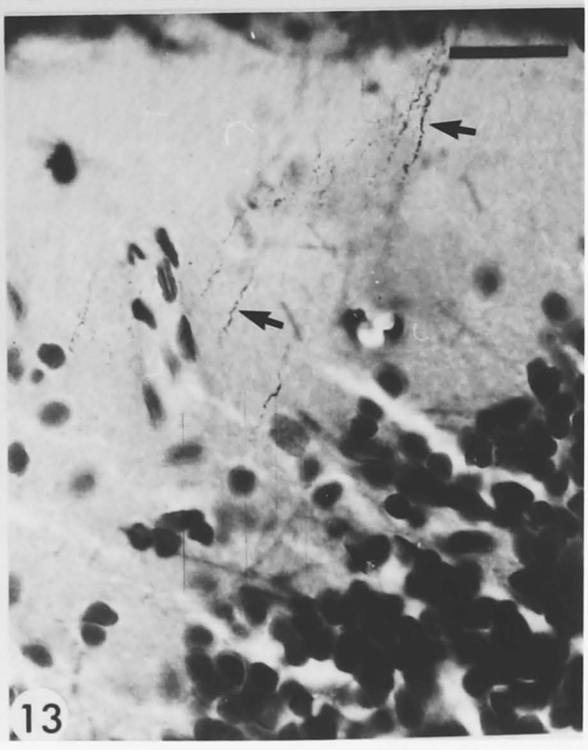

13

the tectum than in the caudal part. An ipsilateral retino-tectal projection was also found. It did not extend as far caudally (by about 200μm) as the contralateral one (Fig.5). The projection was extremely small and restricted to the mediodorsal and ventrolateral areas of the tectum (Figs. 5, 10-13). In preparations where uptake appeared to be the greatest, a small number of terminals and fibres were also observed in the more ventral part of the optic neuropile (Fig. 11).

The amount of ipsilateral staining varied somewhat between animals. However, as the strength of the reaction on the ipsilateral side was matched by the relative strength on the contralateral side (i.e. the animal showing the strongest reaction on the contralateral side, showed the strongest ipsilateral reaction), I feel that the variability is in the technique (e.g. HRP diffusion along the optic nerve) rather than an actual difference in the extent of the projection. Two animals showed no detectable ipsilateral retino-tectal projection at all (one from each light microscopic method); however in these cases the contralateral one was also weakly stained.

3.1.b Electron Microscopic Results (Figs. 14, 15, 32, 35)

Optic axons and boutons filled with HRP are clearly visible in low power, unstained electron micrographs of both contralateral and ipsilateral tecta (Figs. 14, 15). The synaptic vesicles and synaptic appositions of the synapses can still be seen (Figs. 32, 35). The mitochondria have an electron-lucent matrix and tubular inner membrane similar to that described in the optic synapses of the rat suprachiasmatic nucleus (Güldner, 1978a, b). Terminals of both the ipsilateral and the contralateral projections showed similar features. In the areas compared (i.e. rostral, mediodorsal optic neuropile), the number of HRP filled terminals in the ipsilateral tectum amounted to about 3% of that in the contralateral tectum. This means that taking the optic neuropile as a whole, the percentage is probably less than 1%.

FIGS. 14, 15 Survey electron micrographs of axolotl tectum (unstained). OB, Optic bouton; OA, Optic axon; M, Mitochondrion. Calibration bar = 1μm.

FIG. 14 Contralateral tectum.

FIG. 15 Ipsilateral tectum.

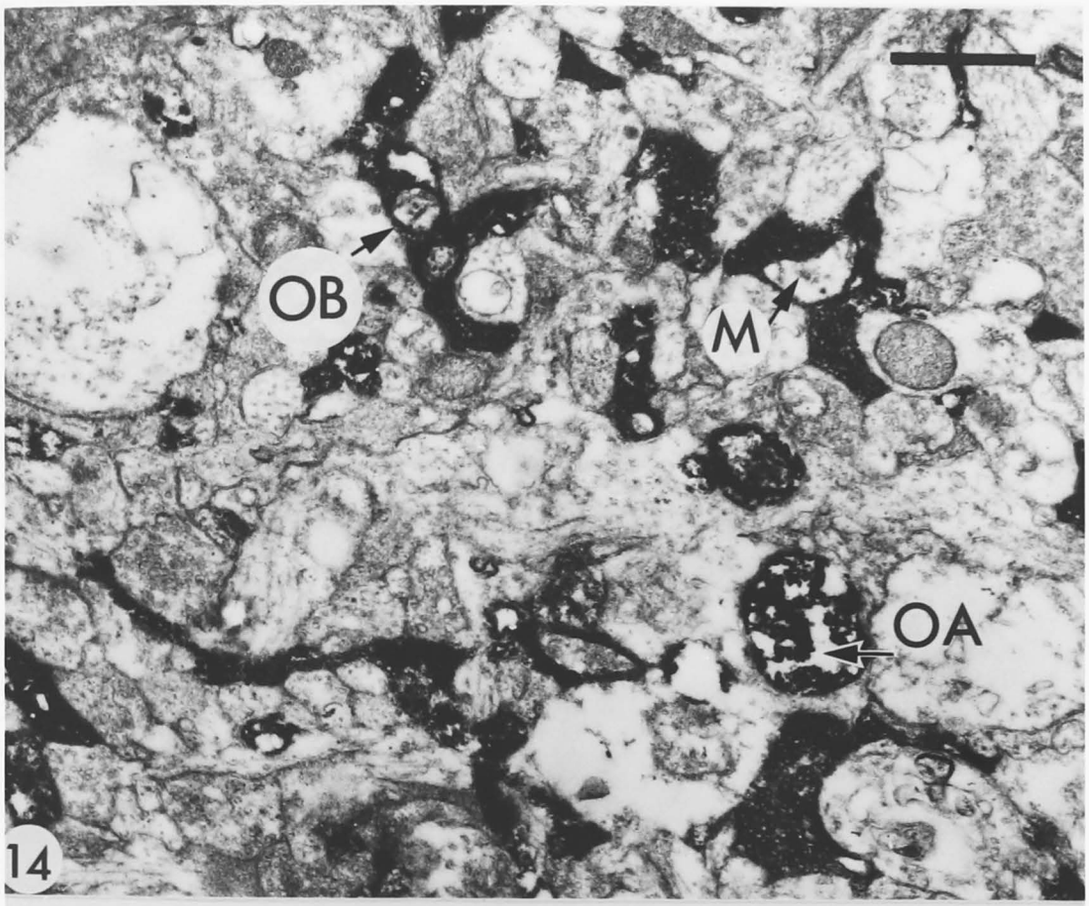

14

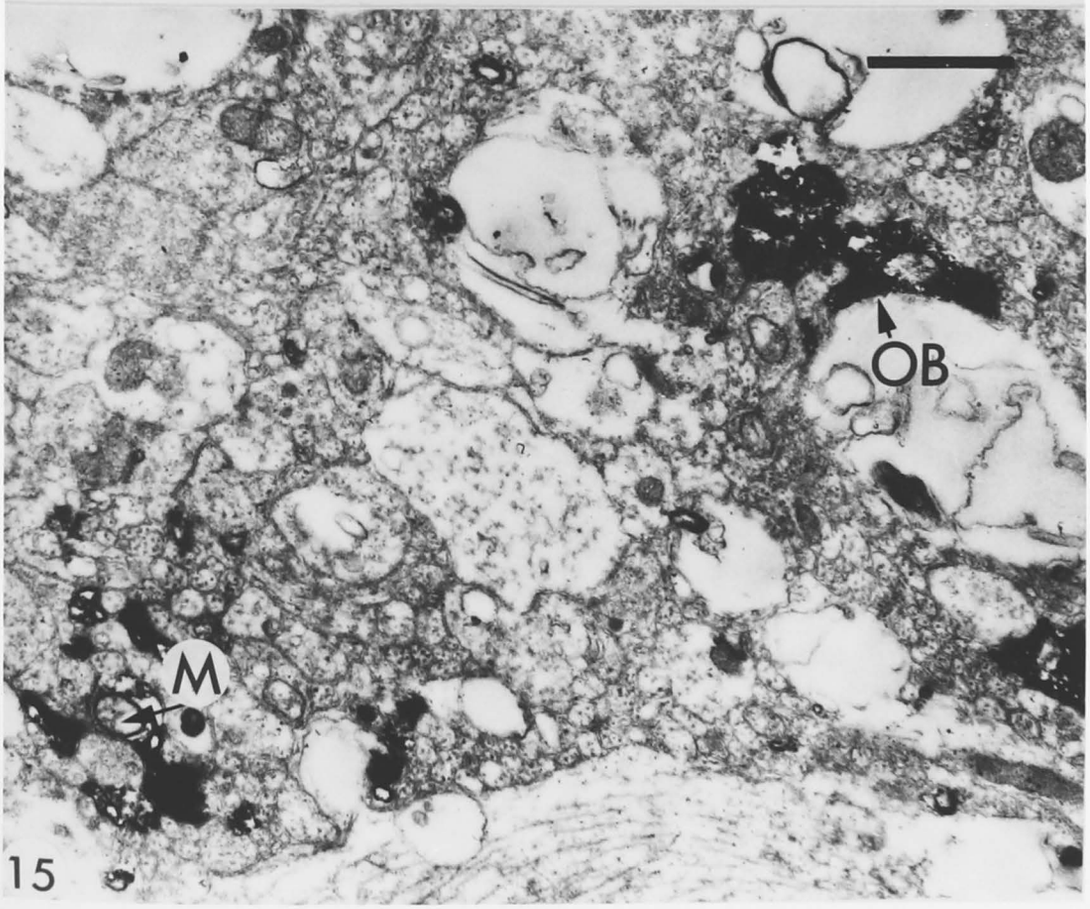

15

3.2 GOLGI STUDY

The cell sizes in the axolotl tectum did not vary much in size, ranging from about 15-30μm in diameter. The cells were usually pear-shaped, their height being greater than their width. The cells occurring in the outer plexiform layer were usually slightly smaller and rounder (see Table 2). Nearly all cells that were stained well enough to study lay in the outermost part of the cellular layer (CL1).

The cell types as categorised in this study will now be described in detail.

Radial, widely branching cells (RW) (Figs. 16 - 19, 22)

The majority of cells stained were of this type. Of the 23 cells of this kind studied quantitatively, 19 occurred in layer CL1, 3 slightly lower in CL2 and 1 in the deeper part of the cellular layer CL3. They were radially-oriented. One apical dendrite left the dorsal side of the cell body, it branched in the innermost part of the outer plexiform layer (PL3). Most of the branches coursed at an angle towards the dorsal surface of the tectum. The widest part of the dendritic tree was generally just below the optic layer in PL2 where many of the branches appeared to terminate. Some branches continued into the optic layer where a fairly wide dendritic tree was maintained. It is possible that the width of the dendritic tree was underestimated in the optic layer (PL1) due to incomplete staining or inability to follow the processes to their termination. Many of the finer branches had a slightly beaded appearance (Figs. 16, 17, 19). The beads were 2-4μm in diameter and resembled longitudinal sections through post-synaptic elements (P1) in electron micrographs both in size and shape (cf. Fig. 51). The dendrites sometimes possessed protuberances or spines, many of which were drumstick-shaped (Figs. 16-18). A similar shape was occasionally seen in the electron microscope (Fig. 52). Fifty percent of this type of cell had basal dendrites. They had a much narrower dendritic spread than the apical ones. The dendrites and the cell bodies sometimes

CELL TYPE	METHOD	CELL BODY		DENDRITIC FEATURES					
		HT	WTH	RADIAL	BASAL	CELLULAR LAYER	PLEXIFORM LAYERS		
							PL3	PL2	PL1
WR (23)	GR GK GC	22 ± 5 (23)	17 ± 4 (23)	212 ± 70 (12)	43 ± 17 (11)	57 ± 31 (15)	81 ± 57 (18)	108 ± 62 (16)	96 ± 83 (5)
NR (8)	GR GK GC	21 ± 3 (7)	18 ± 4 (7)	230 ± 69 (8)	30 ± 3 (3)	27 ± 10 (5)	15 ± 6 (6)	14 ± 8 (4)	63 ± 54 (4)
H (4)	GK GC	21 ± 6 (4)	17 ± 4 (4)	110 ± 12 (4)	25 ± 7 (2)	25 ± 7 (2)	178 ± 81 (4)	187 ± 96 (3)	-
M (3)	GR GC	20 ± 0 (3)	20 ± 0 (3)	133 ± 42 (3)	80 ± 28 (2)	90 ± 42 (3)	107 ± 11 (3)	-	-
S (9)	GR GC	18 ± 8 (9)	16 ± 5 (9)	116 ± 70 (9)	-	-	133 ± 59 (4)	96 ± 36 (8)	116 ± 27 (5)

TABLE 2 Table showing the quantitative results on measurements of different cell types. Measurements are in µm, figures in parenthesis represent numbers studied.

FIG. 16 Camera lucida drawing of an RW cell stained using the Golgi-Kopsch method. Arrows show areas of beading.
Calibration bar = 20μm.
a, High power micrograph of beading. Calibration bar = 5μm.
b, Low power camera lucida drawing showing position of cell in the tectum; PL, plexiform layer; CL, cellular layer.
Calibration bar = 50μm.

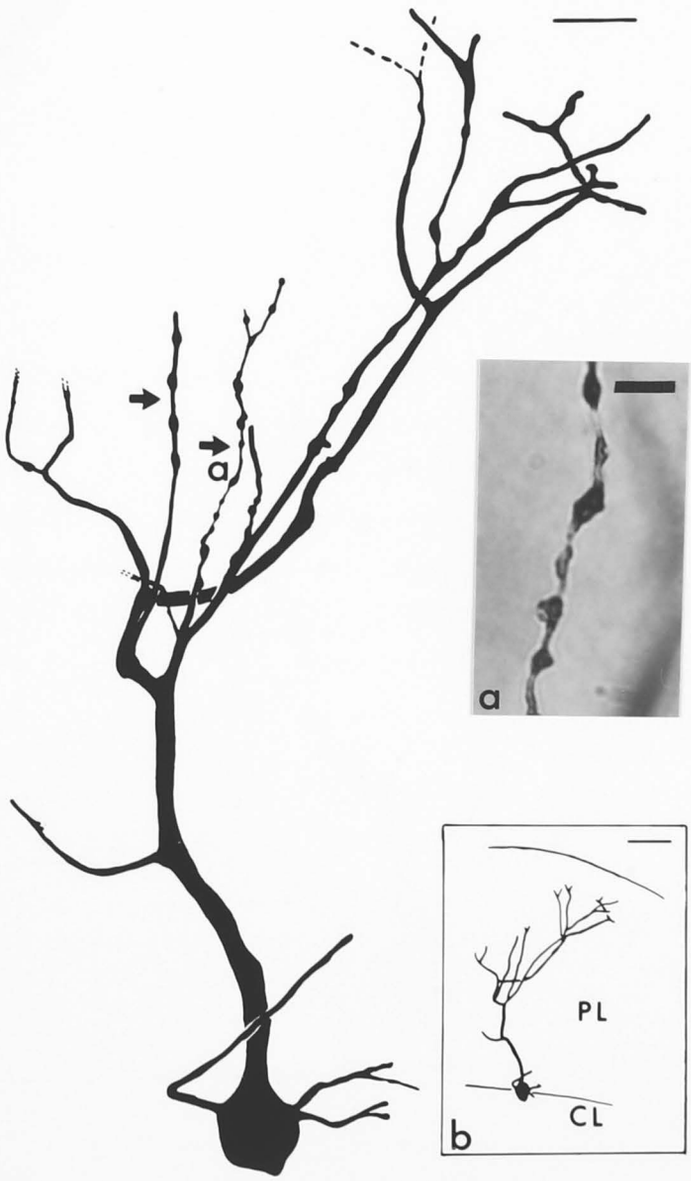
a
a
PL
CL
b

FIG. 17 Camera lucida drawing of an RW cell stained using the rapid Golgi method. Arrows, asterisk and arrowhead show beads, spines and possible axon respectively. Calibration bar = 20µm. a, High power micrograph of beading. Calibration bar = 5µm. b, Low power camera lucida drawing showing position of cell in the tectum; PL, plexiform layer; CL, cellular layer. Calibration bar = 50µm.

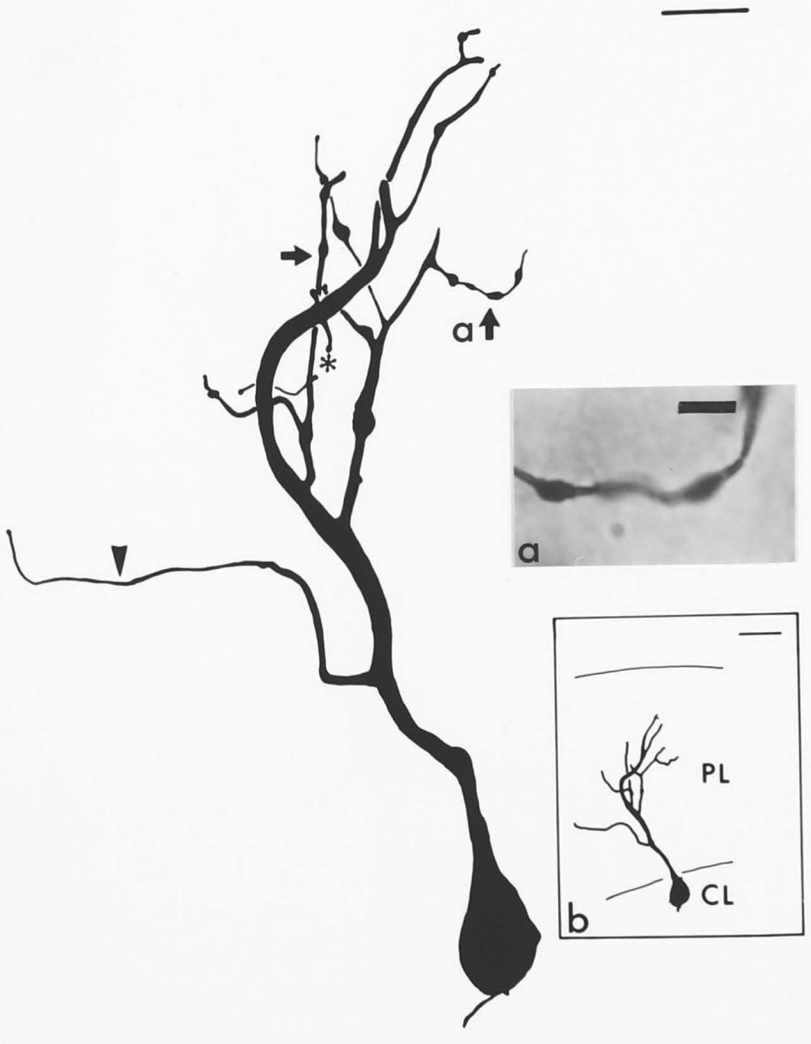
a
a
PL
CL
b

FIG. 18 Camera lucida drawing of an RW cell stained using the rapid Golgi method. Asterisk show spines. Calibration bar = 20μm. a, Low power camera lucida drawing showing position of cell in the tectum; PL, plexiform layer; CL, cellular layer. Calibration bar = 50μm.

apid
20µm.
cell

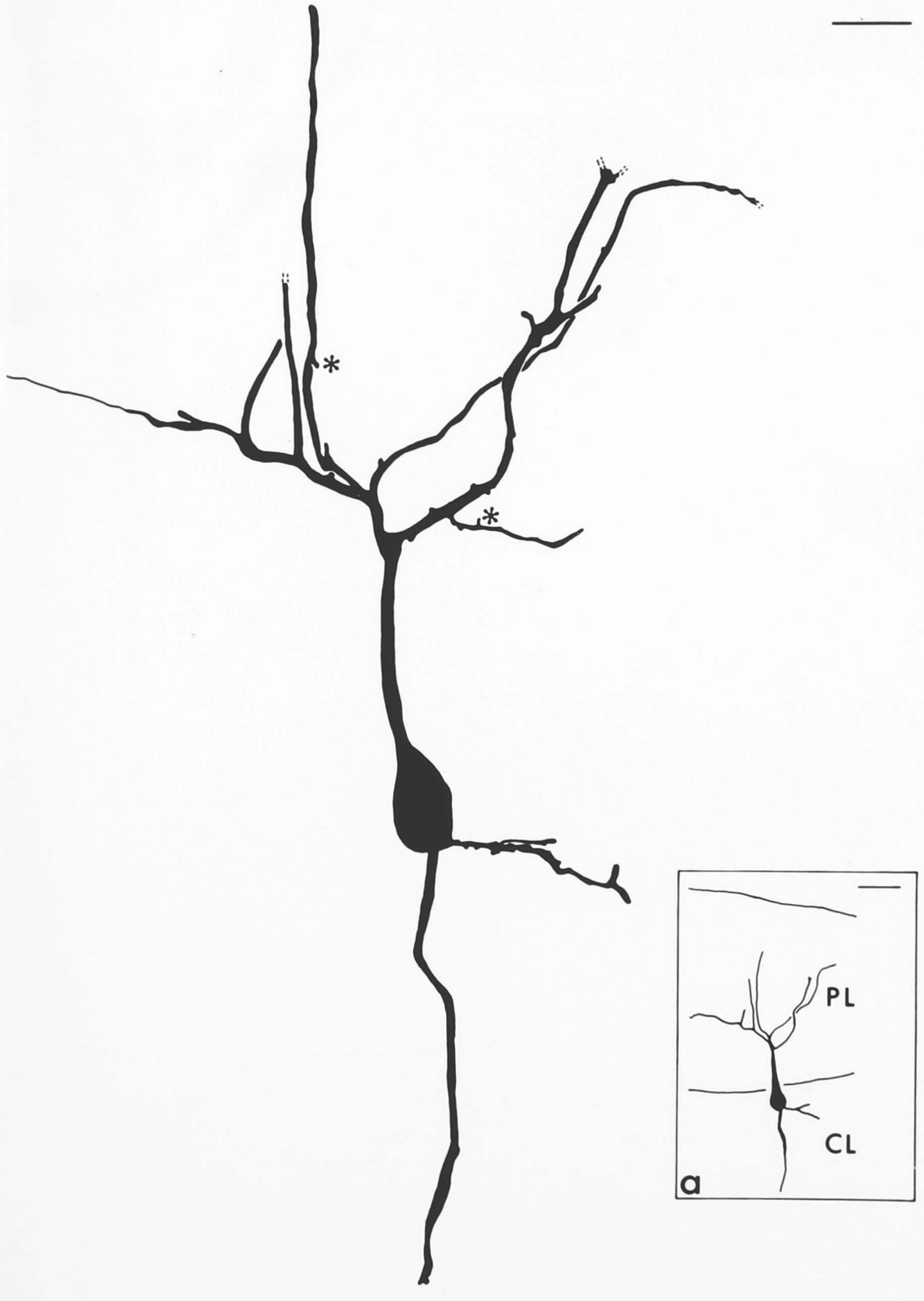

FIG. 19 Micrograph of an RW cell stained using the Golgi-Kopsch method. Arrows show areas of beading. Calibration bar = 20µm.
a, High power micrograph of beading. Calibration bar = 5µm.
b, Low power camera lucida drawing showing position of cell in the tectum; PL, plexiform layer; CL, cellular layer. Calibration bar = 50µm.

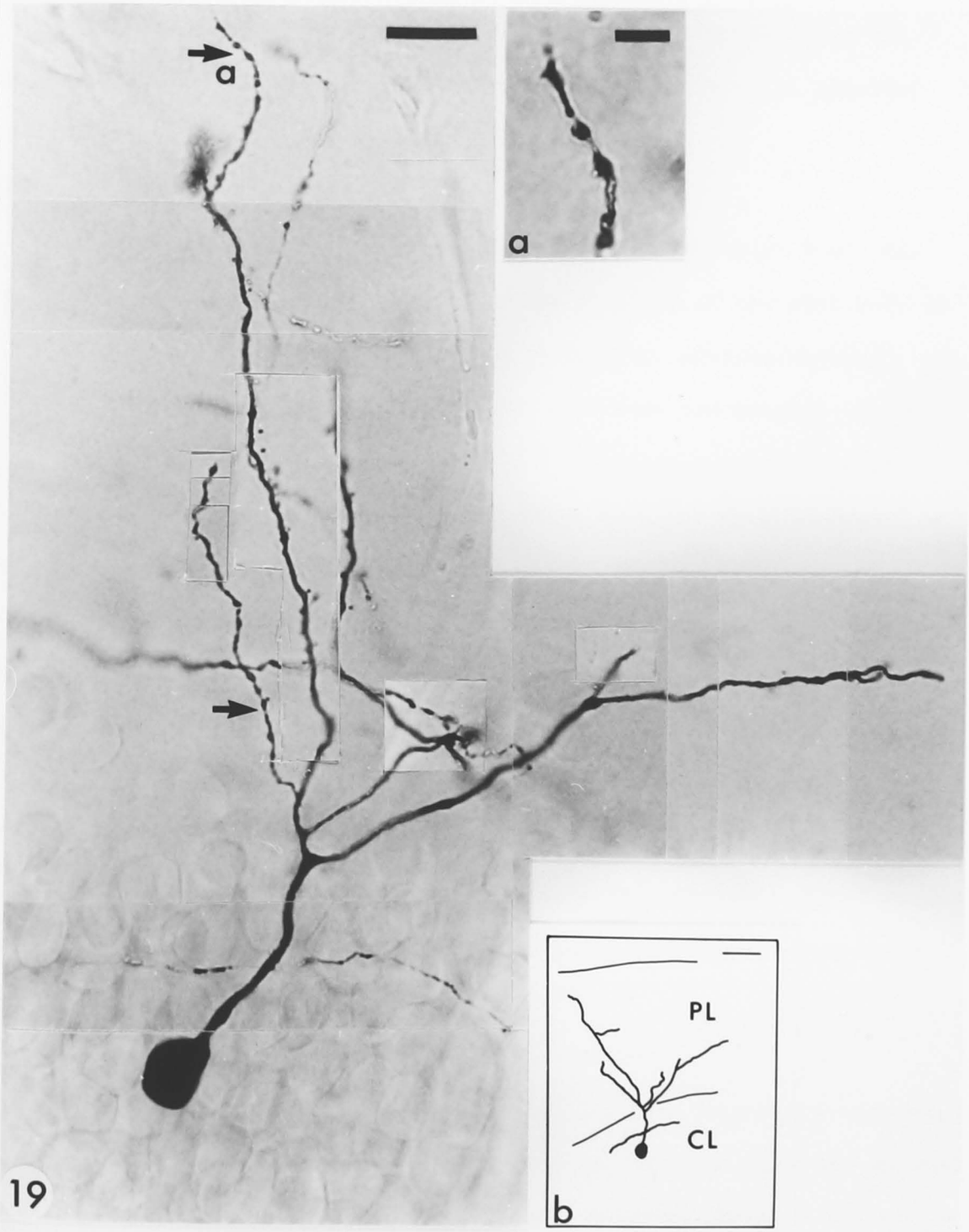
a
a
PL
CL
b
19

bore spines and beads. If axons were present they were difficult to recognise (Fig. 17) and could not be followed more than about 50µm. It is possible that they continued on adjacent sections and were not recognised as such. Terminal arborisations of these axons were never observed. Nine of the cells possibly had axons, they emerged from the cell body or the apical dendrite in layer PL3. One of the cells sent a process from the ventral surface of the cell body into the cellular layers (i.e. bipolar). It did not branch in the lower layers (Fig. 18).

Radial, narrow dendritic tree (RN) (Figs. 20, 21)

Of the eight cells of this type studied quantitatively, 5 of them occurred in layer CL1, 2 in layer CL3 and the position of the cell body of the remaining neuron was obscured. These cells were radially-oriented; the apical dendrite left the dorsal side of the cell body and coursed towards the surface of the tectum, without any major branching until the optic neuropile. The apical dendrites were smooth or gave off small branches or drumstick-shaped spines and protuberances (Figs. 20,21). The more peripheral branches were sometimes beaded and looked similar to those described in the previous cell type (Fig. 20). Axons were difficult to identify but if present they emerged from the cell body or the apical dendrite in layer PL3, and could not be followed more than 100µm in the horizontal direction. In one cell (Fig. 21) the axon appeared to follow a similar course to the apical dendrite and remain in close contact with it. Terminal arborisations were never observed. Three of the cells had basal dendrites, whose horizontal extension was limited (Table 2).

Horizontal cells (H) (Figs. 23, 24)

All these cells occurred in layer CL1. The most completely stained dendrite profile seen branched near the cell body. The two branches coursed in opposite directions in the horizontal plane, spanning 300µm of the tectum. Tertiary branches were given off which generally took a radial course; they appeared to terminate just below the optic layer. Incomplete staining and difficulty in following more peripheral branches could possibly have caused

FIG. 20 Camera lucida drawing of an RN cell stained using the rapid Golgi method. Arrows and arrowhead show beading and possible axon respectively. Calibration bar = 20μm.
a, High power micrograph of beading. Calibration bar = 5μm.
b, Low power camera lucida drawing showing position of cell in the tectum; PL, plexiform layer; CL, cellular layer. Calibration bar = 50μm.


a
a
PL
CL
b

FIG. 21 Micrograph of an RN cell stained with the rapid Golgi method. Asterisk and arrowheads show spines and possible axon respectively. Calibration bar = 20μm. a, High power micrograph of cell body region and spine (asterisk). Calibration bar = 5μm. b, Low power camera lucida drawing showing position of cell in the tectum; PL, plexiform layer; CL, cellular layer. Calibration bar = 50μm.

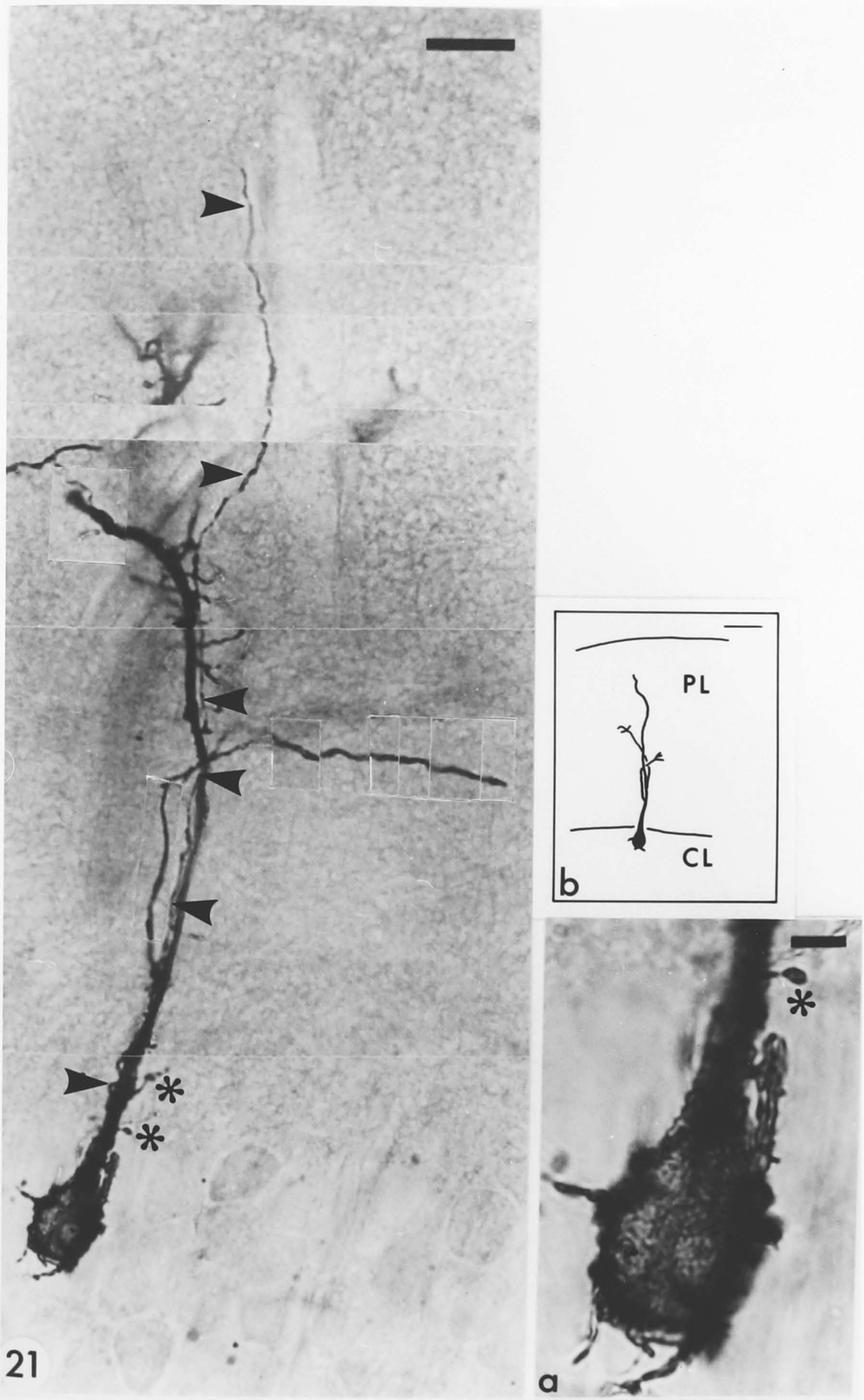
PL
CL
b
a
21

FIG. 22 Camera lucida drawing of an RW cell stained with the rapid Golgi method. Arrow, asterisk and arrowhead show beading, spines and possible axon respectively. Calibration bar = 20µm.
a, High power micrograph of a spine. Calibration bar = 5µm.
b, Low power camera lucida drawing showing position of cell in the tectum; PL, plexiform layer; CL, cellular layer. Calibration bar = 50µm.

FIG. 23 Camera lucida drawing of an H cell stained with the Golgi-Kopsch method. Arrow and asterisk show beading and spines respectively. Calibration bar = 20µm.
a, Low power camera lucida drawing showing position of cell in the tectum; PL, plexiform layer; CL, cellular layer. Calibration bar = 50µm.

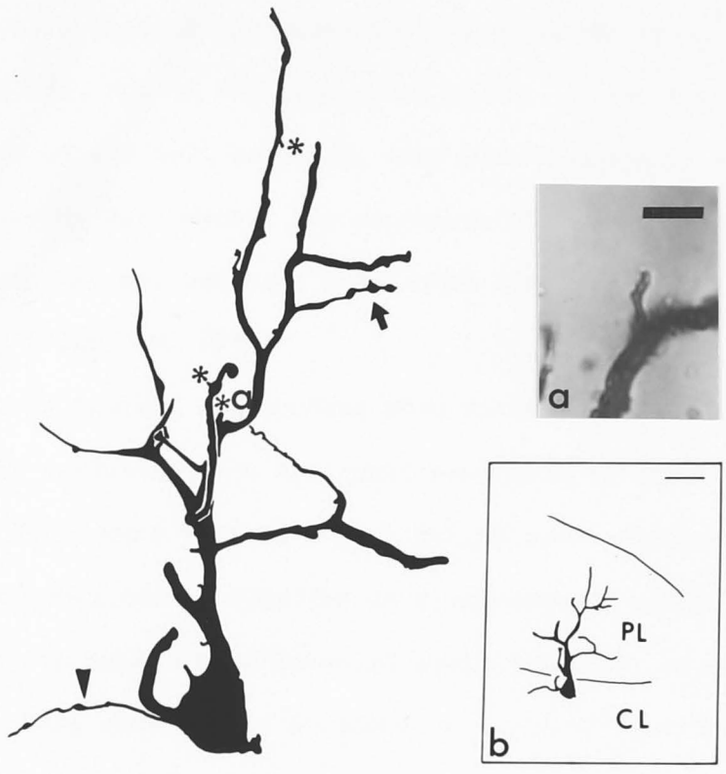

(22)

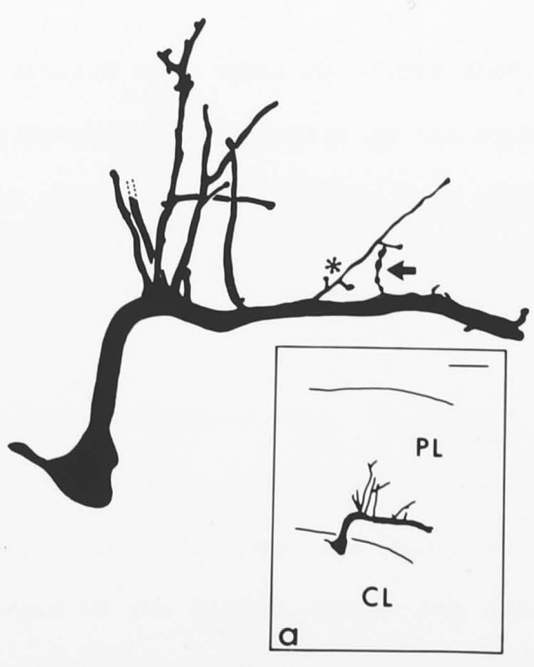

(23)

an underestimation of the radial extension of the dendrites. Nothing resembling an axon was observed on this type of cell.

Multipolar cells (M) (Fig. 25)

Three of the cells stained and examined were situated in layer CL1. They could not be put into any of the categories above. Dendrites emerged from more than 2 sides of the cell body i.e. they were multipolar and not oriented in any particular direction. The processes stretched a similar distance in all directions, for not more than 100μm (see Table 2).

Superficial cells (S) (Figs. 26, 27)

Nine of the cells stained and studied were situated in the outer plexiform layer. They occurred below the optic neuropile in layer PL2 or the PL2/PL3 border. There were various shapes encountered, consequently these cells should probably not be regarded as a homogeneous group. It was not feasible, however, to make a more detailed classification, as so few of them were collected. They were either oriented in a radial direction, a horizontal direction, or no particular direction (Fig. 26). They usually sent processes into optic (PL1) and non-optic (PL2, PL3) layers, but never into the cellular layers. The Golgi-Cox technique appeared to stain these cells most reliably (7 out of the 9). Processes resembling axons were not observed. The cell body and dendrites sometimes had spines.

The features of the various cell types described above are reflected in Table 2, showing the quantitative measurements of the various parameters. No attempt was made to judge the extension of cells in a rostro-caudal direction as few sagittal sections were cut.

Glial cells (Fig. 28)

Glial cells stained with all methods used. Ependymal glial cells were most frequently stained (Fig. 28). They lined the ventral surface of the tectum bordering the ventricle. They sent long branched feathery processes to the dorsal surface of the tectum, where they ended in club-

FIG. 24 Micrograph of an H cell stained with the Golgi-Kopsch method. Arrow and asterisk show beading and spines respectively. Calibration bar = 20µm. a, High power micrograph of beading. Calibration bar = 5µm. b, Low power camera lucida drawing showing position of cell in the tectum; PL, plexiform layer; CL, cellular layer. Calibration bar = 50µm.

FIG. 25 Micrograph of an M cell stained with the rapid Golgi method. Asterisk show spines. Calibration bar = 20µm.
c, Low power camera lucida drawing showing position of cell in the tectum; PL, plexiform layer; CL, cellular layer. Calibration bar = 50µm.

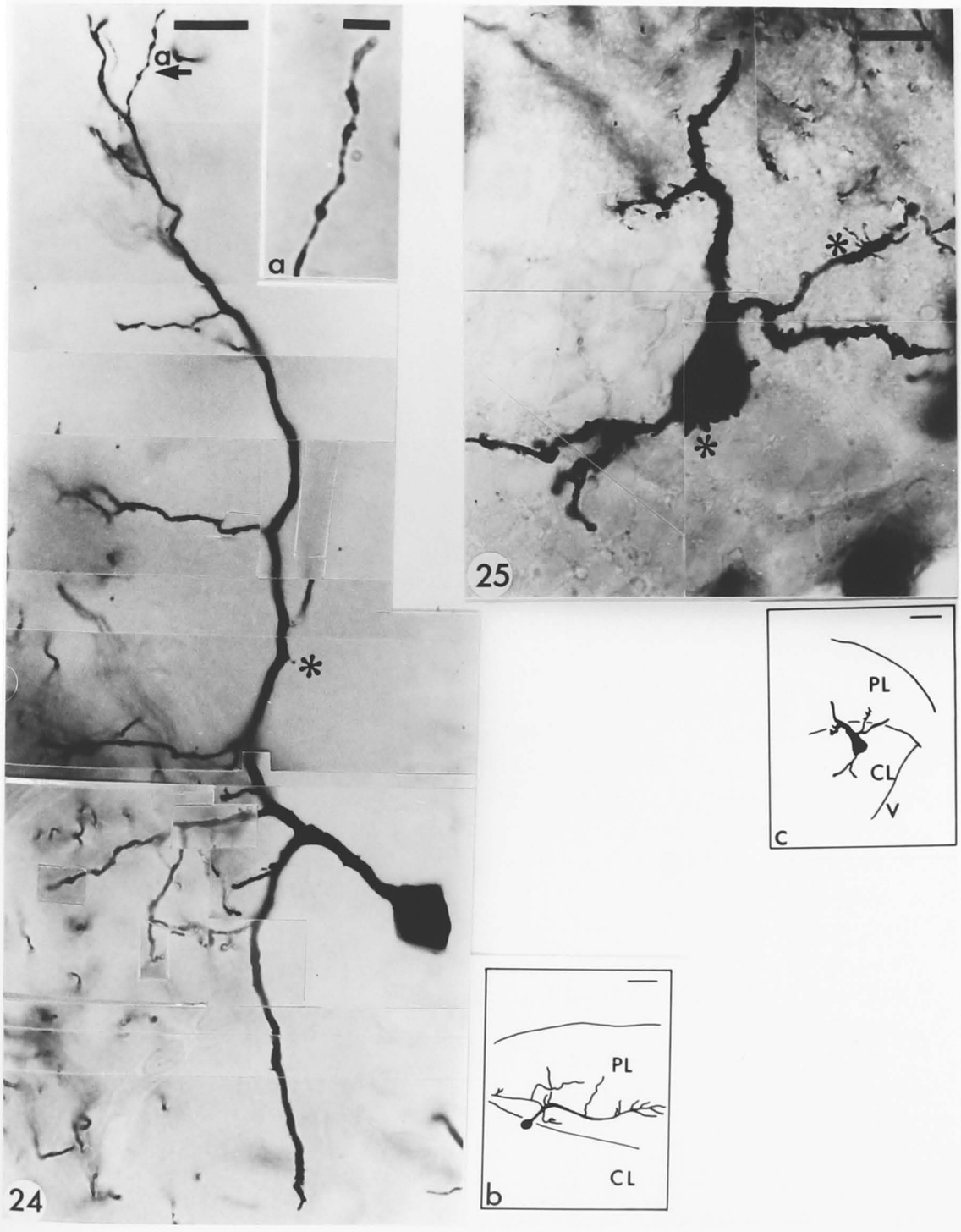
a
a
25
PL
CL
V
c
24
PL
CL
b

FIG. 26 Camera lucida drawings of cells occurring in the outer plexiform layer stained with the Golgi-Cox method. Calibration bar = 20µm.
a, b, c, Low power camera lucida drawings showing position of cells in the tectum; PL, plexiform layer; CL, cellular layer.
Calibration bars = 50µm.

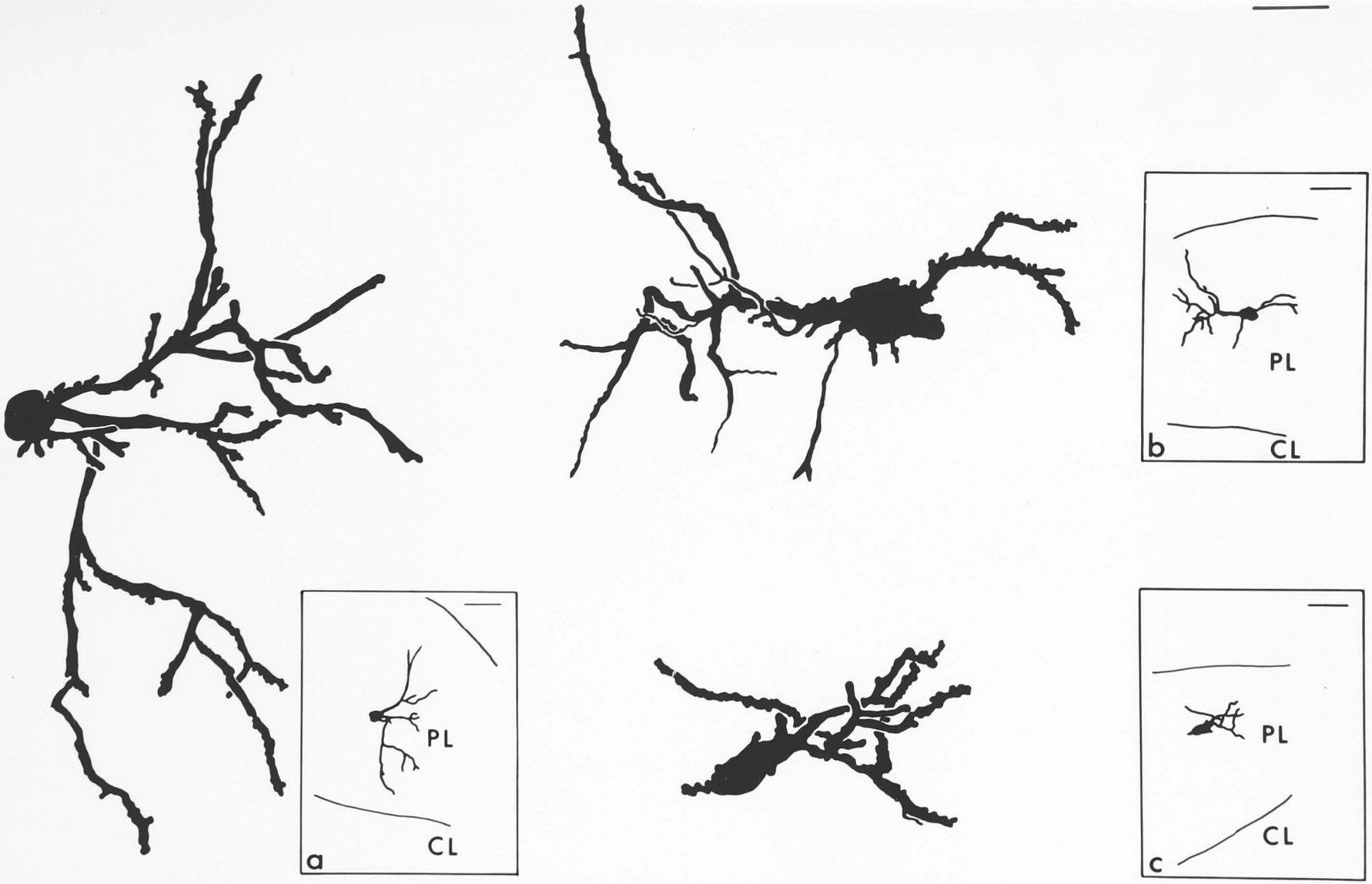
PL
CL
a
PL
CL
b
PL
CL
c

FIG. 27 Micrograph showing a cell stained in the outer plexiform layer, using the Golgi-Cox method. Calibration bar = 20µm. a, Low power camera lucida drawing showing position of cell in the tectum. Calibration bar = 50µm.

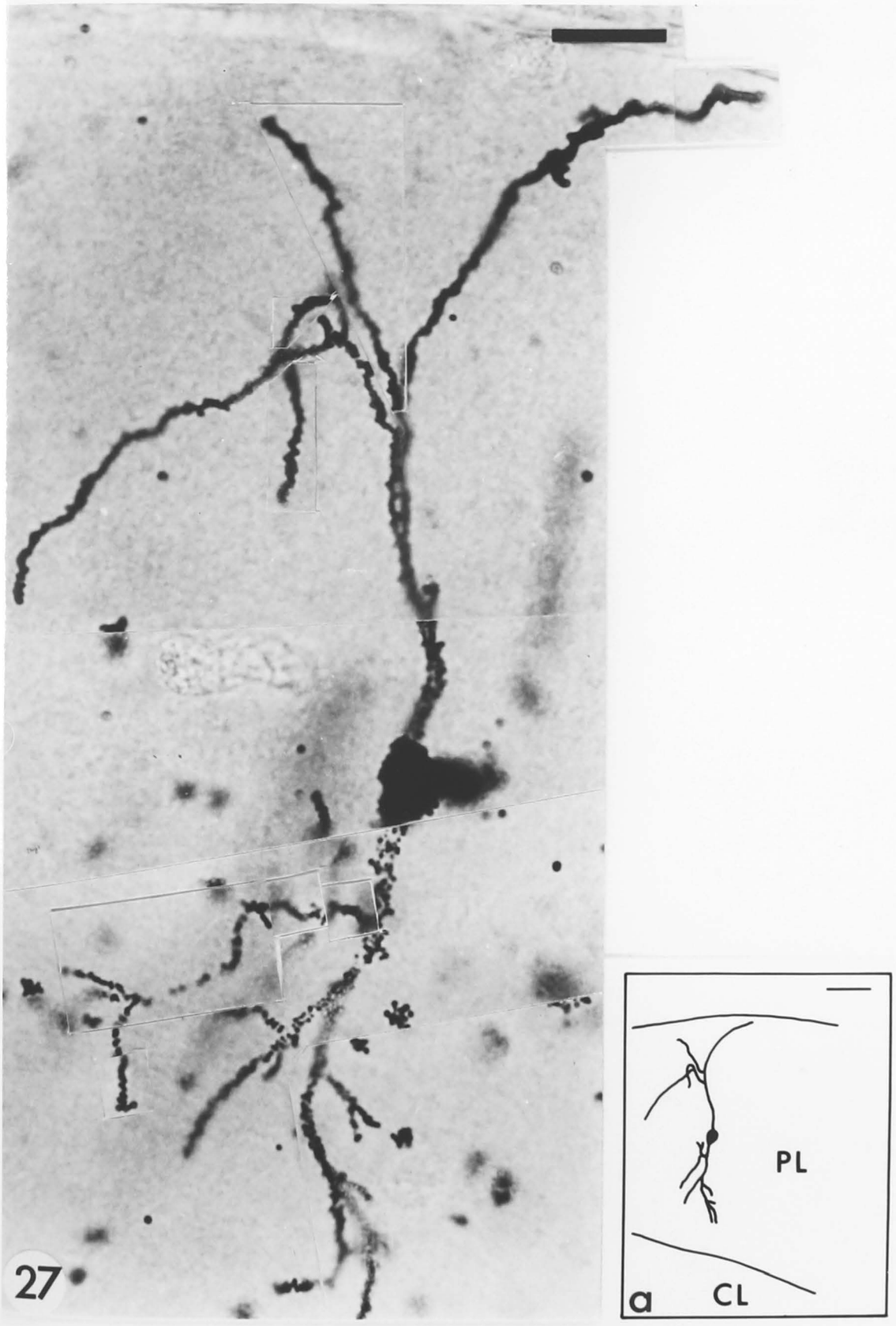
27
PL
a
CL

FIG. 28 Micrograph showing a glial cell stained using the rapid Golgi method. CL, cellular layer; PL, plexiform layer; V, ventricle. Arrows show feathery processes. Calibration bar = 20μm.

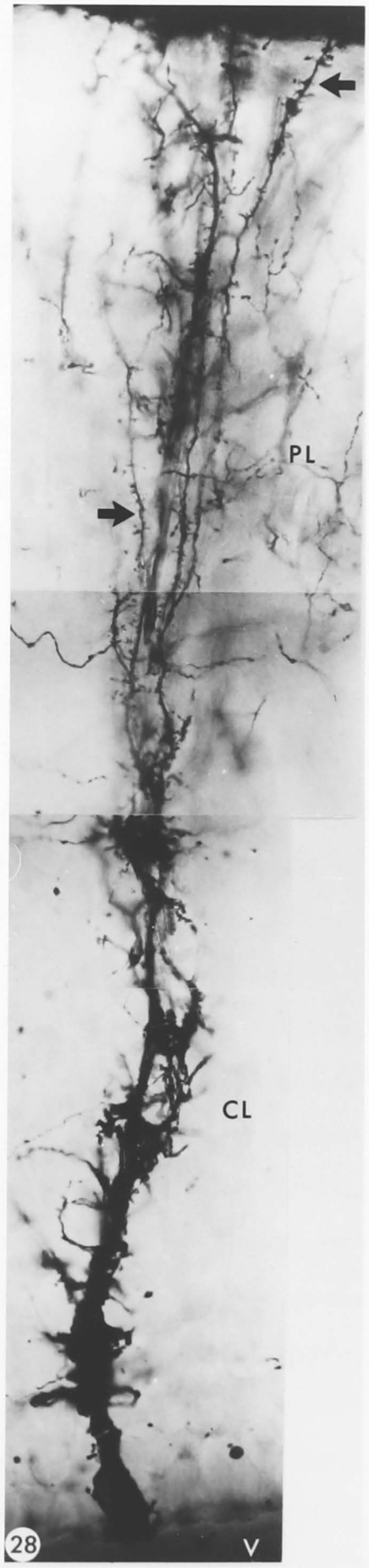
PL
CL
28
V

like swellings. They resembled structures seen under the electron microscope. Other types of glial cells were occasionally observed in the outer plexiform layers. A mass of processes emerged from the cell body, spreading for a short distance in all directions.

Axons

The terminal arbors of axons were not studied. When incoming axons were stained it was generally impossible to trace them to any extent.

3.3 IDENTIFICATION OF OPTIC SYNAPSES BY DEGENERATION AND HRP TECHNIQUES

In normal preparations of axolotl tectum there was always a population of mitochondria which had a lighter matrix than others; they occurred in the superficial 150μm of the tectum, found to receive a retinal projection in this study and previously by autoradiography (Guillery and Updyke, 1976). These pale mitochondria were found in irregularly shaped boutonal elements which had round synaptic vesicles scattered throughout the terminal (Fig. 29a). They were similar to those of retinal origin in the frog optic tectum (Székely *et al*, 1973; Székely and Lázár, 1976). There was no apparent difference in the optic neuropile of animals fixed by perfusion and those fixed by immersion.

The largest amounts of degeneration products could be seen four days after eye removal. Most of the degenerating material appeared as dense bodies in glial cells. Only a very small number of degenerating synaptic boutons, showing a dark reaction of the cytoplasm, were observed (Figs. 36, 37). Earlier stages of degeneration involving vesicle enlargement and boutonal swelling could not be found, although occasionally synapses with synaptic vesicles sequestered within a membrane, as well as membrane-bound dense bodies, were seen (Figs. 38-41). In the animal whose eyes had been removed 4 days before perfusion, the number of presynaptic elements with light mitochondria was about 15% of the number seen in normal animals (Fig. 43). In the animal perfused 14 days after eye removal 99% of the presynaptic

FIG. 29 Survey electron micrographs of the optic neuropile in the axolotl tectum. a, normal animal. b, axolotl whose optic nerve has been filled with horseradish peroxidase. Mitochondria with an electron-lucent matrix are seen in presynaptic (asterisk) and axonal (arrow) elements in a and b. In b they are found in neuronal elements filled with the electron-dense reaction product of horseradish peroxidase.

Calibration bar = 1μm.

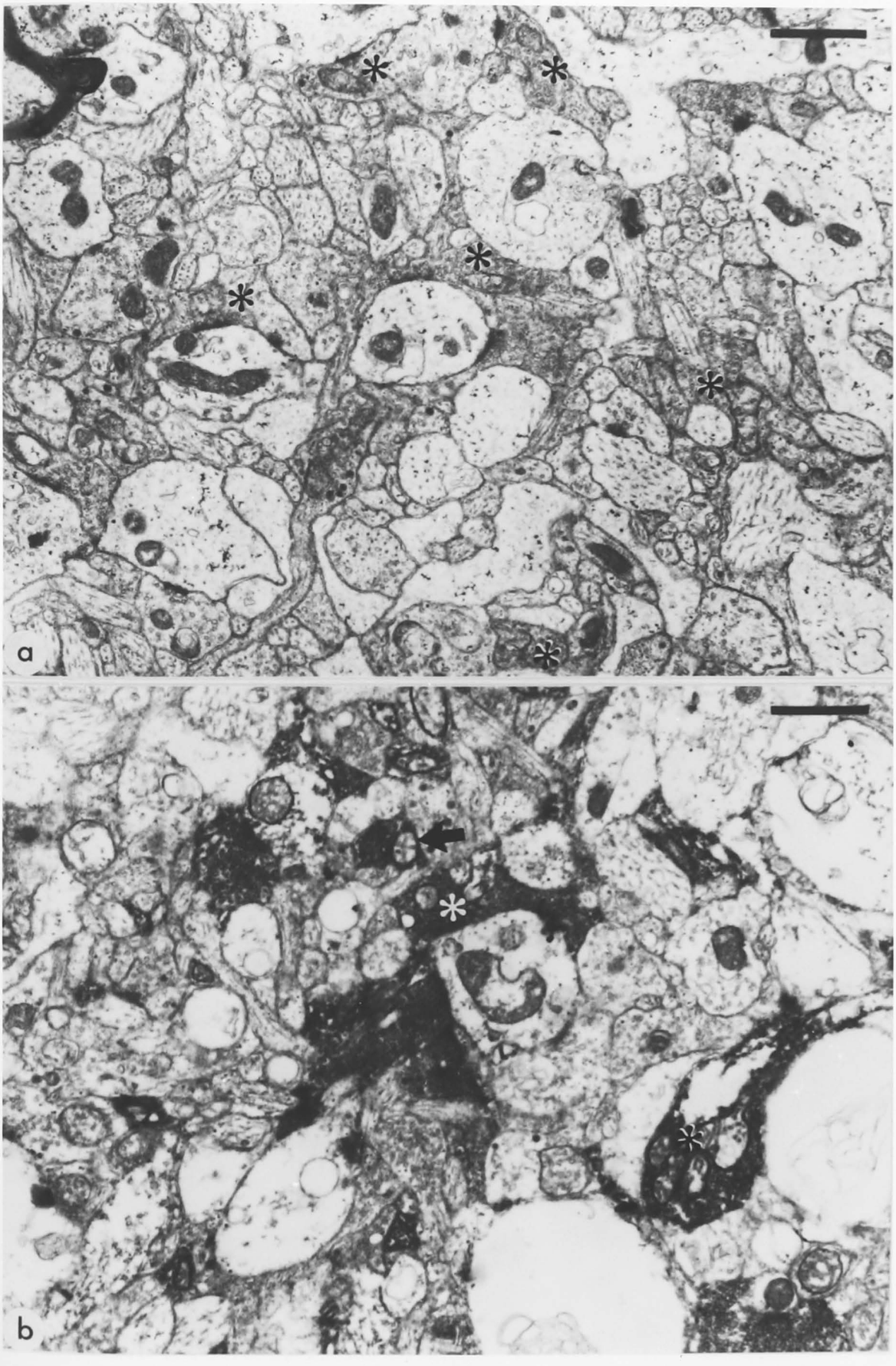
a
b

FIG. 30 Survey electron micrograph of the optic neuropile in the tectum of an axolotl which had both eyes removed 56 days before perfusion. All mitochondria have an electron-dense matrix.
Calibration bar = 1µm.

FIG. 31 Normal optic bouton with pale mitochondrion (M), vacuole (Va), synaptic vesicles (SV), and microtubules (t). It contacts a small postsynaptic element (Ps) and a postsynaptic element (Pl) with a dark mitochondrion (Md). Both contacts are Gray type I (arrows).
Calibration bar = 0.2µm.

FIG. 32 Horseradish peroxidase filled optic bouton with synaptic vesicles (SV), pale mitochondrion (M), synaptic vesicles (SV), and synaptic apposition (SA) contacting a postsynaptic element (Pl'). The cytoplasm shows an electron-dense reaction.
Calibration bar = 0.2µm.

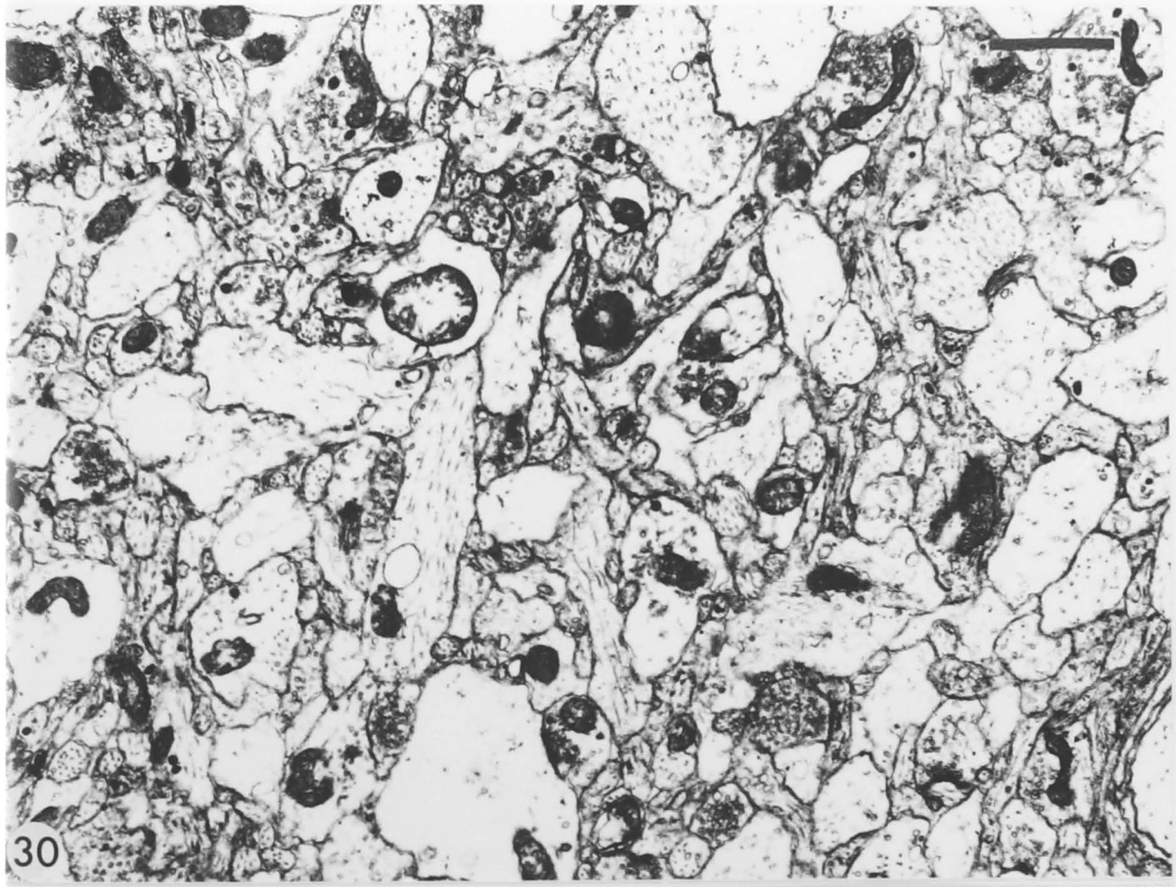

30

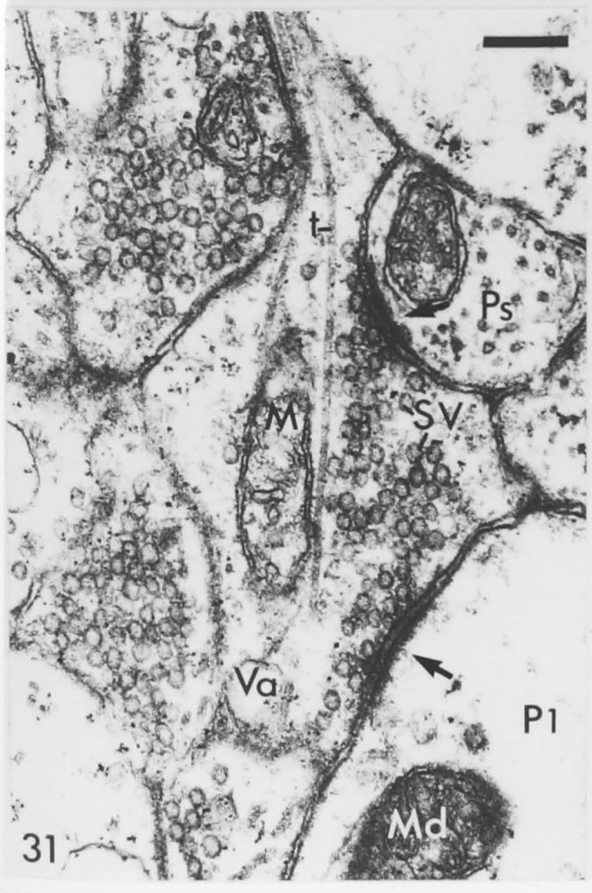

31

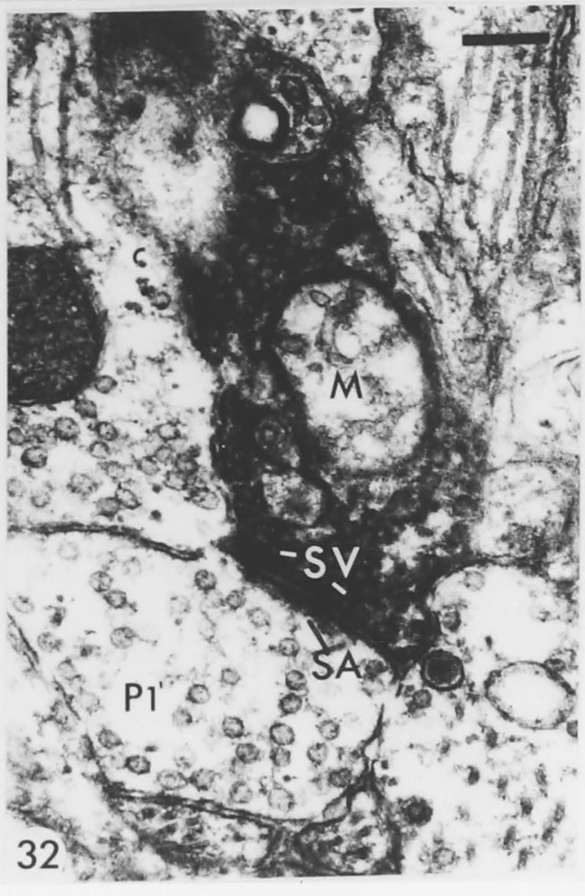

32

FIG. 33 Normal optic bouton with pale mitochondrion (M), vacuole (Va), synaptic vesicles (SV), dense-core vesicle (dcv), and microtubules (t). It contacts a small postsynaptic element (Ps) with a Gray type I synaptic apposition (SA) with a prominent postsynaptic density (psd).
Calibration bar = 0.2µm.

FIG. 34 Normal optic bouton showing a Gray type II (two arrows) as well as a slightly obliquely cut Gray type I (one arrow) synaptic apposition. M, mitochondrion.
Calibration bar = 0.2µm.

FIG. 35 Horseradish peroxidase filled optic bouton contacting small postsynaptic element (Ps). Pale mitochondrion (M), synaptic vesicles (SV) and synaptic apposition (SA) are clearly visible.
Calibration bar = 0.2µm.

FIGS. 36, 37 Degenerating optic boutons in contralateral optic tectum four days after both eyes were removed. Mitochondria (M), synaptic appositions (arrows), and slightly swollen synaptic vesicles (SV) are visible. The cytoplasm shows an electron-dense reaction.
Calibration bar = 0.2µm.

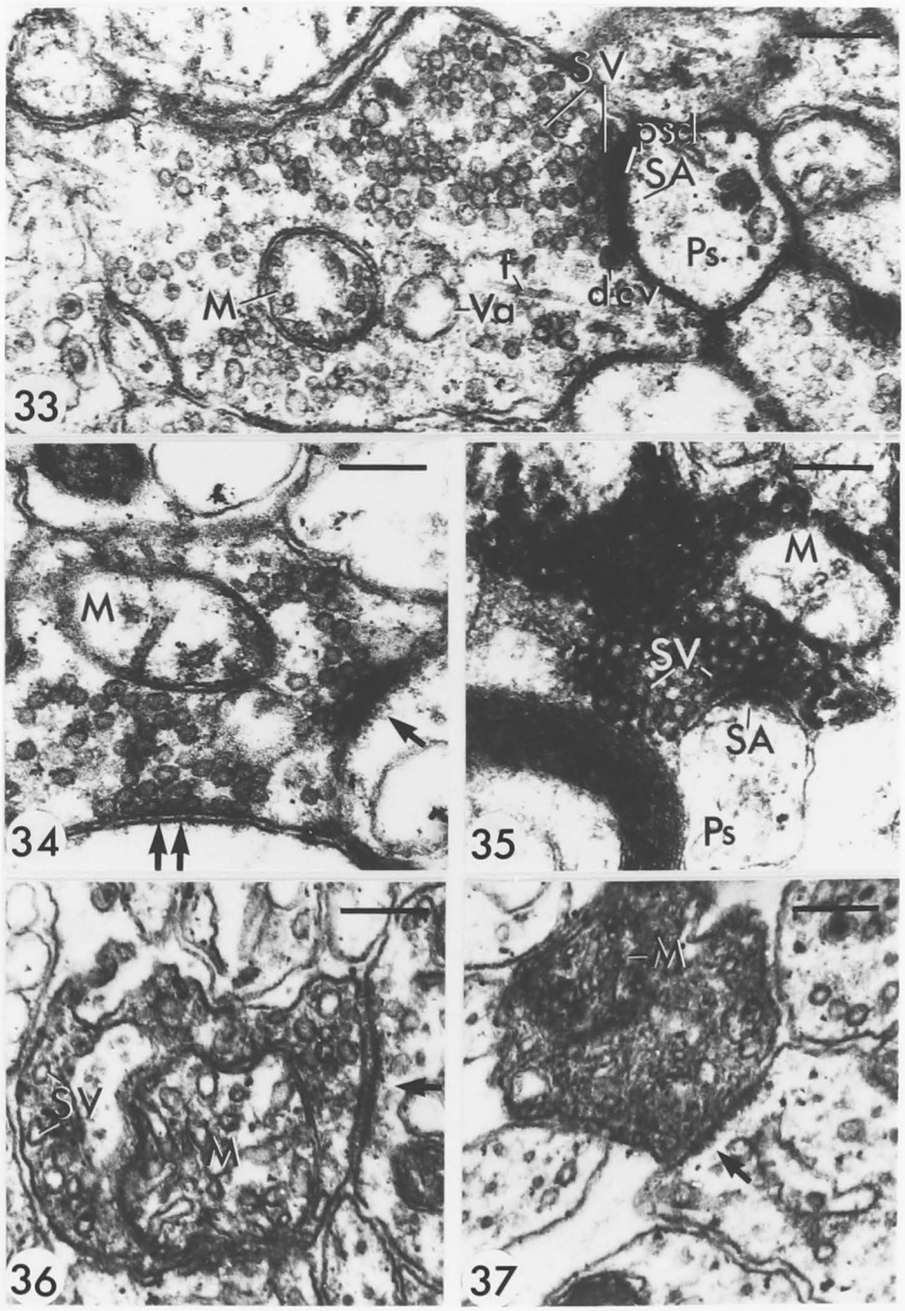
SV
psd
SA
Ps
M
Va
dcv
33
M
34
M
SV
SA
Ps
35
SV
M
36
M
37

FIGS. 38-42 Possible stages in the degeneration of optic boutons. All these stages could be found in the tectum of animals three or four days after both eyes were removed. Calibration bar = 0.2µm.

FIG. 38 Bouton containing synaptic vesicles sequestered within a membrane (asterisk).

FIG. 39 Bouton containing: synaptic vesicles sequestered within a membrane (asterisk); a membrane-bound electron-dense body (DB); and a synaptic apposition (arrow).

FIGS. 40, 41 Boutons containing a membrane-bound electron-dense body (DB), synaptic appositions (arrows) and mitochondria (M).

FIG. 42 Glial cell containing degenerating debris in membrane-bound dense bodies (DB).

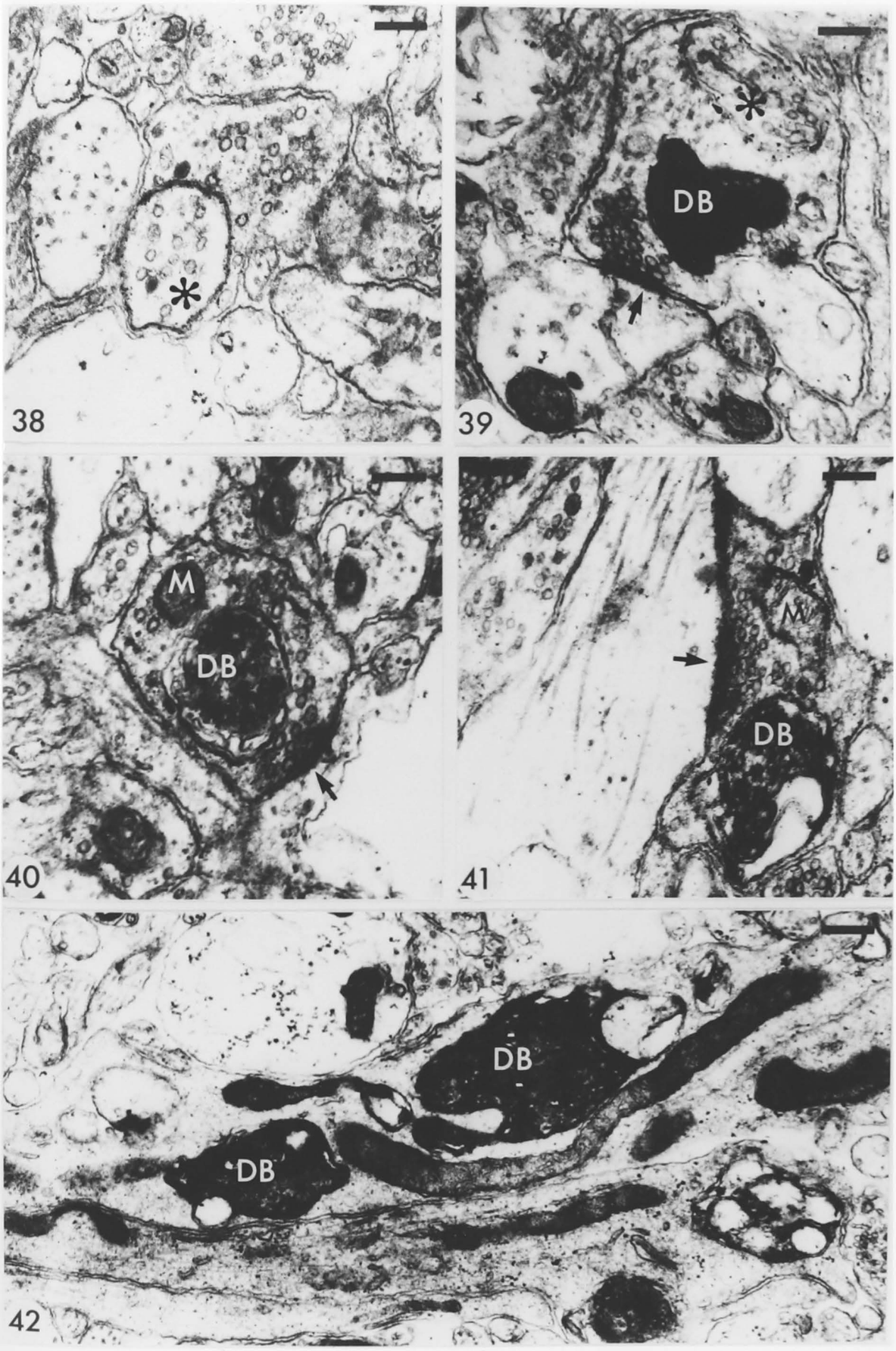
38
39
DB
40
M
DB
41
M
DB
42
DB
DB

FIG. 43 a, Graph showing the number of normal optic boutons in the optic neuropile against the number of days after eye removal. b, The comparison of the percentage of presynaptic elements with dark (D) and light (L) mitochondria in the optic neuropile of a normal (N), an HRP filled, and an axolotl whose eyes were removed 56 days before perfusion (ER). Shading shows the percentage filled with reaction product.

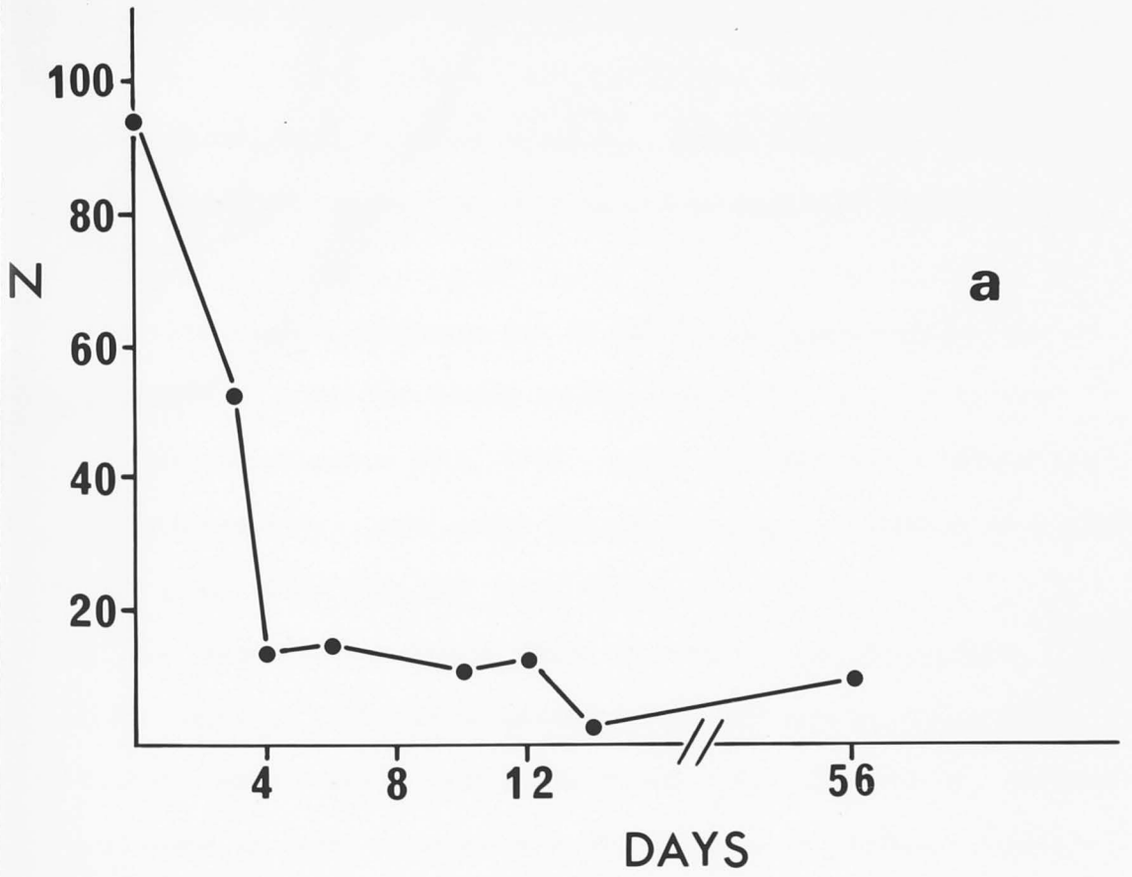
100
80
60
40
20
N
a
4
8
12
56
DAYS

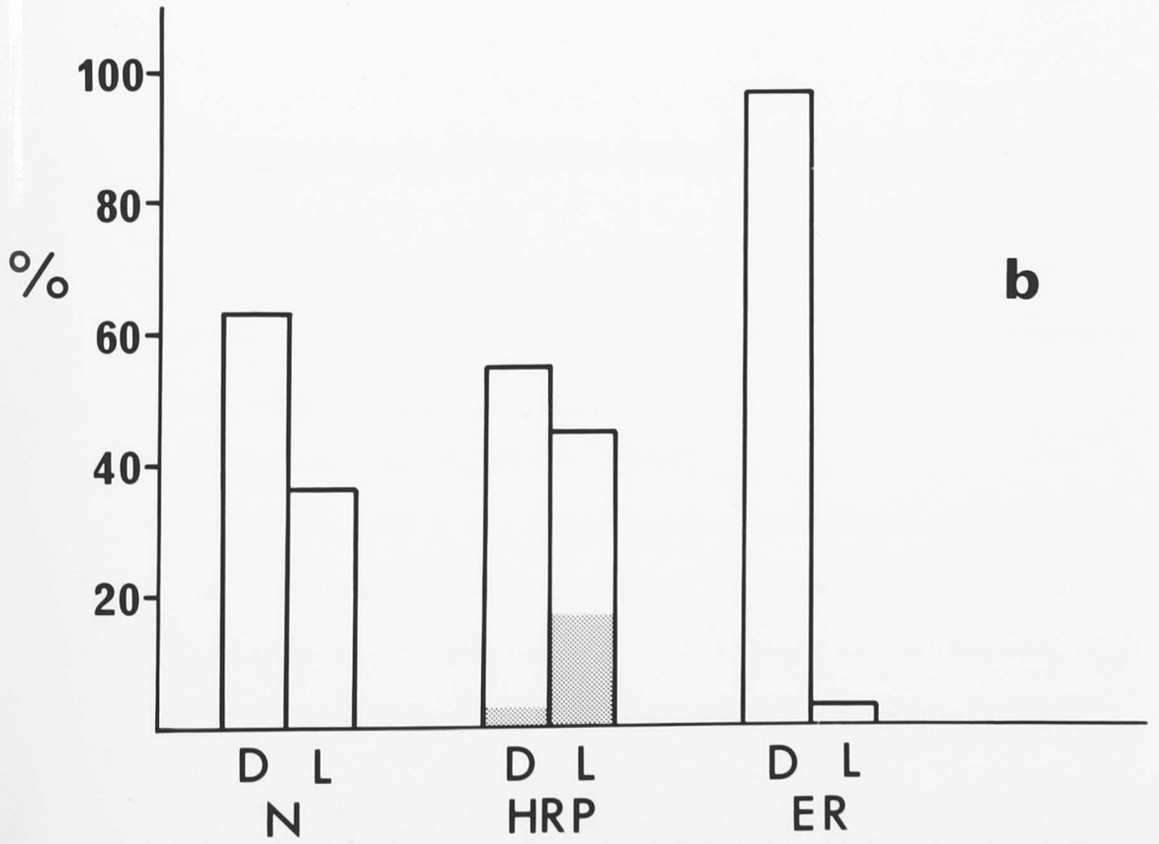
100
80
60
40
20
%
b
D L
N
D L
HRP
D L
ER

boutons had dark mitochondria (Fig. 43). Some neuronal elements which look similar to those assumed to be optic were found ventral to the optic neuropile. Care was therefore taken not to stray into this area during sampling.

In the normal axolotl optic neuropile, about 35% of the presynaptic elements with mitochondria had one that showed an electron-lucent matrix (Fig. 43b).

In the HRP-filled specimens 84% of the filled optic boutons had mitochondria with an electron-lucent matrix, 16% of the boutons having moderately dark mitochnodria (Fig. 43b). Light mitochondria occurred in unfilled structures also. Just under 50% of presynaptic elements with pale mitochondria were filled with HRP (Fig. 43b).

The fact that HRP was rarely found in boutons containing dark mitochondria, together with the observation that the number of boutons containing light mitochondria fell dramatically after eye removal, suggests that the presence of light mitochondria is a diagnostic feature of optic boutons in the axolotl optic tectal neuropile, with only a low probability of error.

3.4 MORPHOMETRIC ANALYSIS OF IDENTIFIED OPTIC BOUTONS AND ASSOCIATED STRUCTURES

The various parameters investigated will be considered in turn. Only those boutons with a light mitochondria and transversely cut synaptic appositions were taken.

Optic Boutons (Figs. 31, 33, 34, 48-50, 53-56)

Diameters ranged from 0.3 - 1.6μm, with a peak between 0.5 and 0.7μm (Fig. 44a). The mean diameter of the boutonal profiles ($\bar{d}$) was 0.72μm; however, the mean diameter of the boutons ($\bar{D}$ = 1.08μm) can be derived from the individual diameters of boutonal profiles with the formula given by

Fullman (see Williams, 1977). This is $\bar{D} = \frac{\pi}{2} \frac{N}{\frac{1}{d_1} + \frac{1}{d_2} + \ldots \frac{1}{d_N}}$, where N = total number of diameter profiles measured and d = diameter measured for any individual profile ($d_1 \ldots d_N$). It is always larger (approximately $\frac{4}{\pi}$ times) than the mean diameter of the profiles, because in spherical structures the largest diameter is statistically less often sectioned than shorter profiles. Perimeters ranged from 1.5 - 8μm with a peak between 2.5 and 3μm (Fig. 44b). Areas ranged from 0.1 - 1.75μm^2 with a peak between 0.25 and 0.5μm^2 (Fig. 44c).

Mitochondria (Figs. 31, 33, 34, 48-50, 53-56)

A section through an optic bouton usually only showed one mitochondrion, although up to 3 have been observed. Their diameters ranged from 0.05 - 0.4μm with a peak between 0.1 and 0.2μm (Fig. 44d). The areas of the mitochondria in relation to those of the boutons ranged from 2% - 50% with a peak between 5% and 15% (Fig. 44e).

Dense-Core Vesicles (Figs. 33, 56)

30% of sections through optic boutons had dense-core vesicles. The number of dense-core vesicles occurring in a section through an optic bouton varied from 0 - 5 (or 0 - 17/μm^2 with a peak at 3/μm^2 - Fig. 47b). Their diameters ranged from 30 - 100nm, with a peak between 60 and 80nm (Fig. 44f).

Clear Vesicles (Fig. 33)

Diameters ranged from 25 - 83nm with a peak between 38 and 42nm (Fig. 46a). The histograms of vesicle diameters in 10 individual boutons were also constructed (Fig. 45). The shape of the curves did not vary very much, nor did the mean vesicle diameters (40-45nm). There were between 5 and 280 vesicles per μm^2 of bouton, with a peak at about 120-140. Subtracting the mitochondrial area shifted the range to between 6 and 320 vesicles with a peak at 140-160 per μm^2 of boutonal cytoplasm (Fig. 46b).

Vacuoles (Fig. 33)

73% of sections through optic boutons did not show any section through a vacuole. The remaining 27% showed 1 or 2 vacuolar profiles. Multivesicular bodies were observed in 2 optic boutons (1%).

Glycogen Granules (Fig. 49)

Glycogen granules were recognised by their size (20-35nm) and dark even staining. Approximately 70% of sections through optic boutons had glycogen granules; there were usually under 10 although occasionally as many as 24 were counted.

Microtubules (Fig. 33)

Approximately 50% of sections through optic boutons had microtubules. Their numbers usually ranged from 1-13 although occasionally as many as 40 were observed. They often lay near the mitochondria.

Length of Direct Contact (synaptic apposition and unspecific membrane contact) between the Membranes of Optic Boutons and those of their Postsynaptic Elements

This ranged from 0.17µm to 2µm with a peak at 0.5µm (Fig. 46c). Sometimes the synaptic apposition was the only contact. The rest of the surface of the optic bouton was contacted by other neuronal elements or by glial processes.

Synaptic apposition (Figs. 31, 33, 34, 48-50, 53-56)

Sections through optic boutons sometimes showed 2 synaptic appositions, although often only one of them was transversely cut. Their lengths ranged from 0.05-0.7µm with a peak between 0.15 and 0.25µm (mean diameter of profiles $\bar{d}$ = 0.25µm, mean synaptic apposition diameter $\bar{D}$ = 0.33µm - cf. boutons) (Fig. 46d). The length of the synaptic appositions made up between 2 and 24% of the perimeter of the optic bouton with a wide peak between 4 and 10% (Fig. 46e).

Dense Projections (Fig. 50)

The height of the dense projections ranged from 10-70nm with a peak

between 30 and 40nm (Fig. 46f). The lengths of the bases of single projections (or width) ranged from 10-90nm with a peak between 40 and 50nm (Fig. 47a).

Synaptic Cleft (Fig. 48)

Since the width of the synaptic cleft can vary in one synaptic apposition, the average width was measured. It ranged in different synaptic appositions from 6-18nm.

Postsynaptic density

The postsynaptic density thicknesses ranged from 0 to 90nm with a peak between 30 and 40nm (Fig. 47c). Thus the majority of synapses (84%) could be classified as Gray type I (Gray, 1959) or asymmetric (Colonnier, 1968) (Fig. 31,33). About 16% of the synaptic appositions showed a post-synaptic density less than 20nm thick and by the criteria of Akert (1972), they can be classified as Gray type II (Gray, 1959) or symmetric (Colonnier, 1968) (Fig. 56). Occasionally an optic bouton had a Gray type I apposition with one postsynaptic element and a Gray type II apposition with another (Fig. 34).

Postsynaptic Elements (Figs. 48-54)

Diameters ranged from less than 0.2 up to almost 2µm. Approximately 70% of them had diameters between 0.2 and 0.6µm (Fig. 47d). Optic synapses were never observed contacting cell bodies which are only rarely found in the optic neuropile. Various postsynaptic elements could be distinguished on morphological grounds.

The first type was characterised by an electron-lucent cytoplasm, dark mitochondria, and few microtubules (Fig. 48). In longitudinal section they appeared to be beaded structures (Fig. 51). The narrower portions had many microtubules. They occurred throughout the optic neuropile and at least 50% of the optic boutons contacted this type of postsynaptic element. They did not have any constant orientation and could be branches of main radial

FIG. 44 Frequency distributions of various parameters of optic boutons. a, DOB - diameters of optic boutons (Ns = 158); b, POB - perimeters of optic boutons (Ns = 158); c, AOB - areas of optic boutons (Ns = 158); d, DMi - diameters of mitochondria in optic boutons (Ns = 178); e, AMi/AOB - relationship between mitochondrial and boutonal area (Ns = 153); f, D dcv - diameters of dense-core vesicles (Ns = 86).

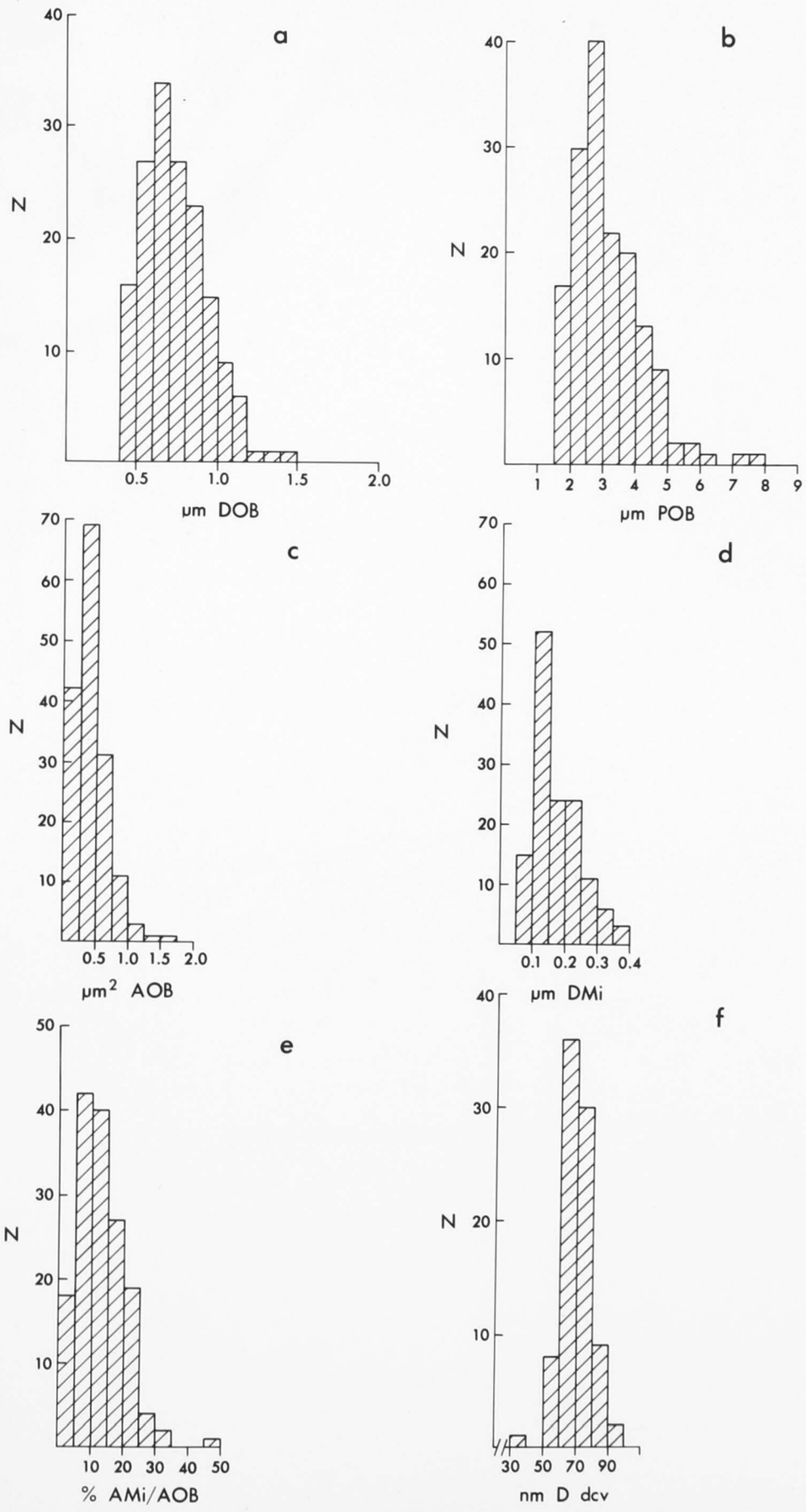
a
b
c
d
e
f
N
μm DOB
μm POB
μm² AOB
μm DMi
% AMi/AOB
nm D dcv

FIG. 45 Frequency distributions of the diameters of clear vesicles (DV) in 10 individual optic boutons.

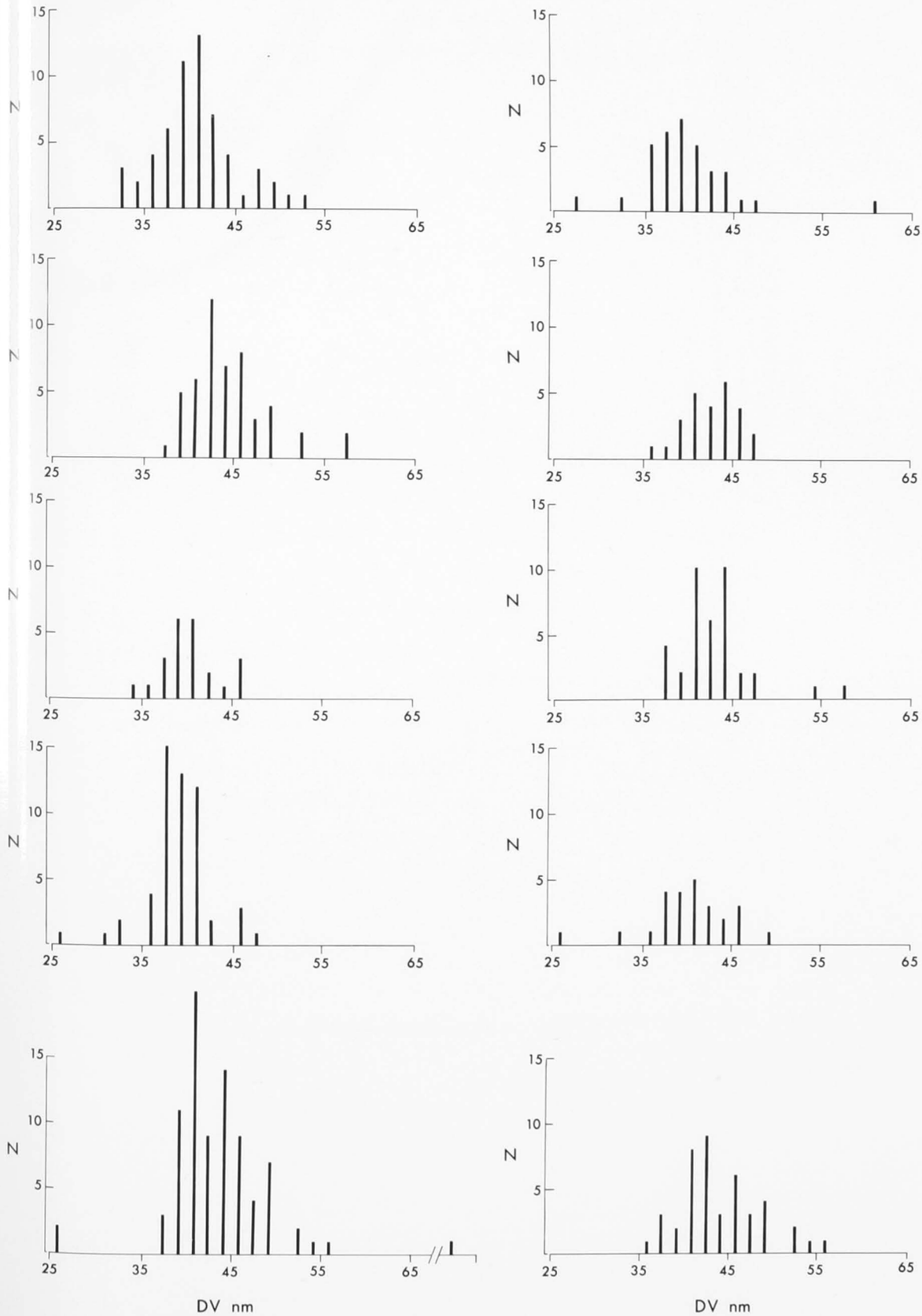
15
10
5
N
25
35
45
55
65
DV nm

FIG. 46 Frequency distributions of various parameters of optic boutons. a, DV - diameters of clear vesicles (Ns = 435); b, NV/AOB - numbers of vesicle profiles per 1μm^2 of boutonal area. Clear columns: mitochondrial areas included; black columns: mitochondrial area excluded (Ns = 158); c, COB:De - lengths of direct (specific and unspecific) contact between optic boutons and their postsynaptic elements (Ns = 173); d, DAZ - lengths of synaptic appositions (Ns = 174); e, DAZ/POB - relationships between lengths of the synaptic appositions and perimeters of optic boutons (Ns = 158); f, ht dp - height of the dense projections (Ns = 98).

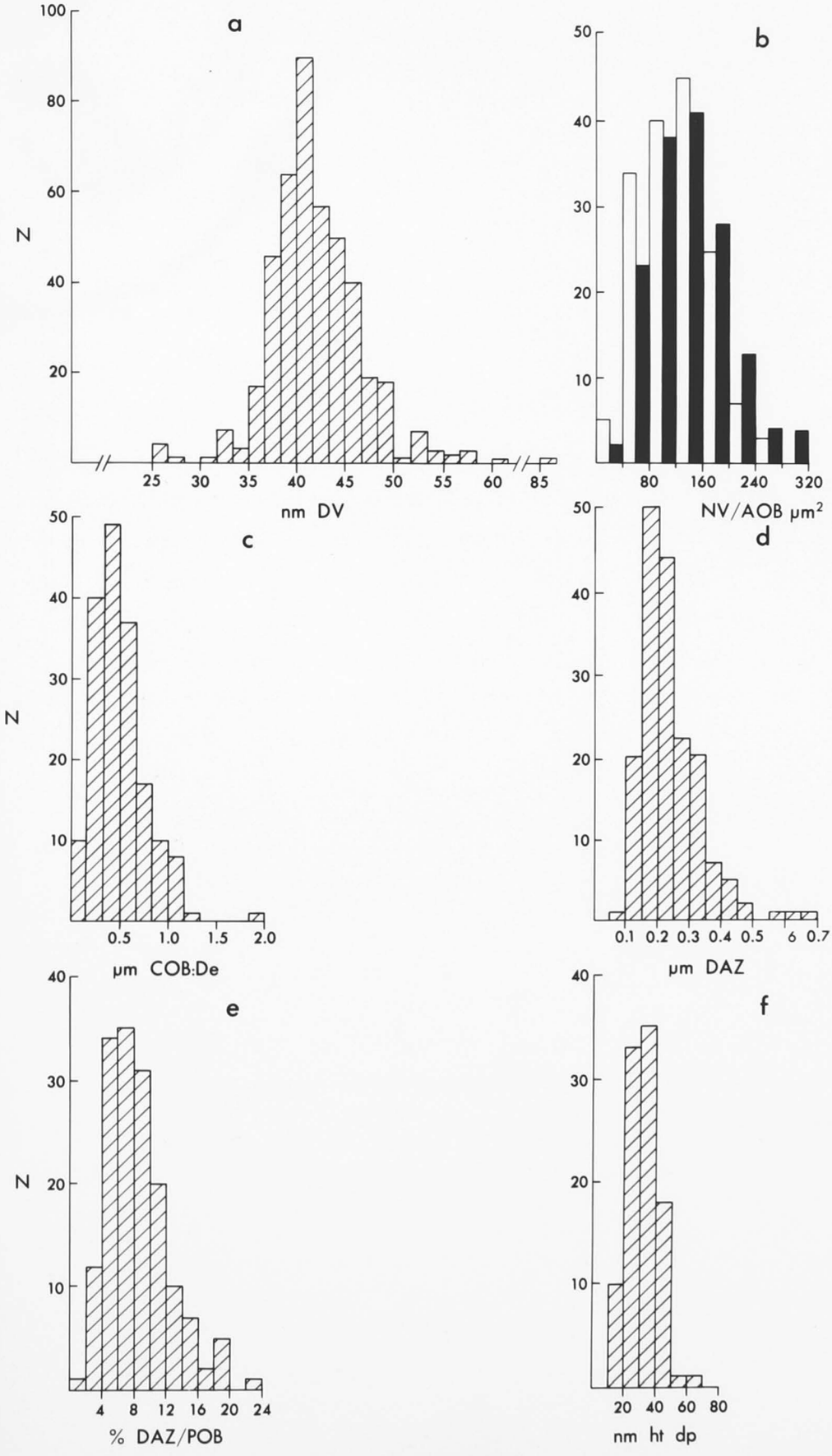
a
N
nm DV
b
NV/AOB µm²
c
µm COB:De
d
µm DAZ
e
% DAZ/POB
f
nm ht dp

FIG. 47 Frequency distributions of various parameters of optic boutons. a, wth dp - width of the dense projections (Ns = 98); b, N dcv/μm^2 - numbers of dense-core vesicle profiles per $1\mu m^2$ of boutonal area, mitochondrial areas included (Ns = 58); c, TPD - thickness of postsynaptic densities (Ns = 172); d, DDe - diameters of the postsynaptic elements (Ns = 170); e, G/B% - percentage of the perimeter of optic boutons contacted by glial cells (Ns = 73); f, G/D% - percentage of the perimeter of postsynaptic elements contacted by glial cells (Ns = 48).

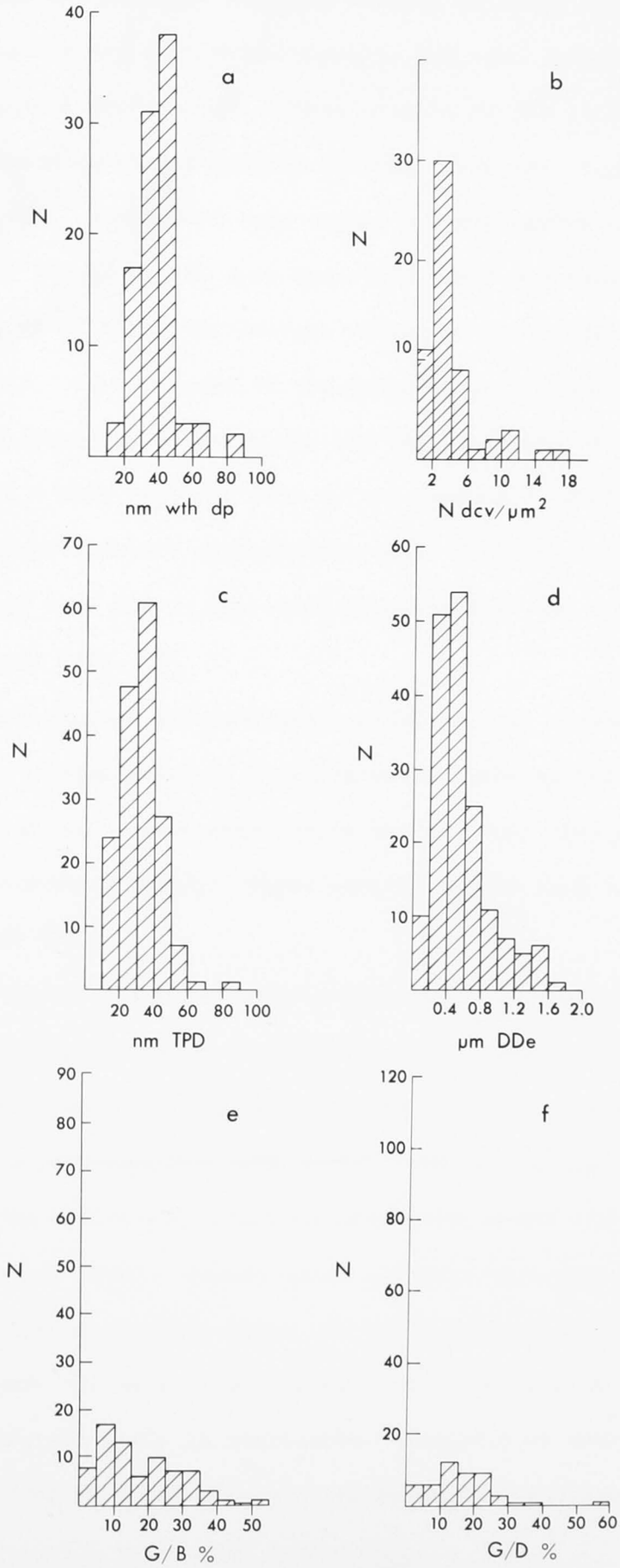
a
N
40
30
20
10
20 40 60 80 100
nm wth dp
b
N
30
20
10
2 6 10 14 18
N dcv/µm²
c
N
70
60
50
40
30
20
10
20 40 60 80 100
nm TPD
d
N
60
50
40
30
20
10
0.4 0.8 1.2 1.6 2.0
µm DDe
e
N
90
80
70
60
50
40
30
20
10
10 20 30 40 50
G/B %
f
N
120
100
80
60
40
20
10 20 30 40 50 60
G/D %

dendrites. They are similar to the dendritic appendages described in the frog (Székely *et al* 1973; Székely and Lázár, 1976). About 14% of optic boutons contacted postsynaptic elements similar to those described above (with pale cytoplasm and dark mitochondria), but with synaptic vesicles scattered throughout the element. Three percent of the latter postsynaptic elements were found to be presynaptic to other profiles, forming serial synapses (Fig. 49). The second type showed a large number of microtubules and was probably formed by the main dendritic stems and their primary branches. Only 4% of the optic boutons contacted this type of postsynaptic element (Fig. 54). Five percent of the optic synapses contacted postsynaptic elements characterised by microtubules and large mitochondria with a pale matrix (Fig. 50). They were not seen in all animals. Twenty seven percent of the postsynaptic elements contacted by optic boutons were small and could not be classified into any of the above groups (Figs. 33, 35, 55).

Attachment Plaques (Fig. 53)

Attachment plaques are membrane specialisations which can be recognised by an accumulation of electron-dense material both pre- and post-synaptically (Fig. 53). Just under 5% of the sections through optic boutons had attachment plaques. Their lengths ranged from 0.05-0.22µm.

Glial cells (Fig. 57)

The most common glial processes could usually be distinguished from neuronal elements in the optic neuropile by their electron-lucent cytoplasm and the frequent occurrence of filaments and vacuoles (Fig. 57). The glial mitochondria showed a homogeneously dark matrix, and few cristae. The processes are similar to the astrocytic processes described in the fish tectum (Laufer and Vanegas, 1974). Darker glial elements were sometimes seen, but no attempt was made to classify them. It was sometimes difficult to distinguish between the pale glial and dendritic elements (Fig. 57). Consequently a certain error is inevitable. Wrapping or covering the bouton and dendrites by glial elements was in fact very sparse. Both

FIGS. 48, 49, 50 Postsynaptic elements contacted by optic boutons (OB) synaptic appositions - arrows.

FIG. 48 Normal optic bouton showing synaptic cleft (SC), contacting pale postsynaptic element (Pl) with dark mitochondrion (Md) and a large pale postsynaptic element (Pl') containing a few clear vesicles (SV). A glial process (G) contacts part of the optic bouton and postsynaptic element. Calibration bar = 0.2µm.

FIG. 49 Normal optic bouton with glycogen granules (g), contacting a postsynaptic element (Pl') with a dark mitochondrion (Md), and containing synaptic vesicles (SV). The element postsynaptic to the optic synapse is presynaptic to another neuronal element, forming a serial synapse (arrows). Calibration bar = 0.2µm.

FIG. 50 Normal optic bouton with a dense projection (dp) contacting a pale postsynaptic element (Pl) with a dark mitochondrion (Md) and a postsynaptic element (Ps) with a light mitochondrion (Ml) and microtubules (t). Calibration bar = 0.2µm.

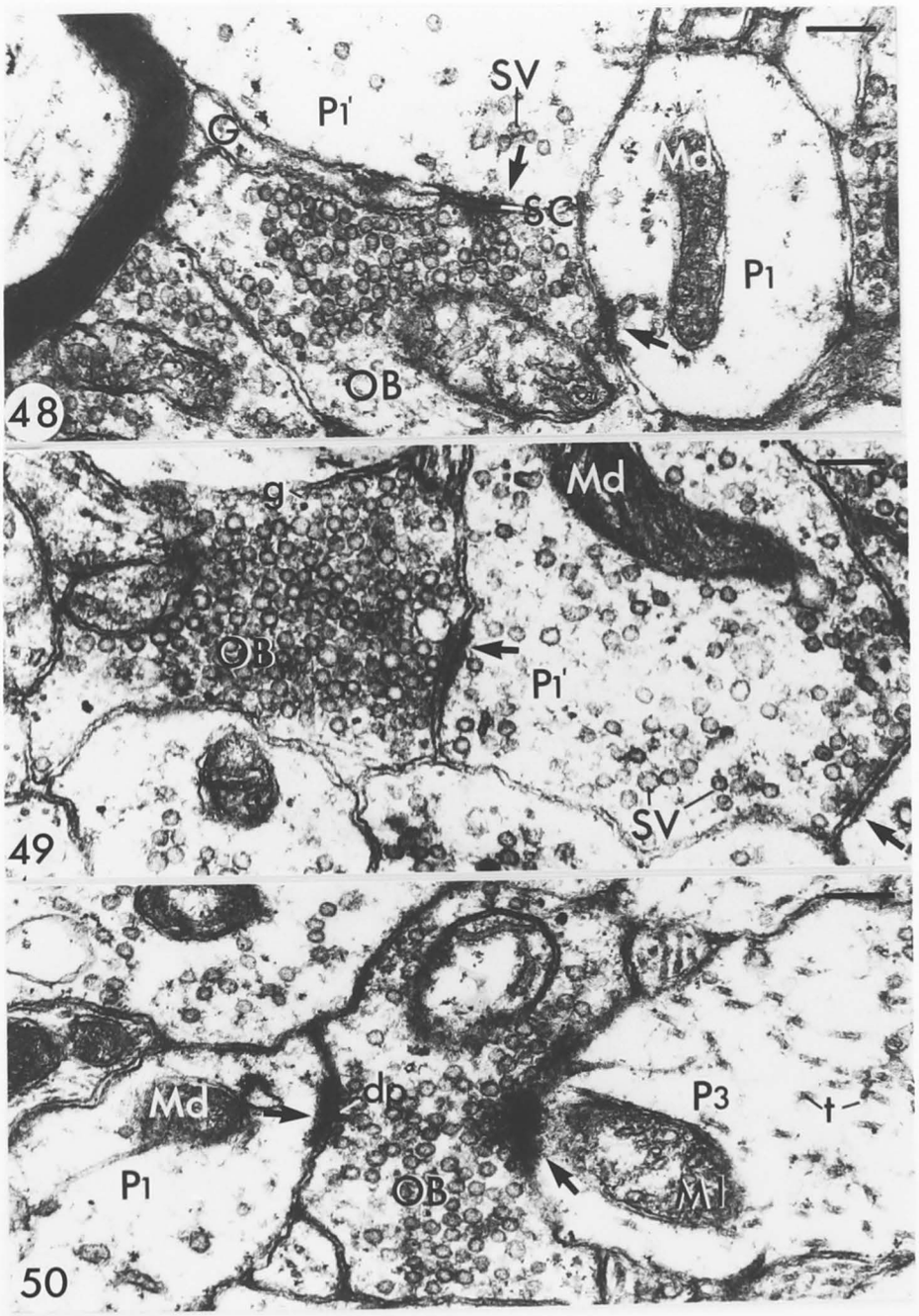
SV
P1'
G
Md
SC
P1
OB
48
g
Md
OB
P1'
SV
49
Md
dp
P3
t
P1
OB
M1
50

FIG. 51 Longitudinal section through a pale postsynaptic element (Pl) with dark mitochondria (Md). It has a beaded appearance. There are many microtubules (t) concentrated in the narrow portion of the postsynaptic element. Calibration bar = 0.5µm.

FIG. 52 Section through a drumstick-shaped postsynaptic element (Pl) which branches from a radially orientated element (arrow). Calibration bar = 0.5µm.

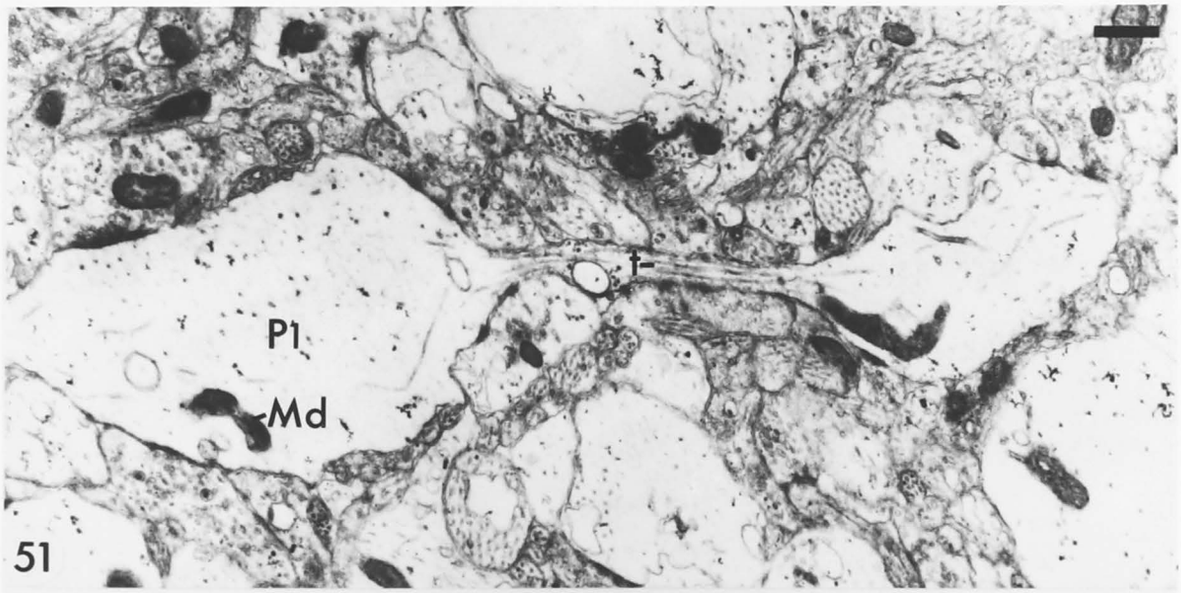

51

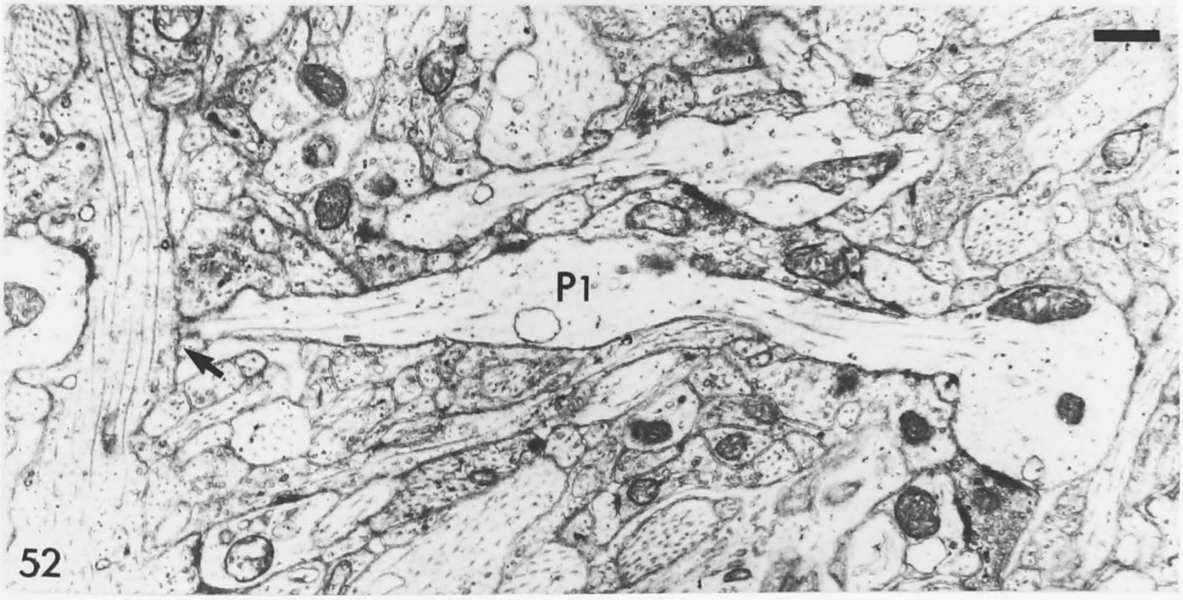

52

FIG. 53 Normal optic bouton with synaptic apposition (SA) and attachment plaque (arrow) contacting the same postsynaptic element. Calibration bar = 0.2µm.

FIG. 54 Normal optic bouton (OB) contacting postsynaptic element (P2) with microtubules (t). Calibration bar = 0.4µm.

FIG. 55 Normal optic bouton contacting (arrows) two small postsynaptic elements (Ps). M, mitochondrion. Calibration bar = 0.2µm.

FIG. 56 Normal optic bouton contacting postsynaptic element (P1) with a Gray type II synaptic apposition (arrows). M, mitochondrion; dcv, dense-core vesicle. Calibration bar = 0.2µm.

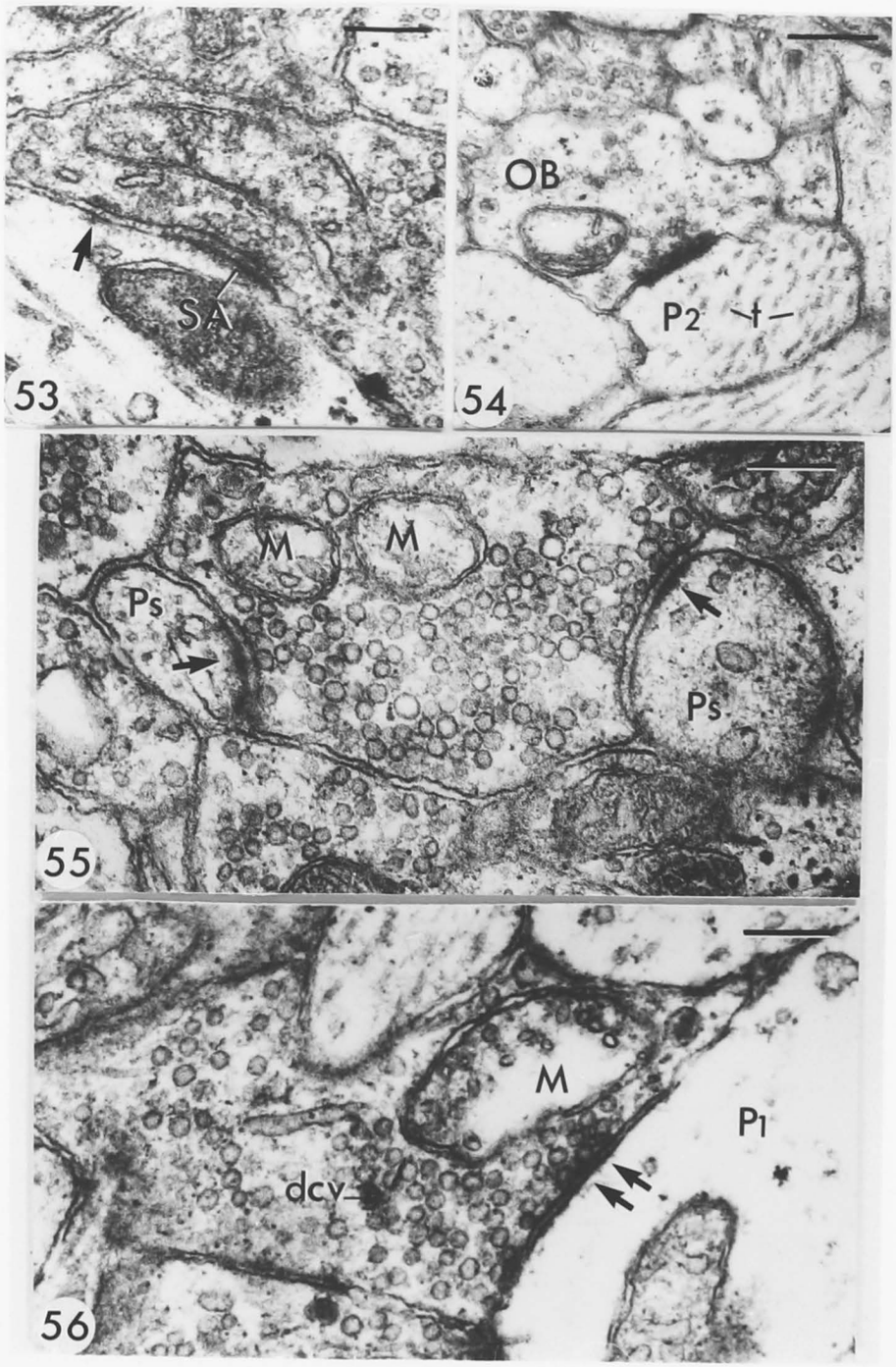
SA
53
OB
P2
t
54
M
M
Ps
Ps
55
M
P1
dcv
56

structures were usually contacted by other neuronal elements. Only 46% of optic boutons showed any glial contact. When glial wrapping was apparent, the percentage of the bouton profile contacted was usually small, but sometimes reached 50% (Fig. 47e). Thirty percent of the postsynaptic elements had glial covering. When present the glial wrapping sometimes contacted 60% of the boutonal profile (Fig. 47f). Glial cells did not obviously surround groups of synapses in glomerular structures, as has been noted in frog tectum (Székely *et al*, 1973; Székely and Lázár, 1976).

FIG. 57 Survey electron micrograph of the optic neuropile, showing glial processes (G) with dark mitochondria (Md) filaments (arrows) and vacuoles (Va). Some glial processes (G?) may be confused with pale postsynaptic elements. OB: optic bouton. Calibration bar = 0.5µm.

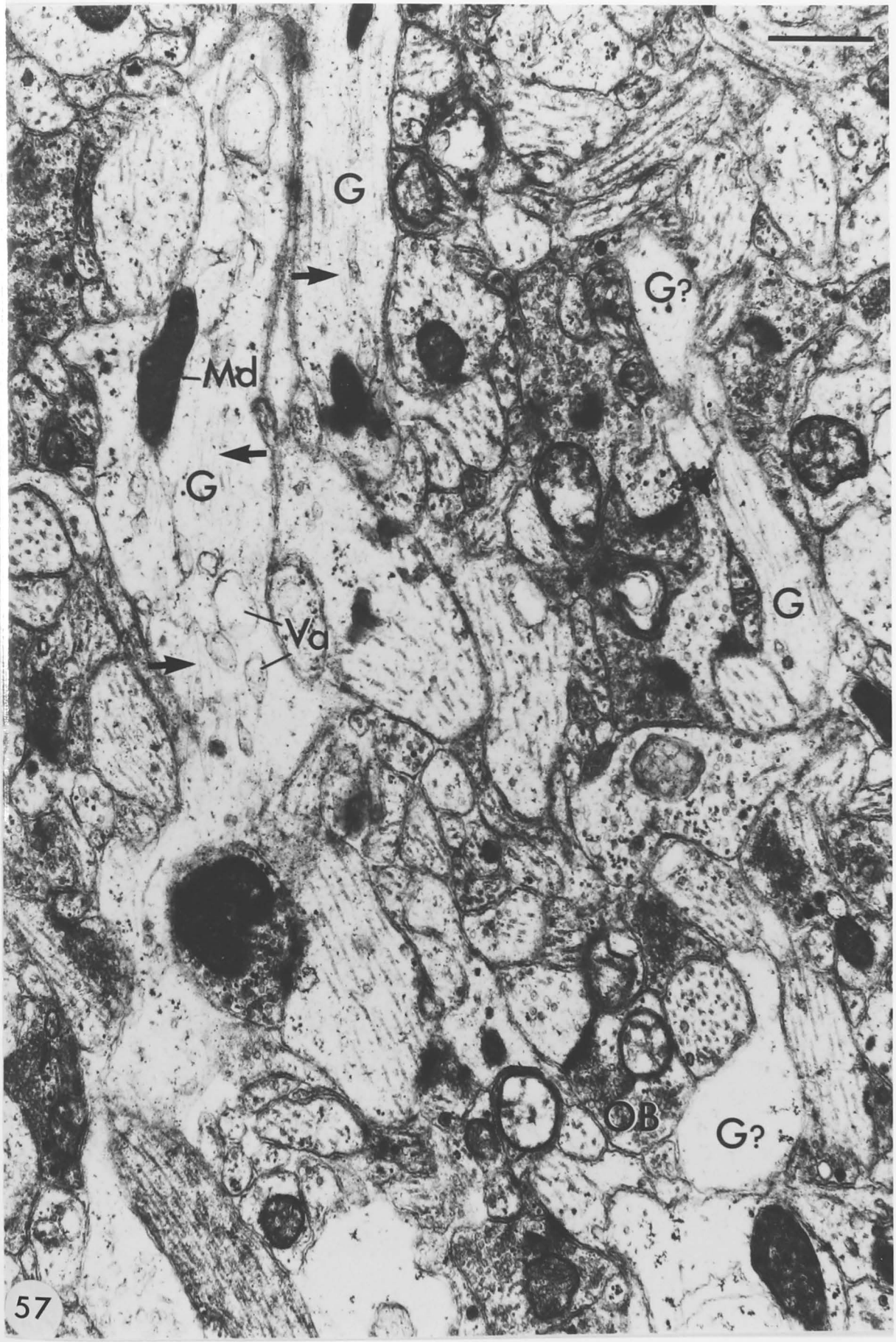

57

4. DISCUSSION

4. DISCUSSION

This thesis has concentrated on the relationship between the retina and the tectum in the axolotl. Ganglion cells in the retina send optic nerve fibres to the tectum, forming one of its largest inputs. The retino-tectal projection has been mapped by light microscopy. The cells in the tectum have also been investigated using Golgi techniques. At least some of these cells must receive direct input from the optic nerve fibre terminations. The ultrastructure of the tectal area receiving retinal input, i.e. the optic neuropile, has been studied in detail. In the following pages these results will be discussed in relation to the findings in other vertebrates, especially anuran amphibians which are phylogenetically the closest vertebrates to urodeles.

The tectum receives inputs from many other areas of the brain and sends fibres to an equally large number. Similarly, as well as sending optic nerve fibres to the tectum, the retina innervates other centres in the brain. These factors have not been well studied in urodeles and have not been investigated for this thesis. What is known about these connections in other vertebrates will be discussed in order to give a more complete picture of the optic tectum and its relationship to the rest of the brain.

4.1 COMPARISON OF THE RETINO-TECTAL PROJECTION IN THE AXOLOTL WITH THAT IN OTHER VERTEBRATES

In the axolotl, the horseradish peroxidase method of tracing the retino-tectal projection gave similar results to the degeneration methods

used by Jackway and Riss (1972), and Gruberg (1973), in the tiger salamander *(Ambystoma tigrinum)*, and Zakon (1978) in the red-backed salamander *(Plethoden cinereus)*. Autoradiographic methods used by Guillery and Updyke (1976) in the axolotl also confirm these results. The optic nerve sends fibres to the superficial half of the tectum. In this study of the axolotl, both the HRP and the Golgi methods provided no evidence that fibres or terminals were separated into layers. Gruberg (1973) found no evidence for a lamination of the terminal fields of retino-tectal fibres, although he did note that the density of degenerating material in the tectum varied with time. Zakon (1978) found no apparent lamination in the red-backed salamander. Jackway and Riss (1972), however, did note a lamination pattern in the tiger salamander. They found that three dense layers alternated with three less dense regions, suggesting that incoming fibres are separated into three, and that the terminal fields are separated from the fibre layers. There is physiological evidence that visual input is to the superficial half of the optic tectum in the tiger salamander (Gruberg, 1969).

In the axolotl a small direct ipsilateral retino-tectal projection was found. Zakon (1978), in the red-backed salamander, found a similar projection by degeneration methods but Riss *et al* in another urodele, *Cryptobranchus allegheniensis*, (1963), Jackway and Riss (1972) and Gruberg (1973) in the tiger salamander did not find an ipsilateral retino-tectal projection (Table Ib). The presence of a direct ipsilateral retino-tectal projection in the axolotl has been suggested by Guillery and Updyke (1976) using labelled amino acids as tracers. However, they also considered trans-neuronal transport as an alternative explanation. These authors found label extending as far caudally on both sides of the tectum, in contrast to my results. This difference could well be due to the different techniques used to reveal the projection. This direct ipsilateral retino-tectal projection must not be confused with an indirect ipsilateral retino-tectal projection first described by Gaze and Jacobson (1962) in *Rana temporaria*.

This projection is far more extensive and found in the dorso-rostral tectum. The latency of the ipsilateral response was found to be 20-30msec longer than that of the contralateral response. Anatomically the pathway goes from the retina to the contralateral tectum, from there to the nucleus isthmi in the caudal tegmentum, and then to the ipsilateral tectum (Gruberg and Udin, 1978; Gruberg and Lettvin, 1978; Glasser and Ingle, 1978). This indirect ipsilateral retino-tectal projection leads to a binocular representation of the binocular visual field in both tecta (Levine, 1980). This indirect ipsilateral retino-tectal pathway was found to develop in axolotls induced to metamorphose by injections of thyroxine (Brändle and Stirling, 1975).

In the axolotl, the direct ipsilateral projection described in this study is consistent between animals. It is small, and concentrated in the rostral tectum, and perhaps the lower part of the contralateral area of termination. Where it has been demonstrated in other amphibians, these features of the projection appear to be fairly consistent. It is always much smaller than the contralateral counterpart and usually concentrated in the rostral tectum (Neary, 1976; Lázár, 1978; Peyrichoux *et al*, 1978; Zakon, 1978; Stelzner, 1979), although a small posterolateral area has also been mentioned (Picouet and Clairambault, 1977; Lázár, 1978). Another fairly common feature is that the projection tends to be in the lower part or even under the contralateral area of termination (Guillery and Updyke, 1976; Peyrichoux *et al*, 1978; Zakon, 1978). It has been suggested that ipsilateral visual units described in the frog tectum could be the result of a direct projection (Gaillard and Galand, 1977).

In fish (Northcutt and Butler, 1976; Kennedy and Rubinson, 1977), and reptiles (Butler, 1973; Northcutt and Butler, 1974; Cruce and Cruce, 1975; Repérant and Rio, 1976; Repérant *et al*, 1978), a similar variability is apparent, although the trends mentioned above also apply. There are no reports of such a projection in birds, but in mammals the presence of an

ipsilateral retino-tectal projection is well established (Laties and Sprague, 1966; Wilson and Toyne, 1970; Tigges and O'Steen, 1974; Mai, 1976). Again it is smaller than the contralateral one, and does not extend to caudal areas of the superior colliculus.

In the frog *(Rana pipiens)*, ipsilateral retinal projections to the diencephalon do not develop until the onset of metamorphosis (Currie and Cowan, 1974). This has also been reported for the ipsilateral retino-tectal projection in the lamprey (Kennedy and Rubinson, 1977). It is therefore interesting that there is an ipsilateral retino-tectal projection in the axolotl, which does not metamorphose.

This study has shown that in the axolotl at any rate, an ipsilateral retino-tectal projection is consistently present. The ipsilateral optic nerve fibres form synapses which appear normal and similar to those in the contralateral tectum. As such they could have a significant function. What this might be in the axolotl or any lower vertebrates, is difficult to envisage. In mammals it is thought to have some function in stereopic vision (Hughes, 1977). In reptiles, no correlation between binocular vision and the ipsilateral retino-tectal projection could be found (for discussion see Repérant and Rio, 1976), nor could it be linked with nocturnal vision (Repérant *et al*, 1978) as had previously been suggested (Northcutt and Butler, 1974).

More detailed morphological and physiological investigation of the ipsilateral retino-tectal projection will be required before its significance is clarified.

4.2 GOLGI STUDY

4.2.a Technical considerations

There are numerous problems involved in carrying out, analysing and drawing conclusions from Golgi studies.

Staining methods There are different methods available for carrying out a Golgi study. Each technique may preferentially stain different cell types, or stain the same cell type in different ways, giving misleading information. Within any one method, staining times and concentrations of the solutions used can be varied. This can give a great deal of variation for any one method used, and even if all controllable factors are kept constant, an intrinsic variability in any method is apparent. The way in which the Golgi stain works is not understood (Ramón-Moliner, 1970). Until it is, intrinsic variability is inevitable.

In this study, all except one cell type was shown up by all three methods used. The cells occurring in the outer plexiform layer could only be reliably studied using the Golgi-Cox technique. The different stains have differing advantages and disadvantages. To carry out a complete study it is important to use as many methods as possible. Variations of each method are also necessary for the same reasons. The Golgi-Cox method did not appear to stain axons very well, as other workers have reported (Ramón-Moliner, 1970; Butler and Ebbesson, 1975). In this study, this apparent disadvantage proved to be useful. In the rapid Golgi method especially, incoming axons stained very well and obscured the dendritic trees in the optic layer. There were too many axons stained, even for studies of the arborisation patterns of the optic terminals. Shortening staining times cut down the number of incoming axons staining, but often led to incomplete staining of other cells. The Golgi-Cox stained cells had a characteristic bumpy appearance which the rapid Golgi and Golgi-Kopsch stained cells lacked, but the Golgi-Cox stained cells could still be categorised into specific groups due to the shape of their dendritic trees. The bumpiness may be an artefact and could obscure other features such as spines and beading. The rapid Golgi and Golgi-Kopsch methods involved perfusion of the animal prior to staining, and it seems reasonable to suppose that the

fixation is superior using these methods. Under the electron microscope the postsynaptic profiles observed resembled the shapes seen under the light microscope using the rapid Golgi and the Golgi-Kopsch methods rather than the shapes seen using the Golgi-Cox method.

One of the theories for a Golgi staining mechanism is that the staining of one cell inhibits the staining of other cells in its vicinity (Ramón-Moliner, 1970). This does not seem to be the case in the Golgi-Kopsch method where clumps of cells were often stained leaving large areas of the tectum unstained. Only the processes of those cells on the border of the clump could be followed in detail.

Glial cell staining The glial cells stained with all methods used, sometimes to the extent of obscuring dendritic patterns. They were easily distinguishable from neurons, could be recognised as such under the electron microscope where their shapes were comparable to those seen under the light microscope, and were similar to those cells identified as glial in other animals (Lázár and Székely, 1967; O'Flaherty, 1970; Vanegas *et al*, 1974).

Axons There are no absolute criteria for the morphological distinction between axons and dendrites. The general criteria used are the smaller diameter, lack of spines, and presence of beading. The origin of an axon on a cell type and its initial course is often so consistent that this is an added criterion, once the cell has been first described (Meek and Schellart, 1978). In this study axons were always difficult to identify and no conclusions could be drawn about the cell type most likely to have an efferent function.

Differential Staining It is quite possible that some cell types stain better than others, and that some may remain completely unknown because they do not stain at all. The relative numbers of cells cannot be established using the Golgi technique, the probability rates of cell types staining may vary considerably and give a totally biased view. Often cells in a particular area stained better than those in another. In this material

cells in the outer cellular layer (CL1) appeared to stain far more frequently than those situated more ventrally. Similarly, cells in the mediodorsal area of the tectum appeared to stain more readily than those situated ventrally and laterally. This could give a wrong impression of relative numbers of cell types. In this material the widely branching cells could be virtually restricted to the outer cellular layer and almost all the cells below this layer could be the narrow branching cells. Selective staining as described above would then lead to few of the narrow branching cells staining and being studied. In the tiger salamander, Gruberg (1969) did find that the widely branching cells occurred dorsal to the narrow ones.

Categories There is a certain amount of subjectivity involved in categorising cells. In this study, an attempt to minimise the subjectivity has been made by making quantitative measurements, and adopting strict rules for dividing cells into groups. But there are always intermediate types, perhaps every cell stained potentially comprises a cell type. The way in which authors categorise cells is bound to differ, since emphasis is laid on different details of neuronal structure. Emphasis can be laid on the cell body shape and the layer it occurs in, rather than the pattern of the dendritic tree. The latter approach however, first suggested by Ramón-Moliner (1962), seems likely to have more bearing on the function of the optic tectum.

It is essential to keep all these considerations in mind when studying a structure using the Golgi method and comparing it with other studies.

4.2.b Lamination of the tectum

In the Golgi study of the axolotl tectum there was no evidence for lamination of the cellular layer. This supports the idea that the urodele tectum is quite different from the anuran and indeed from all other vertebrate tecta (Figs. 58-63). Virtually all the tectal cells were confined to the periventricular border. Plexiform layers ran irregularly through this

cellular portion but on the whole the grey and white matter were separated. There were some cells stained in the outer plexiform layer in this study. They occurred at about the same level and so could comprise a widely spaced cellular layer. In the tiger salamander, Herrick (1942) divided the plexiform layer into five and the cellular layer into three. *Layer 1* was the superficial layer containing mainly optic fibres, *layer 2* he called the intermediate neuropile and considered it to be the main synaptic field of all afferent inputs including optic terminals. *Layer 3* had intermediate fibres in it and comprised the main efferent pathway. *Layer 4* contained commissural fibres and *layer 5* or the deep alba was a narrow zone of dense fibres. *Layer 6* was the outer grey, *layer 7* the intermediate grey and *layer 8* the deep grey or ependymal layer. Gruberg (1969) found that the sensory inputs were not totally mixed and divided the plexiform layer into three (optic layer, contralateral somesthetic layer and a bilateral somesthetic layer). The results on the axolotl support Gruberg's (1969) division of the outer plexiform layer, the optic layer being equivalent to layer PL1 in this study, the contralateral somesthetic layer being equivalent to PL2 and the bilateral somesthetic layer being equivalent to PL3 in this study. Following Herrick (1942), in this study the cellular layer was arbitrarily divided into three.

4.2.c Cell types in the tectum

The axolotl tectum may show columnar organisation in that the majority of cells had a radial orientation. The dendritic branches often had beads and spines. The cells in the outer layer had various shapes but their size was reasonably similar to those occurring in lower layers. Ependymal glial cells were present in the axolotl and looked similar to those in other vertebrates.

There appears to be a reasonable similarity between the axolotl and other urodeles. Gruberg (1969) described 2 main types of cell in the tiger salamander, a widely branching one which occurred in the outer part of the

cellular layer, and a narrow branching one which occurred throughout the cellular layers. The cells are similar to the widely branching and narrow branching cell types in the axolotl. Their differing positions could explain why few narrow branching ones were stained in this material. Gruberg (1969) did not describe a horizontal cell - he could have included them in his widely branching group. In the axolotl, because the main dendrites had a horizontal orientation and the horizontal extension appeared greater than the radial extension, they were considered to be a different group even though many of the tertiary dendrites had a radial orientation. Gruberg (1969) also found occasional cells of various shapes in the plexiform layer. Herrick (1942) gave similar descriptions of the cells in the tiger salamander *(Ambystoma tigrinum)*, but in *Necturus* (Herrick, 1941) there were many cells with huge dendritic trees which spanned the whole tectum. In the axolotl the horizontal cells sometimes spanned approximately half of the medio-lateral extension of the tectum. Due to the difficulty in staining axons, it was not possible to consider which cells had efferent pathways from the tectum.

The results from the light microscopy of the axolotl tectum have shown that the tectum is basically divided into an outer plexiform and an inner cellular layer. The optic input is restricted to the superficial half of the outer plexiform layer. One class of cells (RW) send dendrites to all levels of the plexiform layer. They presumably receive other sensory input such as tactile somesthetic as well as visual input. Radial narrow cells (RN) send a dendrite through all levels of the plexiform layer, but only branch in the outer half of the tectum. Their input is presumably mainly visual. There may also be cells which only send dendrites into the lower layers receiving only non-visual input, possibly the horizontal cells.

4.3 DISCUSSION OF FEATURES OF THE TECTUM IN OTHER AMPHIBIANS AND OTHER VERTEBRATES

The anuran amphibians are the nearest group to the urodeles. The structure of the anuran tectum has been well studied and differs markedly (Fig. 59) from that of urodeles (Fig. 58) in that in frogs the tectum is a highly-laminated structure. It has been studied extensively in two species of anuran - *Rana esculenta* and *Rana catesbeina*, and will be described in detail using information from the following authors: Lázár and Székely, 1967; Potter 1969, 1972; Székely, 1973; Székely and Lázár, 1976. References for the more historic pioneer work were given by Székely and Lázár (1976).

Unlike the urodele, the anuran tectum is clearly laminated in appearance, being divided into many cellular and plexiform layers. Nine layers can be distinguished although Potter (1969) has sub-divided some of these (Fig. 59).

Commencing at the innermost layer next to the ventricle:
Layer one consists of ependymal glial cells which form a single sheet of cells next to the ventricle. They have a single moderately branched feathered process which extends to the surface of the tectum. They are the supporting cells.

Layer two is a cellular layer, one to two cells thick (mainly pear-shaped neurons). In the rostral part of the tectum this layer also contains large cells which form the mesencephalic root of the trigeminal nerve.

Layer three is a plexiform layer containing efferent axons and axons and dendrites from intrinsic cells (Potter's (1969) deep layer).

Layer four is a cellular layer one to two cells thick (mainly pear-shaped cells).

Layer five is a plexiform layer similar to layer three.

Layer six has many layers of cells with two irregular plexiform layers

within it. Cell types within this layer are large pear-shaped neurons, large pyramidal neurons and ganglionic (multipolar) neurons.

Layer seven is a plexiform and cellular layer. Potter (1969) divided it into the deep medullary lamina and the upper multipolar cell lamina. The deeper plexiform portion forms the main efferent pathway comprising part of Potter's (1969) intermediate system.

Layer eight is a loosely packed cellular layer of multipolar cells, small pear-shaped neurons, and vertical bipolar cells.

Layer nine is mainly a plexiform layer taking up approximately one-third of the tectum. It is the layer which receives retinal input and unlike the axolotl it is clearly laminated. Potter (1969) divided it into five layers A-E, and he also added another layer beneath layer eight i.e. G, this being included with the others because of the orientation of the fibres; together, they form Potter's (1969) outer system. C and E are mainly cellular. Large myelinated fibres are found in B, D, F and G while the finer unmyelinated fibres occur in A, C and E. The thickness of layer A (or stratum zonale) diminishes caudally until it disappears.

For comparison with other vertebrates, layers 2-6 correspond to the stratum periventriculare, 7 to the stratum album centrale, 8 to the stratum griseum centrale, C-F of 9 to the stratum fibrosum et griseum superficiale, B to the stratum opticum, and A to the stratum zonale (Scalia, 1976).

Potter (1969) divided the plexiform layers into three groups according to their orientation and position. He found that the *outer system fibres* (A-G) were orientated in an anteroventral-posterodorsal manner although Székely and Lázár (1976) commented on a more mediolateral orientation in the centre of the tectum. The *intermediate system fibres* were orientated in a posteroventral-anterodorsal direction, the main part being in the deep medullary lamina of 7, although they also overlapped with the outer system,

intermediate system fibres being present in layers C, E and F. At the lateral and medial margins of the tectum the fibres converged to form the tectal commissure. It formed the main efferent pathway of the optic tectum. The *deep system fibres* (3 and 5) had a varying orientation. Some of them are probably of thalamic and contralateral tectal origin (Lázár, 1969; Trachtenburg and Ingle, 1974). The thinner ones are probably intrinsic (Székely and Lázár, 1976). The orientation of fibres in the axolotl or other urodeles has not been studied.

In Golgi preparations Potter (1972) studied the termination arbors of retino-tectal fibres. From laminae B and D fibres terminated in layers B, D, C and E, forming densely branched terminals with varicosities along their length. They were elongated in the same orientation as the outer system fibres (30-70μm by 100-200μm). From laminae F and G two types of terminations occurred: a widely branched one which had numerous forks and twigs but not many varicosities; also, thin branching arbors which did not give off many major branches but had branchlets with terminal forks; varicosities were not common. Those from lamina F terminated in the deeper portion of E, F and the superficial portion of 8. Those in lamina G terminated in G and the multipolar cell lamina of 7. Székely and Lázár (1976) suggested a similarity between densely and widely branching terminals, and introduced the possibility that the thinly branching ones might be of interneuronal origin. Lázár and Székely (1967), Székely *et al* (1973), Székely and Lázár (1976) also described terminations which dived from the fibre layer forming bell-shaped arbors. They covered as much as 70μm in diameter and were apparently more common than the elongated terminals. The terminal arbors in the axolotl or other urodeles have not been studied.

The tectal neurons have been studied in detail by Potter (1969) and Lázár and Székely (1967) using Golgi techniques. The latter gave a more comprehensive and up to date review of the situation (Székely and Lázár, 1976), therefore their findings will be presented in detail. Admitting the

somewhat artificial nature of their classification, they described the following six types of neurons.

1. Large pear-shaped neurons

a) With dendritic appendages and ascending axons.

b) With smooth dendritic collaterals, axonless.

The maximum size of these cell bodies was 15-20µm in diameter. A long apical dendrite stretched towards the surface of the tectum. Basal dendrites occurred in varying numbers. These cells made up the majority of those occurring in layers 2, 4 and 6.

Type (a) were the main constituents of layer 6 but also occurred in layer 4. The apical dendrite might or might not begin to arborise in layer 7, the ones that did covered an area of 20-30µm with their terminations. The tertiary and smaller dendrites commonly had dendritic appendages which varied in pattern. Numerous varicosities (2-4µm in diameter) occurred along the length of these appendages; they ended in a club-like protusion. The amount of division and thickness of the side branches varied. They are probably innervated by optic synapses and form dendro-dendritic synapses with other dendrites. The axon originated from the apical dendrite or a large secondary branch.

Type (b) were mainly found in layers 2 and 4 but also occurred in the deeper part of layer 6. The cell body and apical dendrite were slightly larger than in type (a). The main dendrite rarely broke into two but in layer 9 it gave off slender beaded collaterals a few hundred µm long, into the plexiform layers. The basal dendrites were also larger than those of type (a). They entered the adjacent plexiform layers extending 70-150µm. No axons could be found, the dendritic collaterals however bore presynaptic specialisations.

2. Large pyramidal neurons

They occurred mainly in layer 6 and resembled pear-shaped neurons, except that the basal dendrites gave them a more pyramidal shape. The

apical dendrite was short, arborising in layer 6, the dendritic tree covered a much wider area of 160-180μm. The terminal branches were beaded. The axon arose from the apical dendrite passing up to layer 7 via which it left the tectum. They therefore form one of the efferent pathways.

3. Large ganglionic (multipolar, candelabra) neurons

These were found scattered in the top of layer 6, in layer 7, and the deep part of layer 8. They had large cell bodies (30-40μm). Dendrites sometimes ascended to the surface at an acute angle encompassing 250-800μm. These dendrites occasionally crossed to the other tectum in the tectal commissure via layer 7. The finer branches were often beaded. When axons were seen they also left via layer 7 thus comprising another efferent pathway.

4. Small pear-shaped neurons

a) with ascending axons

b) with descending axons

c) axonless, with rich dendritic arbor.

These made up the majority of cells in layer 8 and were found to be similar to their large counterparts except that they rarely had basal dendrites and never had dendritic appendages. The apical dendrite branched at or near the cell body, the secondary and tertiary ones being heavily beaded. The dendritic trees covered an area of 25-30μm in diameter. In type (a) an axon branched close to the dendritic terminations. In type (b) the axon left the opposite pole of the cell body and descended. It could be short ending near the cell body, or descend and terminate in layer 6, or descend a short way and then loop back to end in the lower parts of layer 9, sometimes sending a collateral to terminate in layer 6. In type (c) no axons could be found. The dendrites formed a thick broom-like arborisation.

5. Bipolar neurons

Dendrites emerged at both ends of the cell body; they could be

vertically or horizontally oriented. The vertical bipolars occurred in layer 8, the axon originated on the lower dendrite and probably terminated in layer 6. The horizontal bipolars were present in the cellular laminae of layer 9, i.e. C and E and their axon originated from either of the dendrites terminating in deeper layers.

6. Small neurons (stellate and amacrine)

These only occurred in layer 9. Stellate neurons had dendrites emerging from all round the cell body, they were short, branching, and covered approximately 40μm in diameter. The axon either originated from an axon hillock on the cell body or from one of the dendrites. The amacrine cells were oval in shape (8-10μm in diameter) and depending on the closeness to the surface the dendrites ran downwards or upwards. They are probably axonless. They were less numerous than stellate neurons although they were the only cells of this type that Potter (1969) described (superficial granule cells).

In Golgi preparations, optic terminals could be seen in close association with the apical dendrites and the dendritic appendages of the large pear-shaped cells. The bell-shaped terminal arbors wrapped around the dendrites and formed a glomerulus 10-15μm in diameter. Ascending axons also entered this structure.

From these studies it is obvious that the anurans studied are more complicated than urodeles. Their tecta are highly laminated and the retino-tectal projection is itself laminated. The cells found in the anurans are more varied in size and shape than those of urodeles. However it is also clear that some basic characteristics of the tectum are common to urodeles and anurans.

Gruberg (1969) drew attention to the similarity of the widely branching cells in *Ambystoma tigrinum* to the pyramidal cells in *Rana esculenta*, and considered them to be the most likely candidates for an efferent pathway from the tectum. In this study none of the cells in the

axolotl had such a narrow dendritic field (20-30μm) as the pear-shaped cells in the frog. One of the cells in this study resembled the pear-shaped cell, type (a), in that the axon appeared to follow the dendritic pathway and terminate in the same region.

Schematic diagrams reviewing Golgi studies as well as other light microscopical studies, on the tecta of other vertebrates, are shown in Figs. 58-63. When considering all vertebrates, it would be unwise to compare cell types too critically; however basic similarities and differences are apparent.

1. *Multiple lamination* is present in the tecta of all non-mammalian vertebrates excepting those of urodeles. Division into cellular and plexiform layers is apparent throughout the tectum. Some lamination can be seen in mammals as well; however it is obscured by the increased number of small cells.

2. *Radial organisation*. The majority of cells in all non-mammalian vertebrates have a radial orientation. Many cells originating in the deeper layers of the tectum pass through all the more superficial laminae. In this way information from non-visual and visual layers might be passed on to the same cell, whether it be efferent or intrinsic. In mammals the dendritic fields rarely go further than neighbouring laminae thus each layer maintains a certain amount of independence. Cells contributing to this radial orientation are pyramidal, pear-shaped, vertical bipolars and fusiform cells. The width of the dendritic tree varies enormously.

3. *Horizontal cells* occur in all vertebrates, although in far smaller numbers than the radial cells. Dendrites can stretch for varying distances but usually keep to one lamina.

4. *Small neurons* such as stellate and amacrine cells occur in all vertebrates studied except perhaps urodeles. They have small dendritic fields

KEY TO FIGURES 58-63


Plexiform layers


Cellular layers


Optic termination sites


Axons

Dendritic spines

Dendritic appendages

Beaded structures

Alternative structure

* Commisural in the midline

A	Amacrine cell
B	Bipolar cell
DML	Deep medullary lamina
EG	Ependymal glial cell
F(L)	Fusiform or spindle shaped cell (large)
H	Horizontal cell
HU	Horizontal unipolar cell
IPL	Inner plexiform layer
M	Multipolar (ganglionic, candelabra or polygonal) cell
MCL	Multipolar cell layer
OT	Optic terminal arbors
P	Pyramidal cell
Pr(S,L)	Pear shaped or pyriform cell (small, large)
PI	Pars intermediale
PP	Pars profundum
PS	Pars superficiale
RU	Radial unipolar cell
S	Stellate cell
SAC	Stratum album centrale
SAM	Stratum album marginale
SAP	Stratum album periventriculare
SFGS	Stratum fibrosum et griseum superficiale
SFP	Stratum fibrosum periventriculare
SGC	Stratum griseum centrale
SGM	Stratum griseum medium
SGP	Stratum griseum periventriculare
SGPr	Stratum griseum profundum
SM	Stratum marginale
SO	Stratum opticum
SPV	Stratum periventriculare
SZ	Stratum zonale

n.b. Each cell type is only drawn in full in one layer, its presence in other layers is shown by cell body outline.

FIG. 58 Diagram of the structure of the urodele tectum
(Ambystoma tigrinum, Ambystoma mexicanum).
Cell body sizes:- Pr, P 15-25μm
RU, B, HU cells are extremely rare.
References used:
(1) Herrick '42, '48; (2) Gruberg '69; (3) This study.

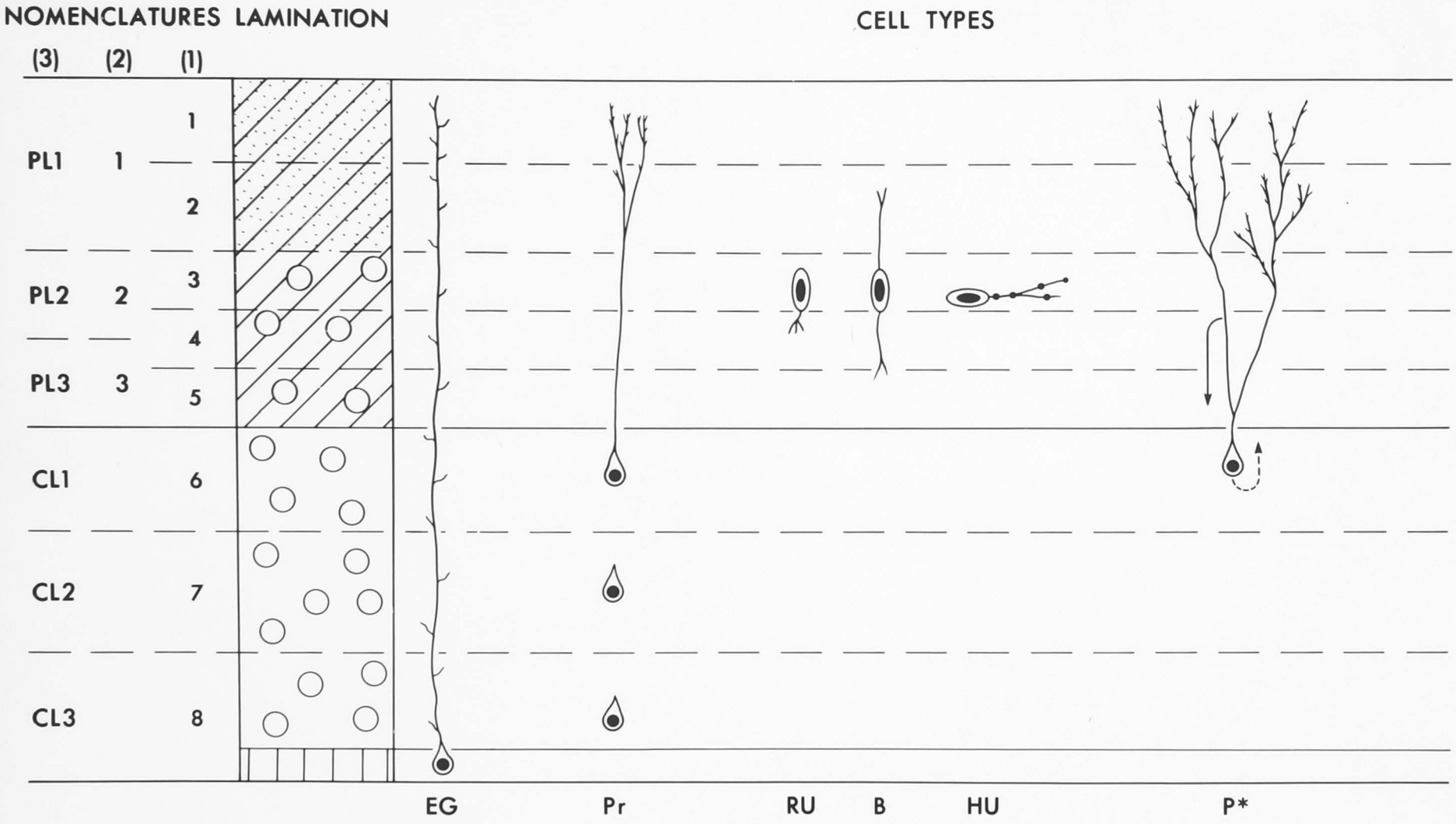
NOMENCLATURES LAMINATION
CELL TYPES
(3)
(2)
(1)
PL1
1
1
2
PL2
2
3
4
PL3
3
5
CL1
6
CL2
7
CL3
8
EG
Pr
RU
B
HU
P*

FIG. 59 Diagram of the structure of the anuran tectum (various species).
Cell body sizes:- Pr(L), P 15-20μm; S, A 8-10μm; S, M 40μm.
Widths of dendritic fields:- Pr(L)a 20-30μm; Pr(L)b 300μm;
Pr(S) 25-30μm; S 40μm; M 600-800μm; P 160-180μm.
Length of OT arbors 100μm.
References used: Lázár and Székely '67; (1) Potter '69, '72;
(2) Scalia '76; Székely and Lázár '76.

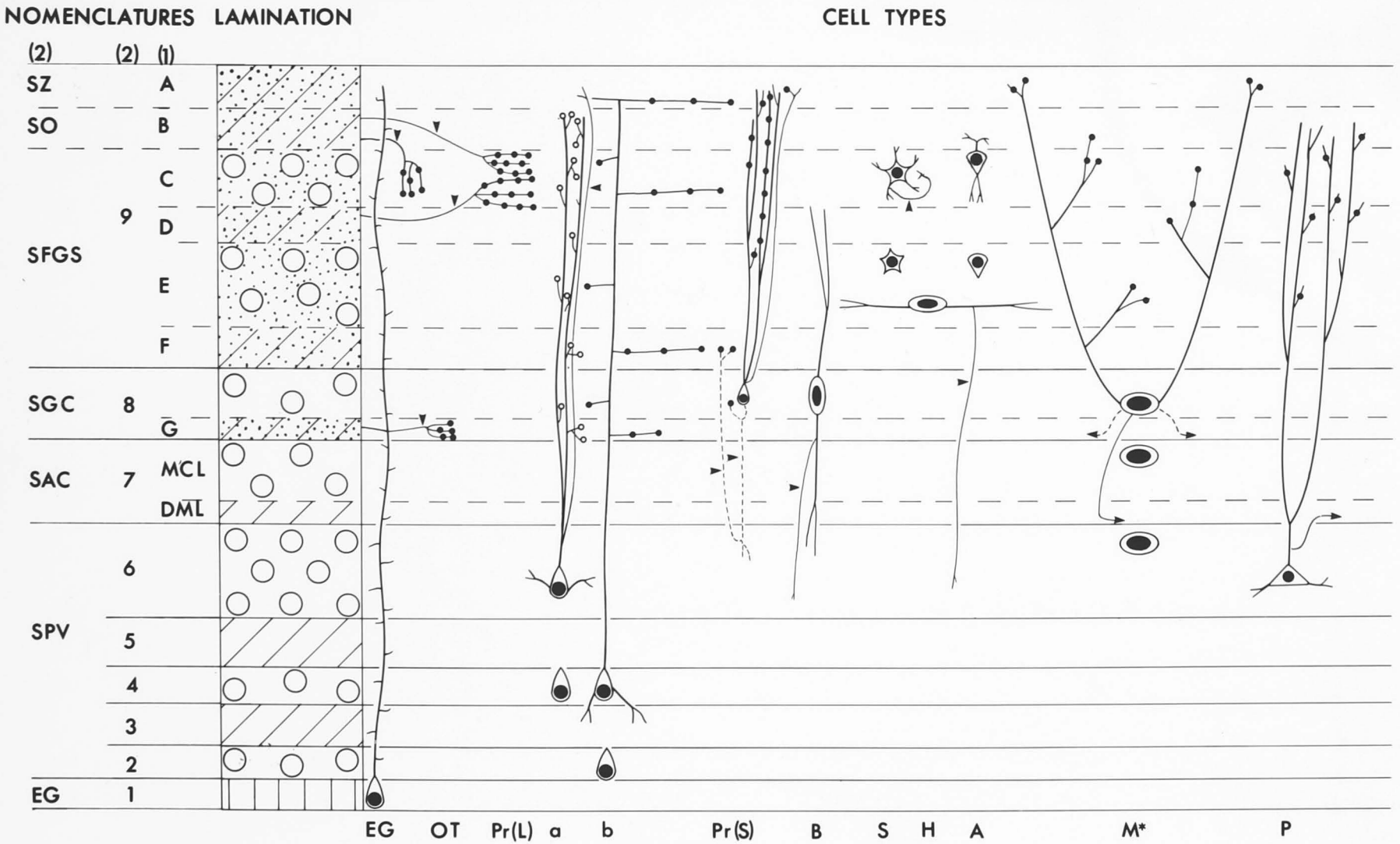
NOMENCLATURES
LAMINATION
CELL TYPES
(2)
(2)
(1)
SZ
A
SO
B
C
9
D
SFGS
E
F
SGC
8
G
SAC
7
MCL
DML
6
SPV
5
4
3
2
EG
1
EG
OT
Pr(L)
a
b
Pr(S)
B
S
H
A
M*
P

FIG. 60 Diagram of the structure of the fish tectum (various species).
Cell body sizes:- Pr(L) 10-15μm; Pr 6-8μm; Pr(S) 5-8μm; F(L) 6-10μm; B 6μm; Ha 6-12μm; Hb 10-15μm; M 15-30μm; P 8-12μm.
Widths of dendritic fields:- F(L), B 150μm; Ha 100-200μm; Hb, M 600μm; P 400-600μm.
References used: (1) Sharma '72; (2) Vanegas, Laufer and Amat '74; (3) Meek and Schellart '78.

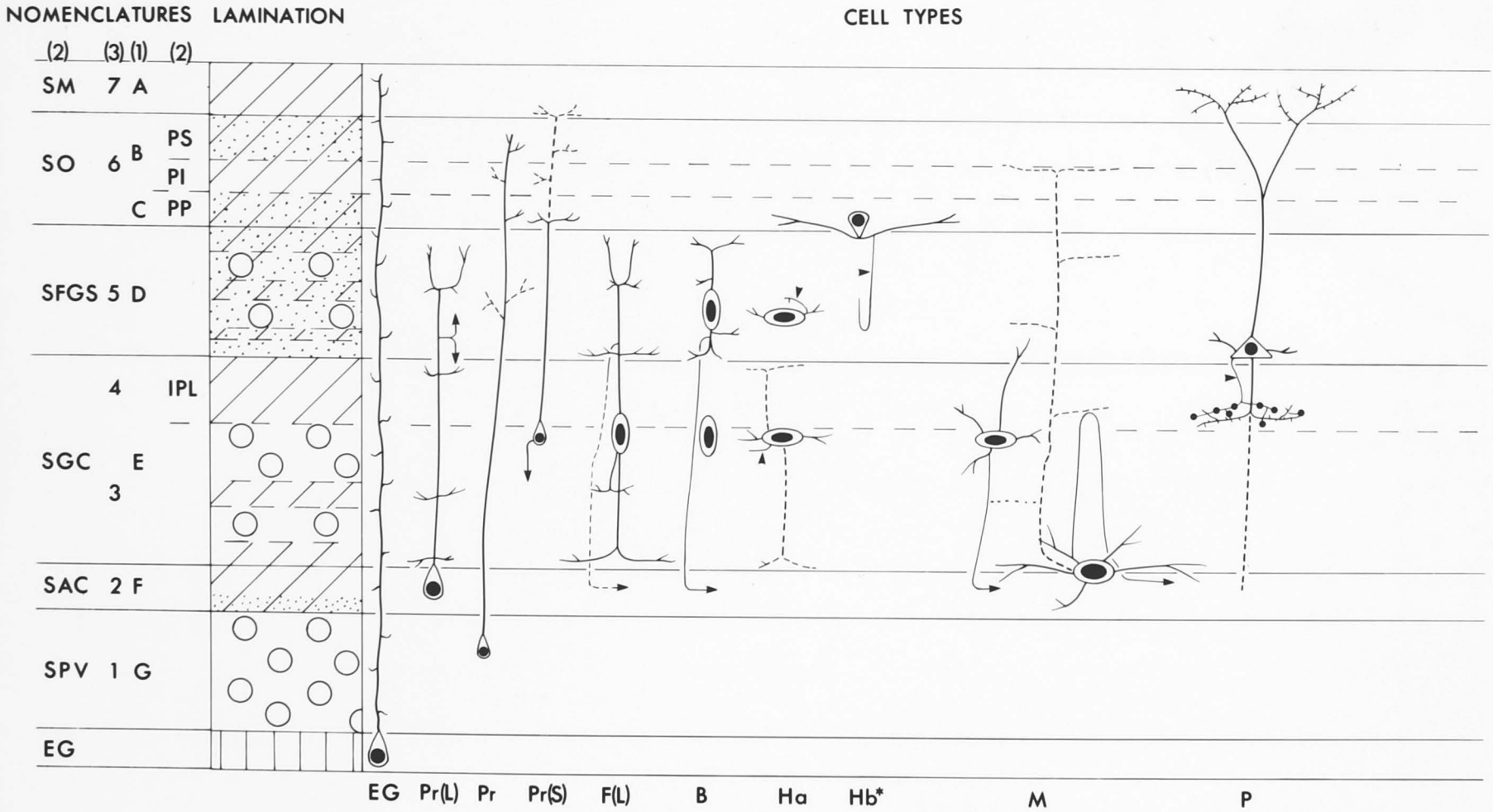
NOMENCLATURES
LAMINATION
CELL TYPES
(2) (3) (1) (2)
SM 7 A
SO 6 B PS
PI
C PP
SFGS 5 D
4 IPL
SGC E
3
SAC 2 F
SPV 1 G
EG
EG Pr(L) Pr Pr(S) F(L) B Ha Hb* M P

FIG. 61 Diagram of the structure of the reptile tectum (various species). References used: (1) Repérant et al '78; (2) Butler and Ebbesson '75. Axons not shown in above references. Cell body sizes and widths of the dendritic fields can not be given accurately using the above authors' material.

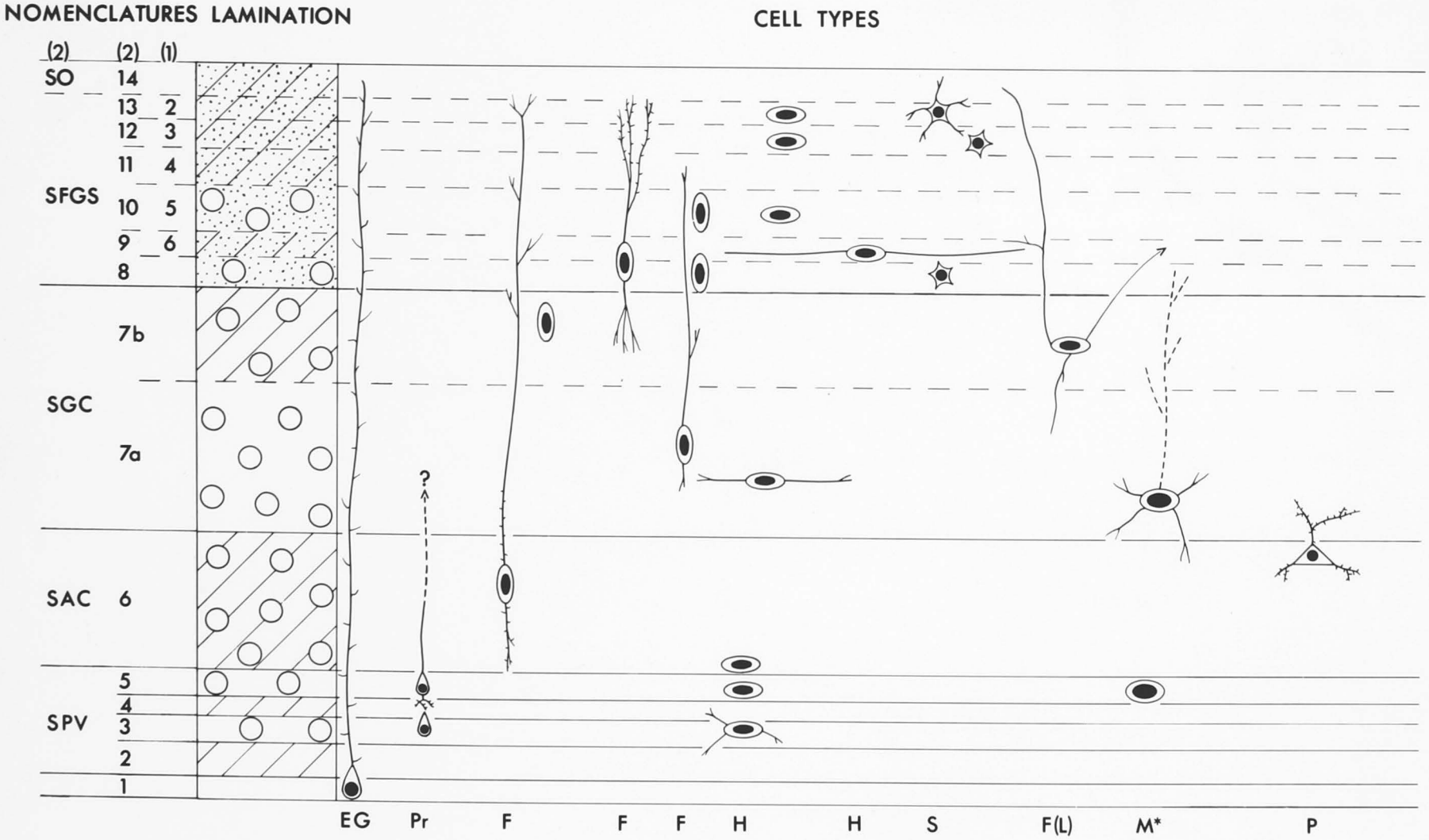
NOMENCLATURES LAMINATION
CELL TYPES
(2) (2) (1)
SO
14
13 2
12 3
11 4
SFGS
10 5
9 6
8
7b
SGC
7a
SAC 6
5
4
SPV 3
2
1
?
EG
Pr
F
F
F
H
H
S
F(L)
M*
P

FIG. 62 Diagram of the structure of the bird tectum (various species). Cell body sizes: M 40μm. Widths of dendritic fields:- H 500μm; M 1000μm. References used: (1) O'Flaherty '70; (2) La Vail and Cowan '71; Stone and Freeman '71; (3) Repérant '73.

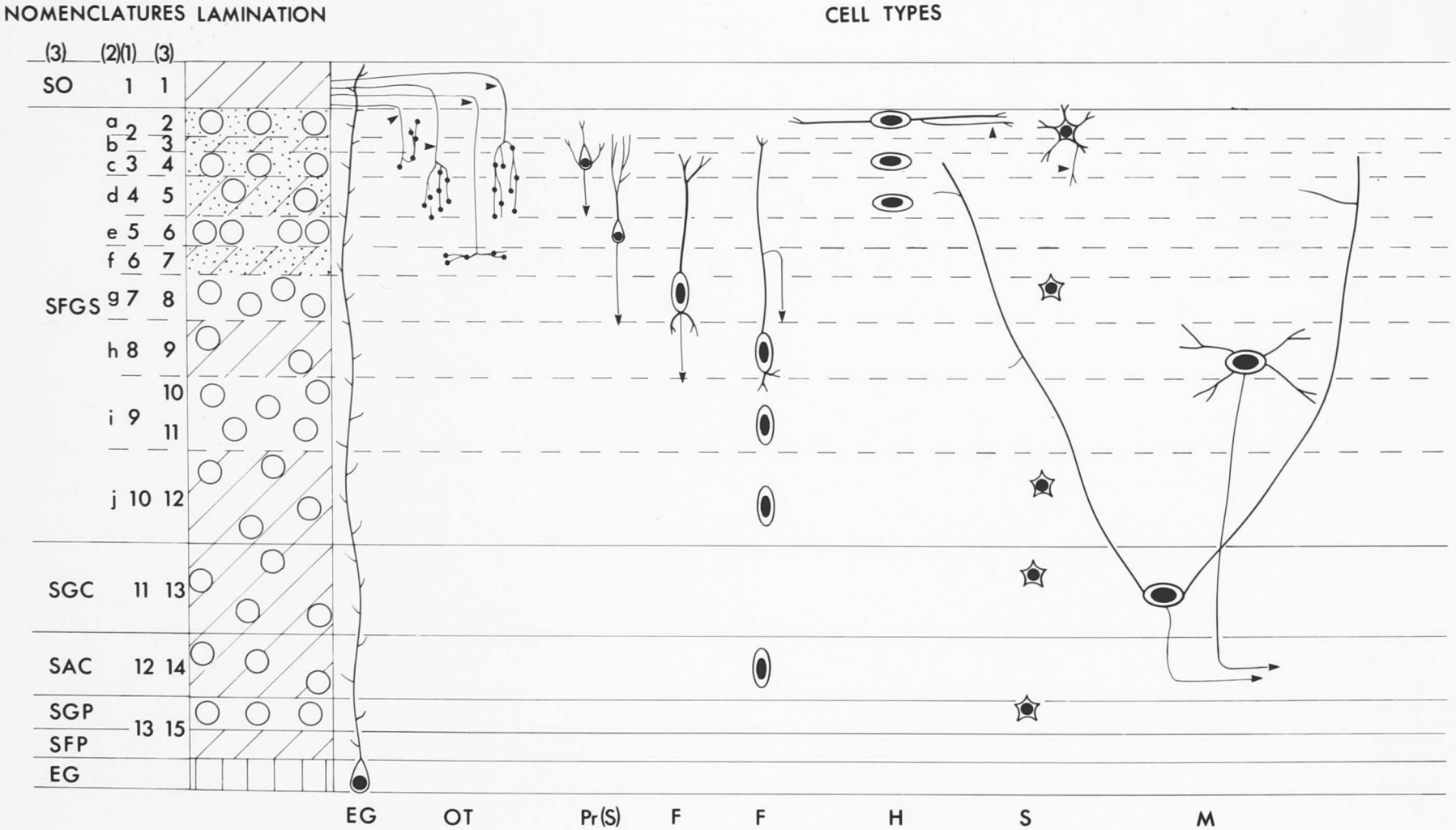
NOMENCLATURES LAMINATION
CELL TYPES
(3) (2)(1) (3)
SO 1 1
a 2 2
b 2 3
c 3 4
d 4 5
e 5 6
f 6 7
SFGS g 7 8
h 8 9
10
i 9 11
j 10 12
SGC 11 13
SAC 12 14
SGP 13 15
SFP
EG
EG
OT
Pr(S)
F
F
H
S
M

FIG. 63 Diagram of the structure of the mammalian superior colliculus (various species). Cell body sizes:- F 8-24μm; H, P 12-15μm; M 50-65μm. References used: Sterling '71; (1) Székely '73; Sprague '73; Mathers '77.

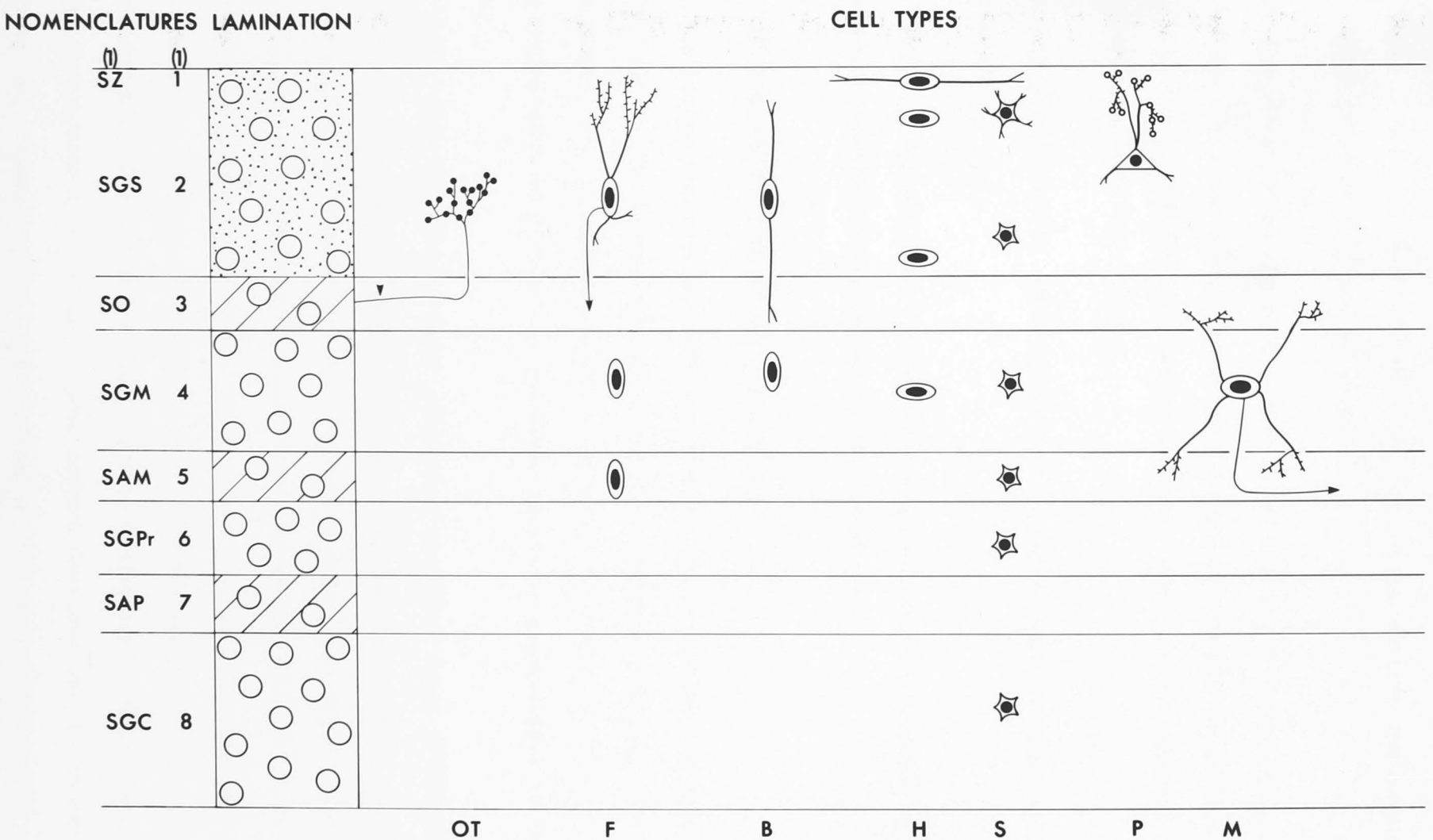
NOMENCLATURES
LAMINATION
CELL TYPES
(1)
(1)
SZ 1
SGS 2
SO 3
SGM 4
SAM 5
SGPr 6
SAP 7
SGC 8
OT
F
B
H
S
P
M

and a short or absent axon. In fish, amphibians and reptiles the small neurons appear to be confined to the superficial optic strata; however in birds and mammals they occur throughout the tectum in increasing numbers. These small neurons are probably interneurons and may reflect the need for more central processing in higher vertebrates.

5. *Large multipolar neurons* also appear to be a constant feature in all vertebrates. They are always large, have a very wide dendritic field often coursing obliquely through many tectal laminae. They form an efferent pathway and are often commissural.

6. *Ependymal glial cells* are a common feature in all vertebrates, lining the ventricles.

Thus, it appears that the axolotl and other urodeles do share most of the basic characteristics common to all vertebrates.

4.4 RETINAL PROJECTIONS IN ALL VERTEBRATES

The retina projects to other areas of the brain besides the optic tectum, in all vertebrates. To gain any understanding of the part the tectum plays in the visual system it is important to realise the relationships of the retina with other areas of the brain and their relationship to the tectum.

Apart from the retino-tectal projection the other areas of retinal termination have not been considered in this study of the axolotl. They have been studied by several authors in other urodeles (see Table Ib). There are seen to be five basic areas of retinal termination. Three are in the diencephalon: the hypothalamus, the thalamus and the pretectum; and two are in the mesencephalon: the accessory optic nucleus and the optic tectum. The projection is often bilateral but the ipsilateral one is always smaller than the contralateral contingent. Some authors have divided the thalamic projection into separate dorsal (the nucleus of Bellonci) and ventral

KEY TO TABLES I-IV

A *Autoradiography technique*
B *Bilateral*
Be *Neuropile of Bellonci*
BO *Basal optic nucleus*
C *Contralateral*
Co *Cobalt technique*
CN *Corticalis nucleus*
CO* *Central optic nucleus*
D *Degeneration technique*
DLA *Nucleus dorsolateralis anterior thalami*
DLG *Dorsal lateral geniculate nucleus*
DLO* *Dorso-lateral optic nucleus*
DLT *Dorsolateral thalamic nucleus*
DMO* *Dorsomedial optic nucleus*
EC *Nucleus ectomamillaris*
EX *Nucleus externus de Rendahl*
GL *Nucleus geniculatus lateralis*
GP *Nucleus geniculatus pretectalis*
GT *Nucleus griseum tectalis*
H *Horseradish peroxidase technique*
I *Ipsilateral*

* Ebbesson's (1972) nomenclature

LA *Nucleus lateralis anterior*
LG *Lateral geniculate neuropile*
LM *Nucleus lentiformis mesencephali*
LP *Large celled pretectal nucleus*
ND *Nucleus decussationis supraopticae ventralis pars anterior*
P *Pretectal nucleus*
Pd *Nucleus posterodorsalis*
PD *Nucleus pretectalis diffusus*
PL *Nucleus pretectalis lateralis*
PT *Posterior thalamic nucleus*
SS *Nucleus superficialis syencephali*
SGFS *Stratum griseum et fibrosum superficiale*
SFS *Stratum fibrosum superficiale*
SZ *Stratum zonale*
U *Unicate nucleus*
VL(D,V) *Ventrolateral nucleus (Dorsal, Ventral)*
VLG *Ventral lateral geniculate nucleus*
VLO* *Ventrolateral optic nucleus*
VLT *Nucleus ventrolateralis thalami*
VMO* *Ventromedial optic nucleus*

TABLE I: RETINAL PROJECTION SITES IN AMPHIBIANS

Techniques, reference, species	Hypothalamus (Preoptic)	Thalamus DLO* Be	Thalamus VLO* LG	Pretectum PT	Pretectum LP	Pretectum U	Accessory VMO* BO	Tectum (Showing layers) C	Tectum (Showing layers) I
a) Anurans									
D Knapp et al '65 *Rana pipiens*	C I	C I	C I	C I	C		C	9	
D Scalia et al '68 *Rana pipiens*	C?	C I	C I	C I	C		C	9,8(G)	
D Lázár et al '69 *Rana esculenta*		C I	C I		C I		C	9,8(G)	
D Lázár '71 *Rana esculenta*		C I[1]	C I[1]	C I[1]	C I		C	9,8(G)	
A Scalia '73 *Rana pipiens*								9(ABCDEF),8(G)	
D Scalia et al '74 *Rana pipiens*		C I[1]	C I[1]	C I[1]	C	C I[1]	C	9,8(G)	
H Scalia et al '74 *Rana pipiens*								9(ABCDEF),8(G)	
D Vullings et al '75 *Rana temporaria*	C I								
A Neary '76 5 sp.		C I	C I	C I	C I		C I[2]	9,8(G)	See 3
A Picouet et al '77 *Discoglossus pictus*	C? I?	C I	C I	C I	C I		C	9,8(G)	See 4
Co Lázár '78 *Rana esculenta*	C	C I	C I	C I	C I	C I	C I	9(BCDEF),8(G)	F,G[5]
A Peyrichoux et al '78 *Rana esculenta*	C I	C I	C I	C I	C		C	9(ABCDEF),8(G)	F[10]
A Stelzner '79 *Rana pipiens*		C I	C I	C I	C	C I	C	9,8(G)	See 11
A Levine '80 *Xenopus laevis*	C I	C I	C I	C I[12]	C I[12]	C I	C I	9	See 13
b) Urodeles									
D Riss et al '63 *Cryptobranchus alleghenienses*	C I	C	I		C I		C	See 6	
D Jackway et al '72 *Ambystoma tigrinum*	C I	C	I		C I		C	See 6	
D Gruberg '73 *Ambystoma tigrinum*		C	I		C		C	See 6	
A Guillery et al '76 *Ambystoma mexicanum*	C I	C I	C I		C I		C I	See 6	See 7
D Zakon '78 *Plethoden cinereus*		C I	C I		C I		C	See 8	See 9

1 mainly from temporal retina
2 In *Bombina orientalis, Xenopus laevis*
3 In *Bombina orientalis, Xenopus laevis, Rana catesbeiana, Bufo americanus*
4 9,8 especially posterolateral tectum
5 In anterior half, and posterolateral tectum
6 In superficial half of plexiform layers in anterior two thirds of tectum
7 Below C projection in anterior two thirds of tectum
8 Superficial half of plexiform layers throughout tectum
9 Anterior one third of tectum, below C projection
10 Especially anterior part
11 Anterior and lateral tectum - restricted to a band in superficial third of 9
12 Not homologous to PT and LP in *Rana* sp.
13 Rostral pole of layer 9

(lateral geniculate) nuclei (see Table Ib).

In anuran amphibians the situation is again more complex. Although there are the same five areas of termination, these areas can be subdivided into various nuclei. As shown by Table Ia the optic nerve terminates in six diencephalic (one hypothalamic, two thalamic, three pretectal) and two mesencephalic centres (accessory optic system, optic tectum).

1. Hypothalamus (preoptic nucleus)

Until recently a direct retinal projection to this region has not been shown (see Table Ia). However, an electron microscopical study proved the existence of a small bilateral termination in the preoptic nucleus (Vullings and Heussen, 1975). The contralateral projection at any rate, has now been verified using a cobalt complex diffusion technique, by light microscopy (Lázár, 1978).

2. Thalamic

The lateral geniculate body receives a bilateral retinal projection as does the more dorsally situated neuropile of Bellonci. They are not nuclei in the true sense of the word in that there are no cell bodies present. Like most optic terminations, they contact dendrites. The cells of origin of the dendrites have been studied by Scalia and Gregory (1970) and are situated more medially.

3. Pretectal

The posterior thalamic nucleus, the large-celled pretectal nucleus, and the unicate nucleus all receive a bilateral retinal projection.

The thalamic and pretectal projections are generally retinotopically organised (Lázár, 1971; Scalia and Fite, 1974). The unicate nucleus is too small for any topographical arrangement to be seen, although it does receive projections from all parts of the retina and should be considered as a separate nucleus (Scalia and Fite, 1974). This retinotopic organisation

is a mirror image of that found in the tectum, suggesting a reversal of polarity across the di-mesencephalic junction during development, with differentiation beginning at the di-mesencephalic border and proceeding both rostrally and caudally (Scalia, 1976).

4. Accessory Optic Nucleus (basal optic nucleus, ectomammilary nucleus)

This is situated near the junction between the hypothalamus and ventral tegmental region of the mesencephalon. It receives a mainly contralateral projection. Lázár (1973) has shown it to be vital for the optokinetic response.

5. Tectum

The tectal projection is mainly contralateral. On reaching the antero-lateral border of the optic tectum, the optic nerve bifurcates into mediodorsal and ventrolateral portions which encircle the tectum. The optic fibres course in several layers within the tectum and send off terminations into the surrounding tissue. There has been some controversy in recent years over the presence or not of optic terminals in the most superficial layer of the tectum, the stratum zonale. Although not shown by any degeneration techniques, they have been demonstrated by Scalia (1973) using autoradiography and Scalia and Coleman (1974) using anterograde transport of horseradish peroxidase. Lázár (1978) found only a small number of terminals in this layer. The explanation that light microscopic degeneration techniques do not show these terminals up because they take a longer time (21 days) to degenerate being unmyelinated (Scalia and Coleman, 1974) does not explain why Székely *et al* (1973) in their electron microscopical investigation found no sign of degeneration in the stratum zonale between one and thirty days after enucleation.

When comparing the projection sites of the retina in all vertebrates, (Table II), it can be seen that the 5 main areas of termination (hypothalamus, thalamus, pretectum, accessory optic system and tectum) remain unchanged.

TABLE II: RETINAL PROJECTION SITES IN FISH, REPTILES, BIRDS AND MAMMALS

FISH

Techniques, reference, species	Hypothalamus (Preoptic)	Thalamus LG	Pretectum DMO* DLT	Pretectum P	Pretectum CN	Accessory VMO* BO	Tectum (showing layers) C	Tectum (showing layers) I
D Campbell et al '69 *Holocentrus*	C	C	C	C	C	C	BCDF [1]	
D Sharma '72 Goldfish	C	C	C	C	C		BCDF [1]	
D Vanegas et al '73 *Euggerres*	C	C	C I	C	C		BCDF [1]	
A Landreth et al '75 *Hemichromis*							BCDF	
A Lemire et al '76 Trout	C I	C	C I	C		C	BCDF	
D Northcutt et al '76 Gar	C I	?[2]	C I	C I		C	BCD	See 3
A Repérant et al '76 9 teleosts	C I	C	C I	C I	C	C	BCDEF	
D Voneida et al '76 *Astynax mexicanus*	C	C	C I	C I	C	C	BCDE	
D Kennedy et al '77 Lamprey		C	C I	C I[4]			BCDE	See 4

1 Anterior tectum only
2 Describes a lateral and ventral medial nucleus
3 Anterior tectum only
4 Ventro-lateral margin only

REPTILES

Techniques, reference, species	Hypothalamus	Thalamus DLO* DLG	Thalamus VLO* VLG	Thalamus VL D	Thalamus VL V	Pretectum GP	Pretectum LM	Pretectum GT	DMO* Pd	Accessory VMO* BO	Tectum (showing layers) C	Tectum (showing layers) I
a) Squamates (lizards, snakes)												
D Butler '73 *Xantusia vigilis*		C I	C I		C	C I			C I	C	8-14	8,9
D Northcutt '74 *Gekko gecko*	C	C I	C I		C	C	C I		C I	C	8-14	8-14
A Cruce et al '75 *Tupinambis nigropunctatus*		C I	C I			C I			C I		8-14	See 1
A Repérant et al '76 *Vipera aspis*	C	C I				C	C I	C	C I	C I	8-14[2]	8-14[2]
A Repérant et al '78 5 sp. lizards	C	C I[3]	C			C	C	C	C I		8-14	See 4
A Butler et al '78[5] *Iguana iguana*		C I	C I	C	C I	C	C I		C I	C		
Gekko gecko		C I	C I	C	C I	C	C I		C I	C		
b) Chelonians												
D Bradford '73 Crocodile	C I	C	C		C	C	C		C	C	8-14	
A Bass '75 Turtle		C	C		C		C		C	C	8-14	

1 Variable in amount from specimen to specimen
2 Has a stratum zonale which has terminations also
3 Except in *Uromastix acanthinurus*
4 In *Tarentola mauritanica*
5 3 other additional thalamic nuclei described.

BIRDS

Techniques, reference, species	Hypothalamus	Thalamus ND	Thalamus GL	Thalamus LA	Thalamus DLO* DLA	Thalamus VLO* VLT	Pretectum SS	Pretectum GT	Pretectum PD	Pretectum PL	Pretectum EX	Accessory VMO* BO(EC)	Tectum (showing layers) C	Tectum (showing layers) I
Repérant '73	C?	C	C I?	C I?	C I?	C	C	C	C	C	C	C	abcdf	
D Hunt et al '75 Pigeon													abcdf	
D Bons '76 Duck	C													
H Oliver et al '78 Quail	C													

MAMMALS

	Hypothalamus	Thalamus DLO* DLG	Thalamus VLO* VLG	Pretectum	Accessory VMO* BO	Superior colliculus (showing layers) C	Superior colliculus (showing layers) I
A Tigges '74 Squirrel monkey	C I	C I	C I	C I	C I	SZ, SFS	SZ, SFS
A Mai '76 Rat	C I	C I	C I	C I	C I	SZ, SFS	SZ, SFS

Nuclei within these groups increase in number however, presumably paralleling the increasing complexity of the brain during the course of evolution. It is difficult to compare particular nuclei in the various groups as homologies between them cannot safely be established. Ebbesson (1972) attempted to do this with several nuclei and where applicable his new nomenclature is used as well as the more established. Even within the same phylum nuclei are often given different names but in this case it is easier to draw homologies. Another source of confusion is derived from nuclei having the same name but perhaps not being homologous.

4.5 CONNECTIONS OF THE TECTUM

4.5.a Afferent pathways

As well as receiving a major input from the retina, the tectum receives other inputs from other central areas in all vertebrates (Table III). Non-retinal inputs to the tectum have not been studied in the axolotl in this study. Some of the afferent connections of the tiger salamander have been studied (Herrick 1942, 1948; Kokoros and Northcutt, 1977; Gruberg and Solish, 1978).

Herrick (1942, 1948) traced tracts, using conventional fibre staining, from other areas of the brain, whilst the other two studies used degeneration techniques, destroying an area in the brain and then looking for degeneration in the tectum.

Kokoros and Northcutt (1977) found a sparse projection from the telencephalon to the pretectal-tectal areas via the strio-tegmental tract. The inputs were ventral to optic ones. Herrick (1942, 1948) also described this projection. In the diencephalon Herrick (1942, 1948) described pretectal, thalamic and habenular tracts to the optic tectum, and in the mesencephalon he described the tectal commissure connecting the two tecta.

There is an ipsilateral projection to the tectum from the dorsal grey of the cervical spinal cord. Gruberg and Solish (1978) described a

TABLE III: NON RETINAL AFFERENTS TO TECTUM

1a, ANURAN		1b, URODELE		2. FISH	
Telencephalon		*Telecephalon*	I	*Telecephalon*	
				Central region	I?
Diencephalon		*Diencephalon*		*Diencephalon*	
Dorsal lateral nucleus (postero lateral nucleus)	B	Habenula		#* Pretectal nucleus	
#* Large celled prectectal (DMO*)	I	#* Pretectum			
#* Lateral geniculate	I	#* Dorsal thalamus		#* Dorsolateral nucleus (DMO*)	
Mesencephalon		*Mesencephalon*		*Mesencephalon*	
#* Tectum	C	#* Tectum	C	#* Tectum	C
# Tegmentum	I			# Tegmentum	
# Isthmic nucleus	B			# Isthmic nucleus	
Supra peduncular	B			Torus semicircularis	
				# Torus longitudinalis	I
				# Lateral reticular formation Lateralis valvular	
		Rhombencephalon		*Rhombencephalon*	
		Medulla	B^1	Cerebellum	
Spinal Cord		*Spinal Cord*		# *Spinal Cord*	
# Cervical region	I	Ventromedial Spinal grey	B^1		
References and techniques		*References and techniques*		*References and techniques*	
D Trachtenburg and Ingle '74		Herrick '42, '48		D Marotte and Mark '75	
H Wilcynski and Northcutt '77		D Kokoros and Northcutt '77		H Grover and Sharma '78	
H,A,D Gruberg and Udin '78		D Gruberg and Solish '78		D,H Ito and Kishida '77,'78	

3. BIRD		4. MAMMAL	
Telencephalon		*Telencephalon*	
Wulst[2]	B	Visual Cortex[2]	B
		Non visual cortex (somatic sensory, auditory, motor)	
Diencephalon	?	*Diencephalon*	
		#* Lateral geniculate (DLO*,VLO*)	
		Pulvinar (CO*)	
Mesencephalon		*Mesencephalon*	
#* Tectum	C	#* Superior colliculus	C
		Inferior colliculus (acoustic)	
		Rhombencephalon	
		Cerebellum	
		# Reticular formation	
		Medulla	
# *Spinal Cord*		# *Spinal Cord*	
References and techniques		*References and techniques*	
Ebbesson '70		Székely '73	
D Karten et al '73		Sprague '75	
Webster '74			

Notes

\# Receives tectal projections

* Receives direct retinal projection

1 Fibres mediate touch topographically in phase with retino-tectal projections and possibly serotoninergic.

2 Topographically organised.

Reptiles have not been extensively studied (Ebbesson '70).

somatosensory monaminergic pathway entering the deeper layers of the tectal neuropile in the tiger salamander. Sims (1977) however, did not describe this monaminergic pathway in axolotls. Physiologically, fibres in these deeper tectal layers responded to touch, they were found to be topographically organised and in register with incoming visual information (Gruberg, 1969).

A far more complete study of the anuran afferents to the tectum have been made using the retrograde transport of horseradish peroxidase, which revealed the following projections in *Rana pipiens* (Wilczynski and Northcutt, 1977). In contrast to urodeles, and indeed to all other vertebrate groups studied, there is apparently no telencephalic input to the tectum in anurans. The remaining areas will be considered in turn.

1. Diencephalic

Pretectal

a) Bilateral from the dorsal lateral (posterolateral) nucleus.

b) Ipsilateral from the dorsal half of the posterior nucleus.

These nuclei contribute dendrites to the posterior thalamic nuclei (Scalia and Gregory, 1970).

c) Ipsilateral from the large celled pretectal nucleus.

Thalamic

Trachtenburg and Ingle (1974) reported similar results using degeneration techniques. They found an additional ipsilateral projection from the lateral geniculate body, and suggested a telencephalic-geniculate and dorsolateral nucleus pathway. Anatomical studies fit in well with the physiological evidence that these pretectal inputs are inhibitory. Lesions of the pretectal nuclei result in a disinhibition of tectal neurons. Normally frogs habituate to a repeated bug-like stimulus and do not snap at it any more. Also they avoid large objects. Lesion results in a continuous snapping response to any object even if large (Ingle, 1973b).

2. Mesencephalic

Tectum

There is a contralateral input from the other tectum. It enters in layer 7 (SAC) via the tectal commissure and descends as far as layer 2 (SPV).

Tegmentum

There is an ipsilateral projection from the anterodorsal, posterodorsal and anteroventral tegmental fields, bringing in non-visual but also visual information from the contralateral tectum.

Nucleus isthmi

This nucleus sends a bilateral projection to the superficial tectum (Gruberg and Udin, 1978) i.e. that part also receiving retinal input. The visual fields found by Gaze and Jacobson (1962) on the ipsilateral tectum which are retinotopically organised in the same manner as the contralateral projection, may be mediated by this nucleus (Gruberg and Udin, 1978; Glasser and Ingle, 1978). This ipsilateral visual field is unaffected by tectal or posterior commissural cuts. Fite (1969) showed that it was abolished by tectal ablation or tegmental commissural cuts. This projection apparently develops in axolotls induced to metamorphose with thyroxine injections (Brändle and Stirling,1975).

Suprapeduncular nucleus

It sends a bilateral projection to the tectum. It is a cell group dorsal to the interpeduncular nucleus.

3. Spinal Cord

There is an ipsilateral projection from the dorsal grey of the cervical spinal cord.

The non-retinal afferent projections to the tectum in all vertebrates are shown in Table III. When comparing them certain patterns are apparent although the information, particularly on reptiles and birds, is rather scanty. Direct information from the telencephalon enters the tectum in all vertebrates except anurans. In mammals visual information mainly enters

into the upper layers and non-visual into the lower layers. Whether the telencephalo-tectal pathways carry visual information in other vertebrates is not known. Thalamo-telencephalic projections have been reported (Ebbesson and Schroeder, 1971; Gruberg and Ambros, 1974) in some lower vertebrates which carry visual information to the forebrain. Pathways from diencephalic centres which themselves receive retinal information and information from other parts of the brain, are a common feature. Pathways from auditory centres such as the torus semicircularis and the inferior colliculus are often present. The cerebellum, reticular formation and the spinal cord send inputs to the tectum in most vertebrates. It is clear that information of many kinds enters the tectum and integration of visual with other information such as somatic (tactile) and auditory (Dräger and Hubel, 1975) can take place and the appropriate motor action be taken.

4.5.b Efferent pathways

The tectum projects to many other areas of the brain in all vertebrates (Table IV). The efferent pathways were not studied in the axolotl. The probable efferent cells of the tectum could not be discovered due to the difficulty of staining and distinguishing axons reliably. Other methods such as the retrograde and anterograde transport of HRP, or anterograde transport of radioactive substances, would be more reliable techniques for showing the efferent cells and the projection sites. In frogs, using retrograde transport of HRP, Gruberg and Lettvin (1978) showed that *all* cell types previously described in the frog tectum, below Potter's (1969) layer G, sent efferent fibres to the nucleus isthmi. The majority, however, came from pyramidal cells in layer 6.

When the projection sites in all vertebrates are compared they are strikingly consistent. In all vertebrates studied both ascending and descending projections from the optic tectum have been observed. The ascending pathways project to the pretectum, ipsilateral dorsal and ventral thalamic regions, and to the contralateral dorsal and ventral thalamus via

TABLE IV: EFFERENT PATHWAYS FROM TECTUM

1a. ANURAN	
Diencephalon	
#* Pretectum (DMO*)	B
* Bellonci (DLO*, CO*)	B
#* Lateral geniculate (VLO*)	B
* Hypothalamus	B
Mesencephalon	
#* Tectum	C
# Tegmentum	
# Isthmic nucleus	I
Interpeduncular nucleus	I
Lateral reticular formation	I
Medial reticular formation	C
Rhombencephalon	
Lateral reticular formation	I
Medial reticular formation	C
Spinal Cord	
# Cervical region	C
Retina	See 1

References and techniques

D Robinson '68
D Lazar '69
H Wilczynski and Northcutt '77
1H Scalia and Teitelbaum '78
H,A Gruberg and Udin '78
H Gruberg and Lettvin '78

1b. URODELE	
Diencephalon	
#* Pretectum (DMO*)	B
#* Thalamus (VLO*, DLO*)	B
* Hypothalamus	B
# Habenula	
Mesencephalon	
#* Tectum	C
Tegmentum	B
Rhombencephalon	
Lateral medulla	I
Medial medulla	C
Cerebellum	
Spinal Cord	
Lateral	I
Medial	C

References and techniques

Herrick '42, '48
D Gruberg '69

2. FISH	
Diencephalon	
#* Pretectum	I
#* Dorsolateral nucleus (DMO*)	I
* Lateral geniculate	B
Nucleus rotundus (CO*)	B
Mesencephalon	
#* Tectum	C
# Tegmentum	I
# Isthmic nucleus	I
# Torus longitudinalis[1]	
# Lateral reticular formation	I
Medial reticular formation	C
Rhombencephalon	
Lateral reticular formation	I
Medial reticular formation	C
Spinal Cord	C

1 Unique to teleosts

References and techniques

D Ebbesson and Vanegas '76
D,H Ito and Kishida '78

3. REPTILE	
Diencephalon	
* Pretectum	B
* Dorsal lateral geniculate[1] (DMO*)	B
* Ventral lateral geniculate[2] (VLO*)	B
* Nucleus rotundus[3] (CO*)	B
Mesencephalon	
#* Tectum	C
Tegmentum	B
Isthmic nucleus[2,3]	I
Lateral reticular formation	I
Medial reticular formation	C
Rhombencephalon	
Lateral reticular formation	I
Medial reticular formation	C
Spinal Cord	C

1 only in snakes
2 topographically organised from SGFS
3 Not present in snakes

References and techniques

D Foster and Hall '75
D Ulinski '77

4. BIRD	
Diencephalon	
* Pretectum[1]	B
* Dorso-lateralis anterior (DLO*)	B
* Ventrolateralis (VLO*)	B
*Lateral geniculate	I
Mesencephalon	
#* Tectum	C
Tegmentum	B
Isthmic nucleus[2]	I
Lateral reticular formation	I
Medial reticular formation	C
Rhombencephalon	
Lateral reticular formation	I
Medial reticular formation	C
# *Spinal Cord*	C

1 partly from SGFS-topographically organised
2 wholly from SGFS-topographically organised

References and techniques

D Karten '65
A Hunt and Künzle '76

5. MAMMAL	
Diencephalon	
* Pretectum[1] (DMO*)	
#* Dorsal lateral geniculate[1] (DLO*)	B
#* Ventral lateral geniculate[1] (VLO*)	B
Lateral posterior nucleus[1]	B
Mesencephalon	
#* Superior colliculus	C
Tegmentum	B
Lateral reticular formation	I
Medial reticular formation	C
Rhombencephalon	
Lateral reticular formation	I
Medial reticular formation	C
Spinal Cord	
# Cervical region	C

1 From SGS, some topographically organised

References and techniques

Székely '73
A Graham '77

* Receive retinal afferents # Project to tectum

the supraoptic decussation. The descending projections can be divided into two portions. An ipsilateral pathway descends along the ventrolateral edge of the brainstem terminating in adjacent structures. It can project as far as the cervical spinal cord (Foster and Hall, 1975). The contralateral portion descends ventromedially also terminating in neighbouring structures. The consistencies suggest that this part of the connectional organisation of the optic tectum was probably established early in vertebrate evolution.

Looking at the connectional patterns of the retino-tectal system it should be noted that many of the retinal termination sites project to the tectum. The tectum also projects back to some sites reciprocally e.g. the pretectum, thalamus, tegmentum, reticular formation, and the spinal cord.

4.6 THE IDENTIFICATION OF OPTIC SYNAPSES BY CHARACTERISTIC MITOCHONDRIA

This study has shown that in the axolotl the identification of optic nerve terminals is possible in the optic neuropile due to the pale matrix of their mitochondria. Other structures with pale mitochondria occurred only rarely and were found in postsynaptic elements with a different ultrastructure from optic synapses.

In mammals, the ultrastructure of primary visual centres, receiving optic nerve afferents from the retina, such as the superior colliculus and dorsal lateral geniculate nucleus, has been studied in detail. Synapses described as, or assumed to be of retinal origin are characterised by the presence of mitochondria with a pale matrix and tubular formations of the inner membrane (see Lund 1969, Lund 1972, Sterling 1971, Mathers 1977: in the superior colliculus of rabbit, cat, rat, monkey; Szentágothai 1973, Lieberman and Webster 1974, Cullen and Kaiserman-Abramof 1976, Robson and Mason 1979: in the dorsal lateral geniculate nucleus of cat, rat and mouse; Yamada 1974 in the medial terminal nucleus of the accessory system of the mouse; Güldner 1978a in the rat suprachiasmatic nucleus).

In the axolotl mitochondria with the pale matrix did have a tubular

inner membrane, although tubular inner membranes often occurred in mitochondria with a dark matrix also i.e. in non-optic synapses.

In other non-mammalian vertebrates mitochondria showing a tubular inner membrane or combinations of tubules and cristae are observed in neuronal elements other than optic synapses (see Figures in Hayes and Webster, 1975; Angaut and Repérant, 1976 - pigeon; Székely *et al*, 1973; Székely and Lázár, 1976 - frog; Laufer and Vanegas, 1974; Marotte and Mark, 1975 - fish).

In non-mammalian vertebrates it appears that tubular inner membranes cannot be used as a criterion for identifying optic boutons. As in the axolotl, in many cases where the ultrastructure of the optic tectum in non-mammalian vertebrates has been studied, the pale matrix of the mitochondria in optic synapses can be used as a distinguishing feature.

In the pigeon, Hayes and Webster (1975) noted the presence of characteristic mitochondria in boutons assumed to be retinal in origin, showing a prominent space between inner and outer mitochondrial membranes, giving the matrix a moderately dense appearance. In another study on the pigeon optic tectum Angaut and Repérant (1976), made no comment on the mitochondrial structure, although in their micrographs synapses containing mitochondria with a pale matrix can be seen. In the frog *(Rana esculenta)* (Székely *et al*, 1973; Székely and Lázár, 1976), synapses assumed to be optic had mitochondria with swollen inner membranes and a pale matrix. Initial studies using horseradish peroxidase filling of optic synapses in *Xenopus laevis* have shown mitochondria with tubular inner membranes and an electron-lucent matrix in filled structures (unpublished results). In fish, optic nerve terminals could not be identified in the carp *(Carassius carassius)* (Marotte and Mark, 1975), but in *Eugerres plumieri*, the mitochondria had a characteristically pale matrix and large spaces between the sparse cristae as well as between the inner and outer membranes (Laufer and Vanegas, 1974). Initial studies on the goldfish have shown that mitochondria with a dark as well as a pale matrix can occur in optic synapses filled with horseradish peroxidase (unpublished results). Variations in fixation techniques,

different amounts of inner membrane and different degrees of swelling of the matrix could explain the differences found amongst vertebrates. Mitochondrial morphology is obviously a useful tool in identifying synapses of retinal origin, however it seems that unlike the situation in mammals, in other vertebrates the mitochondria are not always an absolute criterion for identifying optic boutons.

In the axolotl mistaken identification may occasionally occur but the author believes the error margin is small and would not greatly affect the frequency distributions provided that the sample number is always large.

4.7 COMPARISON OF OPTIC SYNAPSES IN THE AXOLOTL WITH THOSE IN OTHER VERTEBRATES

To my knowledge, the ultrastructure of the axolotl tectum, or any urodele optic tectum, has apparently not been studied previously. When comparing the features of optic synapses with those of other vertebrates many similarities are apparent.

In the axolotl optic boutons often had an irregular shape conforming to their surroundings. They contained round synaptic vesicles 40-60nm in diameter, dense-core vesicles, glycogen granules and microtubules. These features are common to optic boutons in other studies (Lund 1969, Sterling 1971, Lund 1972, Mathers 1977 - mammals; Hayes and Webster 1975, Angaut and Repérant 1976 - birds; Székely *et al* 1973, Székely and Lázár 1976 - amphibians; Laufer and Vanegas 1974 - fish).

Glial cells did not obviously surround groups of synapses in our material. In other vertebrates optic synapses usually tend to be clustered together in complex synaptic arrangements, sometimes surrounded by glial elements making a glomerulus (Sterling, 1971; Székely *et al*, 1973; Székely and Lázár, 1976). They are similar to those found in the dorsal lateral geniculate nucleus (Szentágothai, 1973). In the axolotl most of the synaptic appositions had a significant amount of postsynaptic density material and could be classified as forming Gray type I or asymmetric synapses. However,

16% showed virtually no postsynaptic density and as such could be classified as Gray type II (Gray, 1959; Akert *et al*, 1972). In the medial terminal nucleus Yamada (1974) found the optic nerve terminals made Gray type II contacts. Elsewhere, in other vertebrates the synaptic appositions are described as always forming Gray type I or asymmetric contacts (Lund 1969, Lund 1972, Mathers 1977 - mammals; Hayes and Webster 1975, Angaut and Repérant 1976 - birds; Székely 1973, Székely and Lázár 1976 - anurans; Laufer and Vanegas 1974 - fish). In the axolotl some of the 16% Gray type II synapses could represent mistakenly-identified optic boutons. The fact that optic synapses occasionally showed a Gray type I and type II apposition on the same bouton speaks against this. In horseradish peroxidase-filled optic nerves the presynaptic dense projections are obscured by reaction product, and although their presence is sometimes strongly suspected, Gray type II synapses cannot be unequivocally identified. Serial sections through the optic boutons were not cut, and so some of these with virtually no postsynaptic density material could be sectioned through the border of a synaptic apposition. In the rat suprachiasmatic nucleus, serial sections have shown that Gray type II appositions extend throughout a junction in most of the cases (Güldner, 1978b). As morphometric analysis of identified optic synapses has not been carried out on the optic tectum of any other vertebrates, it is possible that Gray type II synaptic appositions have been overlooked.

The most common postsynaptic dendrite in the axolotl with its pale appearance and occasional synaptic vesicles is similar to those occurring in the frog optic tectum (Székely *et al*, 1973; Székely and Lázár, 1976). In the frog, Golgi studies have shown that the size and shape of these pale dendritic elements is similar to the dendritic appendages of the large pear-shaped cells (Székely *et al*, 1973; Székely and Lázár, 1976). In virtually all vertebrates studied the retinal afferents in the tectum contact a variety of dendritic types including some containing synaptic

vesicles which are sometimes seen to be making serial synapses (Lund, 1969; Sterling, 1971; Lund, 1972; Hayes and Webster, 1975; Angaut and Repérant, 1976; Székely and Lázár, 1976; Mathers, 1977).

As a detailed morphometric analysis of the optic synapses in the albino rat suprachiasmatic nucleus using the same criteria has been carried out (Güldner, 1978b) it is worthwhile making a direct comparison. The main difference is the size of the optic boutons and their mitochondria. Both tend to be smaller in the axolotl tectum. In the axolotl, mitochondria occupy a smaller proportion of boutonal area. This could be due to less swelling or more shrinkage of the mitochondria in axolotl optic synapses compared with those in the rat suprachiasmatic nucleus during fixation. In pigmented rats (Güldner, personal communication), the size of the optic boutons is smaller than those of albino rats. It is possible that pigmentation of the retina corellates with the size of optic boutons.

The diameters of dense-core and clear vesicles are similar, as are the lengths of the synaptic appositions. The variability of the diameters of clear vesicles in individual boutons in the rat suprachiasmatic nucleus is not apparent in axolotl optic synapses.

The range of postsynaptic density thickness is similar in the two species, although in rat suprachiasmatic optic synapses there is a higher percentage (27%, Güldner and Wolff, 1978) of synapses with postsynaptic density thicknesses less than 20nm (Gray type II). As in the rat, in the axolotl, one optic bouton occasionally made a Gray type II as well as a Gray type I apposition. Microtubules, attachment plaques, vacuoles and glycogen granules are common features although more axolotl tectum optic synapses had microtubules. This might indicate a relatively higher number of *en passant* synapses.

4.8 FUNCTIONAL CONSIDERATIONS

4.8.a Behaviour

Urodeles are generally slow-moving animals, which are carnivorous through all stages of life. They eat a variety of animals in their natural environment ranging from worms to crustaceans and insects. They actively search for food, and will eat virtually any kind of prey so long as it is not too small, too large or too fast (Grüsser-Cornehls and Himstedt, 1976). Visual stimuli are not the only ones releasing a prey-capture reaction; chemical detection via the olfactory organ and mechano-detection via the lateral line organ in aquatic forms also play an important role. Some cave dwelling urodeles manage perfectly well with no light whatsoever (Grüsser-Cornehls and Himstedt, 1976).

When catching prey, the initial orientation to fixate an object binocularly is often made with the head alone. This is followed by a slow approach until the prey is within grasping reach. At this stage an olfaction test is often made after which the prey is seized by a snapping action and swallowed (Grüsser-Cornehls and Himstedt, 1976). Some urodeles, such as the axolotl, lead an aquatic existence all their life. Others become terrestrial at metamorphosis, but move back to the water to breed, while others spend the whole of their life on land. Vision is apparently less important to the aquatic forms where the lateral line plays a major role through the detection of vibrations (Grüsser-Cornehls and Himstedt, 1976). The eyes of the axolotl are small and after both of them have been removed, axolotls soon learn to detect prey with their remaining senses (personal observations).

Anurans tend to be more specialised in their diet; they often catch fast-moving prey such as flies. Orientation towards the prey is with the whole body, and not the head alone. If the prey is outside grasping reach, frogs jump and toads creep up to it. This is followed by a snapping action and swallowing. Vision is obviously more important to the success of such

an action especially when the catching of fast-moving prey is involved. Frogs generally sit and wait for prey to enter their visual field, but toads and most urodeles actively search for prey, the head constantly moving during its search for food (Grüsser-Cornehls and Himstedt, 1976).

One of the main functions of the optic tectum in at least lower vertebrates is the initiation of visually guided movements to or away from objects depending usually on whether the object is prey- or predator-like (Ingle, 1970). The orientation away from predator-like objects has been found to be affected by the thalamic/pretectal input to the tectum. Lesions in these diencephalic areas were found to cause a disinhibition towards both small and large objects (Ewert, 1970; Ingle, 1973b). The tectum is apparently not involved in seeing stationary objects. Ingle (1973c, 1976) found that frogs suffering from unilateral or bilateral tectal ablation avoided stationary objects well, despite their apparent inability to orient to prey or predator-like stimuli. In *Bufo marinus*, Ingle (1976) found that toads with large lesions involving the postero-lateral and pretectal cell complex persistently bumped into barriers whilst pursuing prey stimuli.

Ablation studies have not been carried out on urodeles, but the connections are similar and it seems likely that the tectum in these animals has a similar function.

4.8.b Physiology of the tectum

The physiology of the optic tectum has been studied far more completely in the anuran amphibians than in urodeles. Maturana *et al* (1960) described 5 types of units found in different layers of the superficial optic tectum of *Rana pipiens*. The responses were due to the activity of the retino-tectal terminals, which reflect the properties of the ganglion cells. They were found in distinct layers in the tectum and as the latter was penetrated from the dorsal surface, the following units were defined:

Class 1 or sustained edge detectors; *class 2* or convex edge detectors;

class 3 or changing contrast detectors; *class 4* or dimming detectors; and *class 5* or dark detectors. Class 5 units were not in a distinct layer, occurring in the same layer as the class 3 units. Since the study of Maturana and co-workers (1960), there have been many similar investigations on various anurans (for review see Grüsser and Grüsser-Cornehls, 1976). Class 1 and 2 units have many similarities. They both have a strong inhibitory surround such that they are far more sensitive to small objects which fit within their 2-5° receptive fields than to larger visual objects which readily activate classes 3 and 4. Both class 1 and 2 units respond optimally to moving objects and not to changes in illumination. The chief distinction between them appears to be the greater sensitivity of class 1 units to stationary objects (Ingle, 1976). Class 3 units are sensitive to the illumination of the whole or part of the excitatory receptive field, which elicits an on-off response. Class 4 units respond persistently to a dimming of their excitatory receptive fields (off-units). The excitatory receptive fields of class 3 and 4 units are far larger (7-15°) than those of class 1 and 2 (Grüsser and Grüsser-Cornehls, 1976). Classes 1 and 2 may be most important for the detection of prey, whereas classes 3 and 4 may be more important for the elicitation of avoidance behaviour (Ingle, 1976).

In order to localise the terminals accurately, the extracellular potentials were recorded in the optic tectum of various anurans after stimulation of the optic nerve (Chung *et al*, 1974). Four discrete potentials (m1, m2, u1, u2) were recorded which occurred at different latencies. Using current source analysis, the terminals producing these potentials were localised. The m1 wave had the shortest latency and was generated by myelinated fibres and had the properties of class 4 units, occurring at the appropriate depth. The m2 wave had a slightly longer latency, was also generated by myelinated fibres and by their properties and position were typical of class 3 units. Similarly, u1 and u2 waves were thought to be generated by unmyelinated fibres, the u1 wave sink was superficial to the

u2 wave sink. They corresponded to class 1 and 2 units respectively.

When considering amphibians as a whole Grüsser-Cornehls and Himstedt (1976) suggested as a more generally applicable framework that three main neuronal classes can be found. These consisted of class 1 and 2 as one group and 3 and 4 as the other two groups. In toads, class 1 units could not be found (for review see Ewert, 1976). A similar situation was found in the urodele *Triturus* (Cronly-Dillon, 1968), although the units were not assigned to any particular layers in the superficial portion to the optic tectum. In *Salamandra salamandra* (Grüsser-Cornehls and Himstedt, 1973) functional layering was detected, but no class 1 or 2 units were found. At the surface of the tectum a thin layer of axons showed no response to diffuse illumination of the receptive fields. They responded to small dark objects moved through their excitatory receptive field, which in contrast to those of class 1 and 2 terminals were quite large (12-16°). If objects larger than the excitatory receptive field were moved through the receptive field the discharge rate was lower, the larger the stimulus, indicating the existence of an effective inhibitory surround. Most toads and urodeles actively search for prey, and their heads are constantly moving, so that it may not be adaptive to have units with a very small excitatory receptive field and a large inhibitory receptive field, as the inhibitory receptive field would be continually activated and prevent the response of such units (Grüsser-Cornehls and Himstedt, 1976).

Triturus cristatus has a more differentiated retina than *Salamandra salamandra* (Grüsser-Cornehls and Himstedt, 1976), and probably more complicated than the axolotl (personal observation). The retina of *Necturus* is "in a mild state of phylogenetic degeneration" (Grüsser-Cornehls and Himstedt, 1976). It seems reasonable to predict that the axolotl has units similar to or less complex than those of *Salamandra salamandra*.

The physiological properties of the tectal neurons have been studied very poorly in comparison with the retinal ones. Grüsser-Cornehls and

Himstedt (1973) made some qualitative investigations in *Salamandra salamandra*, recording from action potentials of cells below the retinal projection. They found five types of unit: a) had a large receptive field (> 30°) and could stretch over the whole visual field of one eye; b) responded to an object moving in the z axis towards the eye; c) had an excitatory receptive field between 10° and 20° in diameter which responded to stimuli moving into the excitatory receptive field; d) were binocularly activated units, the receptive fields covered the binocular visual field of both eyes; e) were multisensory neurons, usually located in deeper tectal layers which did not always respond to experimental visual stimuli. They responded to tactile stimuli in many cases. Gruberg (1969), recording from tectal neurons in *Ambystoma tigrinum*, showed that when a micro-electrode is advanced from the surface towards the ventricle of the tectum, it passes through 1) a visual layer; 2) a contralateral somesthetic layer; 3) a bilateral somesthetic layer; and 4) a layer where units respond to both visual and somesthetic stimulation. The tactile as well as the visual stimuli are topographically organised on the tectum (Gruberg, 1969).

In anurans similar types of units to those described above can be found although other more complex kinds are also observed (Grüsser and Grüsser-Cornehls, 1976). Unlike urodeles, frogs possess units with very small receptive fields. Perhaps this is a reflection on the more specialised and refined tectum of the frog. The more generalised stimuli needed to fire tectal neurons in urodeles could reflect the more generalised nature of their food sources.

4.8.c Correlations of the physiology, anatomy and behaviour

In anurans the retino-tectal fibres appear to be laminated from both anatomical and physiological studies. Myelinated fibres are found in the areas corresponding to the m1 and m2 wave sinks (Potter's (1969) layers D, E, G). Myelinated fibres are also found in more superficial laminae (Potter's (1969) layer B). Unmyelinated fibres are more difficult to localise

histologically and their appearance during degeneration is similar to that of terminals, so that it is possible that the unmyelinated fibres have been overlooked in anatomical studies. It is known that the majority of the optic nerve fibres in anurans are in fact unmyelinated (Maturana, 1960). In urodeles there are slightly conflicting reports about the physiological and anatomical presence of lamination. *Triturus* has apparently no functional lamination of units whereas *Salamandra* has (Grüsser-Cornehls and Himstedt, 1976). Anatomically, Jackway and Riss (1972) reported a lamination of retino-tectal fibres in the tiger salamander, but no evidence for a lamination of the retino-tectal fibres in the axolotl was found in this study of the axolotl or other (Gruberg, 1973; Zakon, 1978) studies.

In fish, Winkelmann (1968) and Kishida (1979) studied the structure of the tectum of many species of teleost. They found that the thickness of the layers receiving optic input, and other tectal layers, varied depending on the behaviour and habitat of the fish. Those that apparently had poor vision, had thin optic layers. Kishida (1979) also found that the dendrites of the cells showed restricted branching patterns. However the same basic classes of tectal cells were found in all species. The branching patterns of cells in the axolotl tectum were not restricted, and that part of the tectum receiving optic input is quite thick in relation to other layers (half of outer plexiform layer has optic input). Whereas the fish with thin optic layers and little branching of dendrites in these layers could be described as having a regressed optic tectal strucure, in the axolotl the branching patterns of the tectal cells suggest that this is not the case, even though the tectum does not show the complex structure typical of the anuran tectum. Anurans are more successful than urodeles in that they occupy far more diverse and numerous niches. Their success may be partly due to the specialisation of their visual system.

The ultrastructure of the axolotl optic neuropile appears to be very similar to that of an anuran. The most striking difference is the lack of well defined complex synaptic arrangements or glomeruli. Structures similar

to the glomeruli described in the frog (Székely and Lázár, 1976) are common features in many areas of the brain in vertebrates, including the olfactory bulb, the cerebellum and the thalamus (Szentágothai, 1970; Spacek and Lieberman, 1974; Nemecek, 1972). They generally consist of a collection of synapses of varying origin, surrounded by an astroglial wrapping which isolates the glomerulus. The purpose of isolating such complexes is at present unknown, although it has been suggested (Spacek and Lieberman, 1974) that the astrocytic capsule could serve to limit diffusion from the glomerulus, of extracellular ions (mainly potassium ions) and transmitter, released by the intra glomerular terminals.

Glomeruli may be a refinement of visual processing in the frog, important to it for its specialised vision but not necessary for the visual needs of the axolotl.

In summary, it appears that in urodeles including the axolotl the tectum has fewer laminae, fewer cell types, and a less complex optic neuropile than anurans and other vertebrates. This correlates well with physiological and behavioural results. On the other hand, the tecta of urodeles and other vertebrates show many basic similarities. The comparative simplicity of the urodele tectum means the axolotl would be a useful candidate for further physiological and morphological investigations, which are likely to give a better understanding of tectal functions in vertebrates as a whole.

5. REFERENCES

REFERENCES

AKERT, K; PFENNIGER, K; SANDRI, C; MOOR, H. (1972) Freeze etching and cytochemistry of vesicles and membrane complexes in synapses of the central nervous system. In G. D. Pappas and D. P. Purpura (Eds.), *Structure and Function of Synapses.* NEW YORK: Raven Press, pp. 67-86.

ANGAUT, P. and REPÉRANT, J. (1976) Fine structure of the optic fibre termination layers in pigeon optic tectum: a Golgi and E.M. study. *Neuroscience* 1, 93-105.

BASS, A. H. and NORTHCUTT, R.G. (1975) Retinal projections in Atlantic loggerhead sea turtle *(Caretta caretta)*: an autoradiographic study. *Anat. Rec.* 181, 308.

BONS, N. (1976) Retino-hypothalamic pathway in the duck. *Cell Tiss. Res.* 168, 343-360.

BRADFORD, M. R., Jr. (1973) Retinal projections in *Caiman croccodilus*. *Am. Zoologist* 13, 1345.

BRÄNDLE, K. and STIRLING, R. V. (1975) Development of the ipsilateral visual projection in axolotls treated with thyroxine. *J. Physiol. (Lond.)* 250, 28P-29P.

BUTLER, A. B. (1973) Retinal projections in the night lizard, *Xantusia vigilis* Baird. *Am. Zoologist* 13, 1345-1346.

BUTLER, A. B. and EBBESSON, S. O. E. (1975) A Golgi study of the optic tectum of the Tegu lizard, *Tupinambis nigropunctatus*. *J. Morph.* 146, 215-227.

BUTLER, A. B. and NORTHCUTT, R. G. (1978) New thalamic visual nuclei in lizards. *Brain Res.* 149, 469-477.

CAMPBELL, C. B. G., and EBBESSON, S. O. E. (1969) The optic system of a teleost: *Holocentrus* re-examined. *Brain, Behav. and Evol.* 2, 415-430.

CHUNG, S. H.; BLISS, T. V. P.; and KEATING, M. J. (1974) The synaptic organisation of optic afferents in the amphibian tectum. *Proc. R. Soc. Lond. B.* 187, 421-447.

COLONNIER, M. (1968) Synaptic patterns on different cell types in the different laminae of the cat visual cortex. An electron micro-

scopic study. *Brain Res.* 9, 268-287.

CRONLY-DILLON, J. R. (1968) Pattern of retinotectal connections after retinal regeneration. *J. Neurophysiol.* 31, 410-418.

CRUCE, W. L. R. and CRUCE, J. A. F. (1975) Projections from the retina to the lateral geniculate nucleus and mesencephalic tectum in a reptile *Tupinambis nigropunctatus:* a comparison of anterograde transport and anterograde degeneration. *Brain Res.* 85, 221-228.

CULLEN, M. J. and KAISERMAN-ABRAMOF, I. R. (1976) Cytological organisation of the dorsal lateral geniculate nuclei in mutant anophthalmic and postnatally enucleated mice. *J. Neurocytol.* 5, 407-424.

CURRIE, J. and COWAN, W. M. (1974) Evidence for late development of the uncrossed retinothalamic projections in the frog, *Rana pipiens. Brain Res.* 71, 133-139.

DRÄGER, U. C. and HUBEL, D. H. (1975) Response to visual stimulation and relationship between visual, auditory and somatosensory inputs in mouse superior colliculus. *J. Neurophysiol.* 38, 690-713.

EBBESSON, S. O. E. (1970) On organisation of central visual pathways in vertebrates. *Brain, Behav. and Evol.* 3, 178-194.

EBBESSON, S. O. E. (1972) A proposal for a common nomenclature for some optic nuclei in vertebrates and the evidence for a common origin of two such cell groups. *Brain, Behav. and Evol.* 6, 75-91.

EBBESSON, S. O. E. and SCHROEDER, D. M. (1971) Connections of the nurse shark's telencephalon. *Science* 173, 254-256.

EBBESSON, S. O. E. and VANEGAS, H. (1976) Projections of the optic tectum in two teleost species. *J. Comp. Neurol.* 165, 161-180.

EWERT, J. P. (1970) Neural mechanisms of prey catching and avoidance behaviour in the toad *Bufo bufo. Brain, Behav. and Evol.* 3, 36-56.

EWERT, J. P. (1976) The visual system of the toad: behavioural and physiological studies on a pattern recognition system. In K. V. Fite (Ed.), *The Amphibian Visual System.* NEW YORK, SAN FRANCISCO, LONDON: Academic Press, pp. 141-202.

FITE, K. V. (1969) Single unit analysis of binocular neurones in the frog tectum. *Expl. Neurol.* 24, 475-486.

FOSTER, R. E. and HALL, W. C. (1975) The connections and lamina organisation of the optic tectum in a reptile (*Iguana iguana*). *J. Comp. Neurol.* 163, 397-426.

GAILLARD, F. and GALAND, G. (1977) New ipsilateral visual units in the frog tectum. *Brain Res.* 136, 351-354.

GAZE, R. M. and JACOBSON, M. (1962) Projection of the binocular visual field on the optic tecta of the frog. *Quart. J. exp. Physiol.* 47, 273-280.

GLASSER, S. and INGLE, D. J. (1978) The role of the nucleus isthmus in the ipsilateral visual projection to the frog's optic tectum. *Soc. Neurosci. Abst.* 4, 630.

GRAHAM, J. (1977) An autoradiographic study of the efferent connections of the superior colliculus in the cat. *J. Comp. Neurol.* 173, 629-654.

GRAY, E. G. (1959) Axo-somatic and axo-dendritic synapses of the cerebral cortex: an electron microscopic study. *J. Anat. (Lond.)* 93, 420-432.

GROVER, B. G. and SHARMA, S. C. (1978) Tectal afferents in goldfish as revealed by retrograde HRP label. *Soc. Neurosci. Abst.* 4, 103.

GRUBERG, E. R. (1969) Functional organisation of the tectum of the tiger salamander *Ambystoma tigrinum. Ph.D. thesis,* submitted to University of Illinois, Urbana Ill.

GRUBERG, E. R. (1973) Optic fiber projections of the tiger salamander *Ambystoma tigrinum. J. Hirnforsch.* 14, 399-411.

GRUBERG, E. R. and AMBROS, V. R. (1974) A forebrain visual projection in the frog (*Rana pipiens*). *Expl. Neurol.* 44, 187-197.

GRUBERG, E. R. and LETTVIN, J. Y. (1978) The distribution and shapes of tectal cells projecting to the nucleus isthmi in frogs. *Soc. Neurosci. Abst.* 4, 631.

GRUBERG, E. R. and SOLISH, S. P. (1978) The relationship of a monoamine fiber system to a somatosensory tectal projection in the salamander *Ambystoma tigrinum. J. Morph.* 157, 137-151.

GRUBERG, E. R. and UDIN, S. B. (1978) Topographic projections between the nucleus isthmi and the tectum of the frog *Rana pipiens. J. Comp. Neurol.* 179, 487-500.

GRÜSSER-CORNEHLS, U. and HIMSTEDT, W. (1976) Urodele visual system. In K. V. Fite (Ed.), *The Amphibian Visual System.* NEW YORK, SAN FRANCISCO, LONDON: Academic Press, pp. 203-266.

GRÜSSER, O-J and GRÜSSER-CORNEHLS, U. (1976) Neurophysiology of the

anuran visual system. In R. Llinás and W. Precht (Eds.), *Frog Neurobiology*. BERLIN, HEIDELBERG, NEW YORK: Springer-Verlag, pp. 278-294.

GUILLERY, R. W. and UPDYKE, B. V. (1976) Retinofugal pathways in normal and albino axolotls. *Brain Res.* 109, 235-244.

GÜLDNER, F-H. (1978a) Synapses of optic nerve afferents in the rat suprachiasmatic nucleus. I. Identification, qualitative description, development and distribution. *Cell and Tiss. Res.* 194, 17-35.

GÜLDNER, F-H. (1978b) Synapses of optic nerve afferents in the rat suprachiasmatic nucleus. II. Structural variability as revealed by morphometric examination. *Cell and Tiss. Res.* 194, 37-54.

GÜLDNER, F-H. and WOLFF, J. R. (1978) Retinal afferents form Gray type-I and type-II synapses in the suprachiasmatic nucleus (rat). *Exp. Brain Res.* 32, 83-89.

HAYES, B. P. and WEBSTER, K. E. (1975) An electron microscope study of the retino-receptive layers of the pigeon optic tectum. *J. Comp. Neurol.* 162, 447-466.

HERRICK, C. J. (1941) Optic and postoptic systems of the fibres in the brain of *Necturus*. *J. Comp. Neurol.* 75, 487-544.

HERRICK, C. J. (1942) Optic and postoptic systems in brain of *Ambystoma tigrinum*. *J. Comp. Neurol.* 77, 191-353.

HERRICK, C. J. (1948) The brain of the tiger salamander *Ambystoma tigrinum*. University of Chigaco press.

HUGHES, A. (1977) The visual system in vertebrates. In F. Crescitelli (Ed.), *Handbook of Sensory Physiology*, VII/5. NEW YORK: Springer-Verlag, pp. 626-630.

HUNT, S. P. and KÜNZLE, H. (1976) Observations on the projections and intrinsic organization of the pigeon optic tectum: an autoradiographic study based on anterograde and retrograde, axonal and dendritic flow. *J. Comp. Neurol.* 170, 153-172.

HUNT, S. P. and WEBSTER, K. E. (1975) The projection of the retina upon the optic tectum of the pigeon. *J. Comp. Neurol.* 162, 433-446.

INGLE, D. (1970) Visuomotor functions of the frog optic tectum. *Brain, Behav. and Evol.* 3, 57-71.

INGLE, D. (1973a) Evolutionary perspectives on the function of the optic tectum. *Brain, Behav. and Evol.* 8, 211-237.

INGLE, D. J. (1973b) Disinhibition of tectal neurons by pretectal lesions in the frog. *Science* 180, 422-424.

INGLE, D. J. (1973c) Two visual systems in the frog. *Science* 181, 1053-1055.

INGLE, D. J. (1976) Behavioural correlates of central visual function in anurans. In R. Llinás and W. Precht (Eds.), *Frog Neurobiology*. BERLIN, HEIDELBERG, NEW YORK: Springer-Verlag, pp. 435-451.

ITO, H. and KISHIDA, R. (1977) Tectal afferent neurons identified by the retrograde HRP method in the carp telencephalon. *Brain Res.* 130, 142-145.

ITO, H. and KISHIDA, R. (1978) Afferent and efferent fiber connections of the carp torus longitudinalis. *J. Comp. Neurol.* 181, 465-476.

JACKWAY, J. S. and RISS, W. (1972) Retinal projections in the tiger salamander, *Ambystoma tigrinum*. *Brain, Behav. and Evol.* 5, 401-442.

KARTEN, H. J. (1965) Projections of the optic tectum of the pigeon *(Columba livia)*. *Anat. Rec.* 151, 369.

KARTEN, H. J.; HODOS, W.; NAUTA, W. J. H. and REVZIN, A. M. (1973) Neural connections of the 'visual wulst' of the avian telencephalon. Experimental studies in the pigeon *(Columba livia)* and owl *(Speotyto cunicularia)*. *J. Comp. Neurol.* 150, 253-278.

KEATING, M. J. and KENNARD, C. (1976) The amphibian visual system as a model for developmental neurobiology. In K. V. Fite (Ed.), *The Amphibian Visual System*. NEW YORK, SAN FRANCISCO, LONDON: Academic Press, pp. 267-315.

KENNEDY, M. C. and RUBINSON, K. (1977) Retinal projections in larval, transforming and adult sea lamprey, *Protomyzon marinus*. *J. Comp. Neurol.* 171, 465-480.

KISHIDA, R. (1979) Comparative study on the teleostean optic tectum. Lamination and cytoarchitectural. *J. Hirnforsch.* 20, 57-67.

KNAPP, H.; SCALIA, F; and RISS, W. (1965) The optic tracts of *Rana pipiens*. *Acta neurol. (Scand.)* 41, 325-355.

KOKOROS, J. J. and NORTHCUTT, R. G. (1977) Telencephalic efferents of the tiger salamander *Ambystoma tigrinum*. *J. Comp. Neurol.* 173, 613-628.

LANDRETH, G. E.; NEALE, E. A.; NEALE, J. H.; DUFF, R. S.; BRADFORD, M. R. Jr.; NORTHCUTT, R. G.; and AGRANOFF, B. W. (1975)

Evaluation of (^{3}H) proline for radioautographic tracing of axonal projections in the teleost visual system. *Brain Res.* 91, 25-42.

LATIES, A. M. and SPRAGUE, J. M. (1966) The projection of optic fibres to the visual centers in the cat. *J. Comp. Neurol.* 127, 35-70.

LAUFER, M. and VANEGAS, H. (1974) The optic tectum of a perciform teleost. II. Fine structure. *J. Comp. Neurol.* 154, 61-96.

LA VAIL, J. H. and COWAN, W. M. (1971) The development of the chick optic tectum II. Autoradiographic studies. *Brain Res.* 28, 421-441.

LÁZÁR, G. (1969) Efferent pathways of the optic tectum in the frog. *Acta. biol. hung.* 20, 171-183.

LÁZÁR, G. (1971) The projection of the retinal quadrants on the optic centres in the frog. A terminal degeneration study. *Acta morph. hung.* 19, 325-334.

LÁZÁR, G. (1973) The role of the accessory optic system in the optokinetic nystagmus of the frog. *Brain, Behav, and Evol.* 5, 443-460.

LÁZÁR, G. (1978) Application of cobalt-filling technique to show retinal projections in the frog. *Neuroscience* 3, 725-736.

LÁZÁR, G. and SZÉKELY, G. (1967) Golgi studies on the optic center of the frog. *J. Hirnforsch.* 9, 329-344.

LÁZÁR, G. and SZÉKELY, G. (1969) Distribution of optic terminals in the different optic centers of the frog. *Brain Res.* 16, 1-14.

LEMIRE, M. and REPÉRANT, J. (1976) Neuro-anatomie - Analyse radioautographique des projections visuelles primaires chez la truite, *Salmo irideus* Gibb. (comparison avec quelques autres téléostéens d'eau douce). *Comptes Rendus* 283, série D 951.

LEVINE, R. L. (1980) An autoradiographic study of the retinal projections in *Xenopus laevis* with comparisons to *Rana*. *J. Comp. Neurol.* 189, 1-29.

LEWIS, P. R. and KNIGHT, D. P. (1977) Staining methods for sectioned material. In A. M. Glauert (Ed.), *Practical methods in electron microscopy*, V. 5 pt. I. AMSTERDAM, NEW YORK, OXFORD: North-Holland Publishing Company, pp. 45-46.

LIEBERMAN, A. R. and WEBSTER, K. E. (1974) Aspects of the synaptic organization of intrinsic neurons in the dorsal lateral geniculate nucleus. *J. Neurocytol.* 3, 677-710.

LUND, R. D. (1969) Synaptic patterns of the superficial layers of the superior colliculus of the rat. *J. Comp. Neurol.* 135, 179-208.

LUND, R. D. (1972) Synaptic patterns in the superficial layers of the superior colliculus of the monkey, *Macaca mulatta*. *Exp. Brain Res.* 15, 194-211.

MAI, J. (1976) Quantitative autoradiographische untersuchungen am subcorticalen optischen system der albino ratte. *Dissertation*, Medizinische Fakultät, Universität Düsseldorf.

MALMGREN, L. T. and OLSSON, Y. (1977) A sensitive histochemical method for light and electron microscopic demonstration of horseradish peroxidase. *J. Histochem. Cytochem.* 25, 1280-1282.

MAROTTE, L. R. and MARK, R. F. (1975) Ultrastructural localization of synaptic input to the optic lobe of carp (*Carassius carassius*). *Expl. Neurol.* 49, 772-789.

MASON, C. A. and ROBSON, J. A. (1979) Morphology of retino-geniculate axons in the cat. *Neuroscience* 4, 79-97.

MATHERS, L. H. Jr. (1977) Retinal and visual cortical projection to the superior colliculus of the rabbit. *Expl. Neurol.* 57, 698-712.

MATURANA, H. R. (1960) The fine anatomy of the optic nerve of anurans - an E.M. study. *J. Biophys. Biochem. Cytol.* 7, 107-120.

MATURANA, H. R.; LETTVIN, J. Y.; McCULLOCH, W. S.; and PITTS, W. H. (1960) Anatomy and physiology of vision in the frog. *J. Gen. Physiol.* 43, suppl., 129-171.

MEEK, J. and SCHELLART, N. A. M. (1978) A Golgi study of goldfish optic tectum. *J. Comp. Neurol.* 182, 89-123.

MESULAM, M-M. (1976) The blue reaction product in horseradish peroxidase neurohistochemistry: incubation parameters and visibility. *J. Histochem. Cytochem.* 24, 1273-1280.

NEARY, T. J. (1976) An autoradiographic study of the retinal projections in some members of 'archaic' and 'advanced' anuran families. *Anat. Rec.* 184, 487.

NEMECEK, ST. (1972) Principles of synaptic ultrastructure in the C.N.S. From the *Collection of Scientific Works of the Faculty of Medicine, Charles University at Hradec Králové*, vol. 15, no. 3. Faculty of Medicine, Charles University, Hradec Králové.

NORTHCUTT, R. G. and BUTLER, A. B. (1974) Evolution of reptilian visual systems: retinal projections in a nocturnal lizard *Gekko gecko*. *J. Comp. Neurol.* 157, 453-466.

NORTHCUTT, R. G. and BUTLER, A. B. (1976) Retinofugal pathways in the longnose gar *Lepisosteus osseus* (Linnaeus). *J. Comp. Neurol.* 166, 1-15.

O'FLAHERTY, J. J. (1970-71) A Golgi analysis of the optic tectum of the mallard duck. *J. Hirnforsch.* 12, 389-404.

OLIVER, J.; BOUILLE, C.; HERBUTE, S.; and BAYLE, J. D. (1978) Retrograde transport of HRP from preoptic-anterior hypothalamic region to retinal ganglion cells in quail. *Neurosci. Lett.* 9, 291-297.

PALAY, S. L. and CHAN-PALAY, V. (1974) In *The Cerebellar Cortex*. BERLIN, HEIDELBERG, NEW YORK: Springer-Verlag, pp. 333-336.

PALAY, S. L. and CHAN-PALAY, V. (1975) A guide to the synaptic analysis of the neuropil. In *The Synapse*. Cold Spring Harb. *Quant. Biol.* 40, 1-16.

PEYRICHOUX, J.; REPÉRANT, J.; and WEIDNER, C. (1978) Les centres visuels primaires chez la grenouille (*Rana esculenta L.*) et le probleme des projections ipsilatérales. Étude radioautographique. *Comptes Rendus* 287, série D, 37-40.

PICOUET, M. J. and CLAIRAMBAULT, P. (1977) Architecture de système visuel de *Discoglossus pictus*. *J. Hirnforsch.* 18, 404-421.

POTTER, H. D. (1969) Structural characteristics of cell and fiber populations in the optic tectum of the frog (*Rana catesbeina*). *J. Comp. Neurol.* 136, 203-232.

POTTER, H. D. (1972) Terminal arborizations of retinotectal axons in the bullfrog. *J. Comp. Neurol.* 144, 269-284.

RAMÓN-MOLINER, E. (1962) An attempt at classifying nerve cells on the basis of their dendritic patterns. *J. Comp. Neurol.* 119, 211-228.

RAMÓN-MOLINER, E. (1970) The Golgi-Cox technique. In W. J. H. Nauta and S. O. E. Ebbesson (Eds.), *Contemporary Research Methods in Neuroanatomy*. NEW YORK: Springer, pp. 33-51.

REPÉRANT, J. (1973) Nouvelles donées sur les projections visuelles chez le pigeon *(Columbia livia)*. *J. Himforsch.* 14 151-187.

REPÉRANT, J.; LEMIRE, M.; MICELI, D.; and PEYRICHOUX, J. (1976) A radioautographic study of the visual system in fresh water teleosts following intraocular injection of tritiated fucose and proline. *Brain Res.* 118, 123-131.

REPÉRANT, J.; RIO, J. P.; MICELI, D.; and LEMIRE, M. (1978) A radioautographic study of retinal projections in type I and II lizards. *Brain Res.* 142, 401-413.

REPÉRANT, J. and RIO, J. P. (1976) Retinal projections in *Vipera aspis*. A reinvestigation using light radioautographic and E.M. degeneration techniques. *Brain Res.* 107, 603-609.

REYNOLDS, E. S. (1963) The use of lead citrate at high pH as an electron-opaque stain in electron microscopy. *J. Cell Biol.* 17, 208-213.

RILEY, J. N. and MARCHAND, E. R. (1978) Improvements in the benzidine dihydrochloride horseradish peroxidase method. *Stain Technol.* 53, 290.

RISS, W.; KNAPP, H.; and SCALIA, F. (1963) Optic pathways in *Cryptobranchus allegheniensis* as revealed by the Nauta technique. *J. Comp. Neurol.* 121, 31-43.

RISS, W. and INGLE, D. (1973) Report of a conference on the anuran visual system. *Brain, Behav. and Evol.* 8, 321-326.

ROBSON, J. A. and MASON, C. A. (1979) The synaptic organization of terminals traced from individual labelled retino-geniculate axons in the cat. *Neuroscience* 4, 99-111.

RUBINSON, K. (1968) Projections of the tectum opticum of the frog. *Brain Behav. and Evol.* 1, 529-561.

SCALIA, F. (1973) Autoradiographic demonstration of optic nerve fibres in stratum zonale of frog's tectum. *Brain Res.* 58, 484-488.

SCALIA, F. (1976) Optic pathway of the frog: nuclear organization and connections. In R. Llinás and W. Precht (Eds.), *Frog Neurobiology*. BERLIN, HEIDELBURG, NEW YORK: Springer-Verlag, pp. 386-406.

SCALIA, F.; KNAPP, H.; HALPERN, M.; and RISS, W. (1968) New observations on the retinal projection in the frog. *Brain, Behav. and Evol.* 1, 324-353.

SCALIA, F. and COLEMAN, D. R. (1974) Aspects of the central projection of the optic nerve in the frog as revealed by anterograde migration of HRP. *Brain Res.* 79, 496-504.

SCALIA, F. and FITE, K. (1974) A retinotopic analysis of the central connections of the optic nerve in the frog. *J. Comp. Neurol.* 158, 455-478.

SCALIA, F. and GREGORY, K. (1970) Retinofugal projections in the frog. Location of the post synaptic neurons. *Brain, Behav. and Evol.* 3, 16-29.

SCALIA, F. and TEITELBAUM, I. (1978) Absence of efferents to the retina in frog and toad. *Brain Res.* 153, 340-345.

SCHROEDER, D. M. (1973) Peripheral zone impregnation with Golgi-Cox procedure using egg yolk coated tissue. *Stain Technol.* 48, 352.

SHARMA, S. C. (1972) The retinal projections in the goldfish: an experimental study. *Brain Res.* 39, 213-223.

SIMS, T. J. (1977) The development of monamine-containing neurons in the brain and spinal cord of the salamander *Ambystoma mexicanum*. *J. Comp. Neurol.* 173, 319-336.

SPACEK, J. and LIEBERMAN, A. R. (1974) Ultrastructure and three-dimensional organization of synaptic glomeruli in rat somatosensory thalamus. *J. Anat.* 117, 487-516.

SPRAGUE, J. M. (1975) Mammalian tectum: intrinsic organization, afferent inputs and integrative mechanisms. Anatomical substrate. *Neurosci. Res. Progr. Bull.* 13, 204-213.

STELZNER, D. J. (1979) Evidence of collateral sprouting in frog visual system. *Brain Res.* 168, 382-387.

STERLING, P. (1971) Receptive fields and synaptic organization of the superficial gray layer of the cat superior colliculus. *Vision Res.* 11 (Suppl. 3), 309-328.

STONE, J. and FREEMAN, J. A. (1971) Synaptic organisation of the pigeon's optic tectum: a Golgi and current source-density analysis. *Brain Res.* 27, 203-221.

SZÉKELY, G. (1973) Anatomy and synaptology of the optic tectum. In R. Jung (Ed.), *Handbook of Sensory Physiology*, Volume VII/3B. BERLIN, NEW YORK: Springer-Verlag, pp. 1-26.

SZÉKELY, G.; SÉTÁLÓ, G.; LÁZÁR, G. (1973) Fine structure of frog's optic tectum: optic fibre termination layers. *J. Hirnforsch.* 14, 189-225.

SZÉKELY, G. and LÁZÁR, G. (1976) Cellular and synaptic architecture of the optic tectum. In R. Llinás and W. Precht (Eds.), *Frog Neurobiology*. NEW YORK, HEIDELBERG, BERLIN: Springer-Verlag, pp. 407-434.

SZENTÁGOTHAI, J. (1970) Glomerular synapses, complex synaptic arrangements and their operational significance. In Francis O. Schmitt (Ed. in Chief), *The Neurosciences Second Study Program*. NEW YORK: The Rockefeller University Press, pp. 427-443.

SZENTÁGOTHAI, J. (1973) Neuronal and synaptic architecture of the lateral geniculate nucleus. In R. Jung (Ed.), *Handbook of Sensory Physiology*, Volume VII/3B. BERLIN, HEIDELBERG, NEW YORK: Springer-Verlag, pp. 141-176.

TIGGES, M. and O'STEEN, W. K. (1974) Termination of retinofugal fibres in squirrel monkey. A reinvestigation using autoradiographic methods. *Brain Res.* 79, 489-495.

TRACHTENBERG, M. C. and INGLE, D. (1974) Thalamo-tectal projections in frog. *Brain Res.* 79, 419-430.

ULINSKI, P. S. (1977) Tectal efferents in the banded water snake. *J. Comp. Neurol.* 173, 251-274.

VANEGAS, H.; LAUFER, M.; and AMAT, J. (1974) The optic tectum of a perciform teleost. I. General configuration and cytoarchitecture. *J. Comp. Neurol.* 154, 43-60.

VANEGAS, H. and EBBESSON, S. O. E. (1973) Retinal projections in the perch-like teleost *Eugerres plumeri*. *J. Comp. Neurol.* 151, 331-358.

VONEIDA, T. J. and SLIGAR, C. M. (1976) A comparative neuroanatomic study of retinal projections in two fishes *Astynax hubbsi* (the blind cavefish) and *Astyanax mexicanus*. *J. Comp. Neurol.* 165, 89-106.

VULLINGS, H. G. B. and HEUSSEN, M. A. (1975) Electron microscopic observations on retino-preoptic pathway of *Rana temporaria* L. *Cell. Tiss. Res.* 161, 177-182.

WEBSTER, K. E. (1974) Changing concepts of the organisation of the central visual pathways in birds. In R. Bellairs and E. G. Gray (Eds.), *Essay on the Nervous System. A. Feishchrift for Prof. J. Z. Young.* OXFORD: Clarendon Press, pp. 258-298.

WILCZYNSKI, W. and NORTHCUTT, R. G. (1977) Afferents to optic tectum of the leopard frog. An HRP study. *J. Comp. Neurol.* 173, 219-230.

WILSON, M. E. and TOYNE, M. J. (1970) Retino-tectal and cortico-tectal projections in *Macaca mulatta*. *Brain Res.* 24, 395-406.

WILLIAMS, M. A. (1977) Quantitative methods in biology. In A. M. Glauert (Ed.), *Practical Methods in Electron Microscopy*, 6, II. AMSTERDAM: North-Holland, p. 52.

WINKELMANN, E. and WINKELMANN, L. (1968) Vergleichend histologische untersuchungen zur funktionellen morphologie des tectum opticum verschiedner teleostier. *J. Hirnforsch.* 10, 1-16.

YAMADA, H. (1974) Light and electron microscopic analysis of the medial terminal nucleus of the accessory optic system in the mouse. *Z. Mikr.-Anat. Forsch* 88, 997-1017.

ZAKON, H. (1978) Retinofugal projections in the red-backed salamander: evidence for an ipsilateral retinotectal pathway. *Soc. Neurosci. Abst.* 4, 103.